GJBX-222(82)

National Uranium Resource Evaluation

REPORTS ON INVESTIGATIONS OF URANIUM ANOMALIES

Bendix Field Engineering Corporation
Grand Junction, Colorado

Issue Date
October 1982

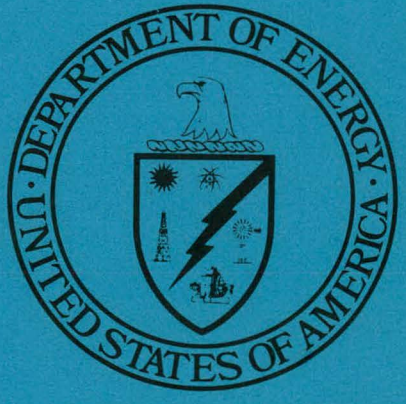

PREPARED FOR THE U.S. DEPARTMENT OF ENERGY
Assistant Secretary for Nuclear Energy
Grand Junction Area Office, Colorado

DISCLAIMER

This report is a result of work performed by Bendix Field Engineering Corporation, Operating Contractor for the U.S. Department of Energy, as part of the National Uranium Resource Evaluation. NURE was a program of the U.S. Department of Energy's Grand Junction, Colorado, Office to acquire and compile geologic and other information with which to assess the magnitude and distribution of uranium resources and to determine areas favorable for the occurrence of uranium in the United States.

Available from: Technical Library
Bendix Field Engineering Corporation
P.O. Box 1569
Grand Junction, CO 81502-1569

Telephone: (303) 242-8621, Ext. 278

Price per Microfiche Copy: $5.00

GJBX-222(82)

DE83 002472

GJBX-222(82)

REPORTS ON INVESTIGATIONS OF URANIUM ANOMALIES

3rd National Uranium Resource Evaluation

Craig S. Goodknight and John A. Burger
Compilers

951 2220

BENDIX FIELD ENGINEERING CORPORATION
Grand Junction Operations
Grand Junction, Colorado 81502

September 1982

PREPARED FOR THE U.S. DEPARTMENT OF ENERGY
GRAND JUNCTION AREA OFFICE
UNDER CONTRACT NO. DE-AC07-76GJ01664

13

THIS PAGE

WAS INTENTIONALLY

LEFT BLANK

FOREWORD

During the National Uranium Resource Evaluation (NURE) program, conducted for the U.S. Department of Energy (DOE) by Bendix Field Engineering Corporation (BFEC), radiometric and geochemical surveys and geologic investigations detected anomalies indicative of possible uranium enrichment. Data from the Aerial Radiometric and Magnetic Survey (ARMS) and the Hydrogeochemical and Stream-Sediment Reconnaissance (HSSR), both of which were conducted on a national scale, yielded numerous anomalies that may signal areas favorable for the occurrence of uranium deposits. Results from geologic evaluations of individual 1° x 2° quadrangles for the NURE program also yielded anomalies, which could not be adequately checked during scheduled field work.

Included in this volume are individual reports of field investigations for six areas initially indicated on the basis of ARMS, HSSR, and (or) geologic data to be anomalous (see p. iv). Field checks were conducted in each case to verify an indicated anomalous condition and to determine the nature of materials causing the anomaly. The ultimate objective of work is to determine whether favorable conditions exist for the occurrence of uranium deposits in areas that either had not been previously evaluated or were evaluated before data from recent surveys were available. Most field checks were of short duration (2 to 5 days). The work was done by various investigators using different procedures, which accounts for variations in format in the following reports.

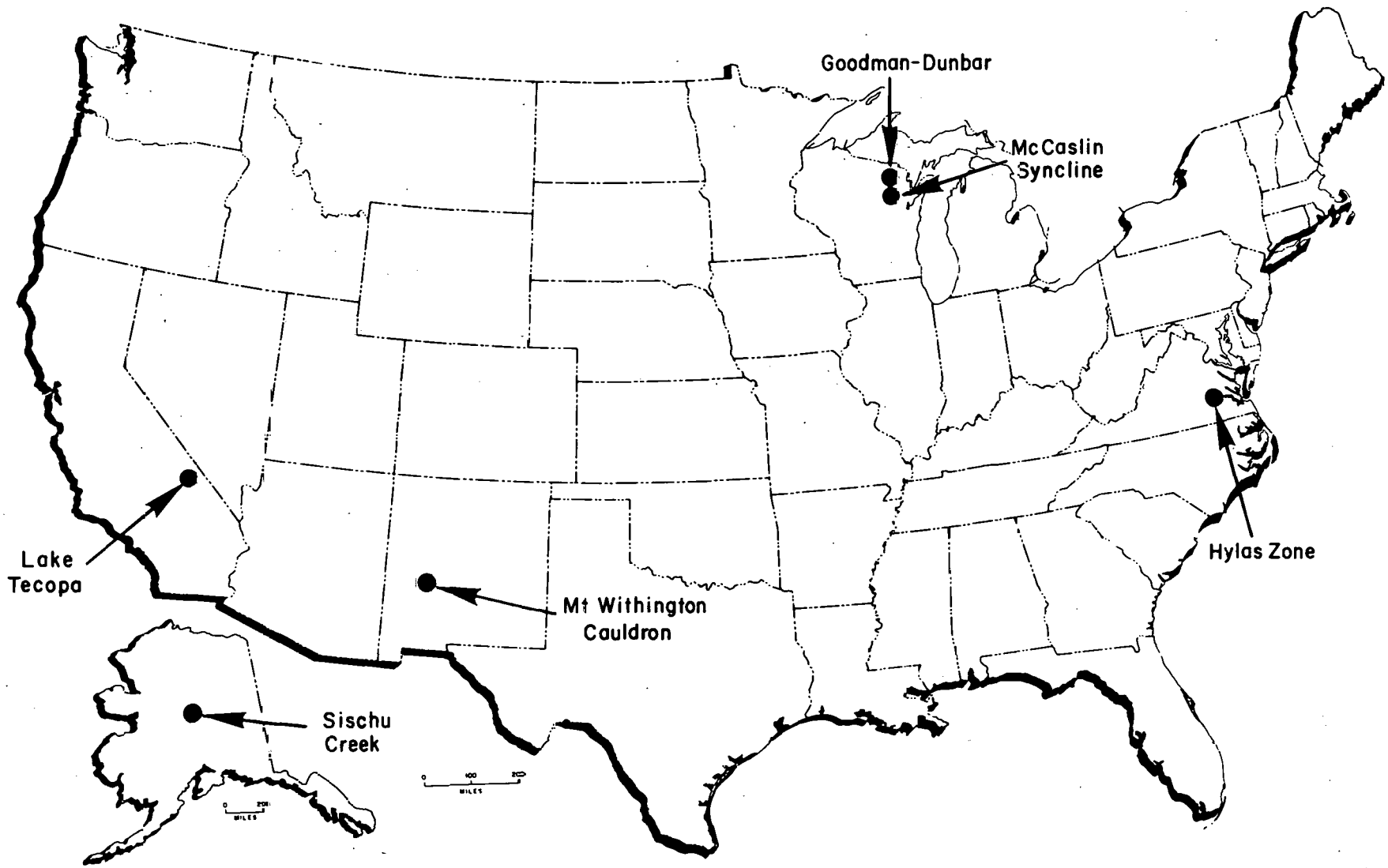

Locations of investigations included in this report.

CONTENTS

CONTENTS (Continued)

CONTENTS (Continued)

CONTENTS (Continued)

CONTENTS (Continued)

I. EVALUATION OF URANIUM ANOMALIES IN THE HYLAS ZONE AND NORTHERN RICHMOND BASIN, EAST-CENTRAL VIRGINIA

Thomas A. Baillieul
and J. J. Dexter

June 1982

BENDIX FIELD ENGINEERING CORPORATION
Grand Junction Operations
Grand Junction, Colorado 81502

INTRODUCTION

The Hylas Zone, a northeast-trending belt of mylonite and ultramylonite, lies in the eastern Piedmont Province of Virginia and borders the northern end of the Richmond Basin (Fig. I-1). The north-trending Richmond Basin is 58 km long and a maximum of 16 km wide. Early indications of anomalous uranium concentrations in the region came from discussions with Jan Krason, GeoExplorers International, Denver, who had worked in the area. Examination of aerial radiometric data (Geodata International, 1975) and HSSR data (Cook, 1981) indicated anomalous values of uranium in the area northwest of Richmond. During June 1981, a 5-day trip to the Hylas area was undertaken to collect rock and ground-water samples and to identify possible source and host rocks of uranium.

METHODS

Field measurements were taken with a portable scintillometer (Mt. Sopris SC-132) and a four-channel gamma-ray spectrometer (Scintrex GAD-6) (Table I-1). Rock samples were analyzed by gamma-ray spectroscopy for potassium, equivalent uranium, and equivalent thorium, and for uranium content by fluorometry (reported as U_3O_8) (Table I-2). Analyses of 35 additional elements by emission spectroscopy are shown in Table I-3. Selected rock samples were also examined in thin section. Ground-water samples were analyzed in the field for radon content using a TSA-RE350 emanometer, for Eh and pH using an Orion Research 407 A/F specific ion meter, and for dissolved CO_2 content by titration. Ground-water data (Table I-4) were examined using the WATEQF computer program. This program is used to calculate chemical equilibria in natural waters. The WATEQF program uses ground-water data to distribute the total concentration of ions among all the known associated and unassociated ions, according to their equilibrium constants. This is accomplished by iteration and correction of the free concentration, ionic strength, and activity coefficients for each successive cycle. The output provides information on the speciation of the dissolved chemical elements, as well as on the state of saturation of the water with respect to solid minerals and compounds (Bloch, 1979).

ACKNOWLEDGMENTS

We thank the Vulcan Materials Company and Luck Quarries, Inc., for permission to visit their operations and to collect samples. Maureen Eatough (BFEC) provided petrographic analyses of the rock samples. The BFEC Data Analysis group assisted with evaluation of water data.

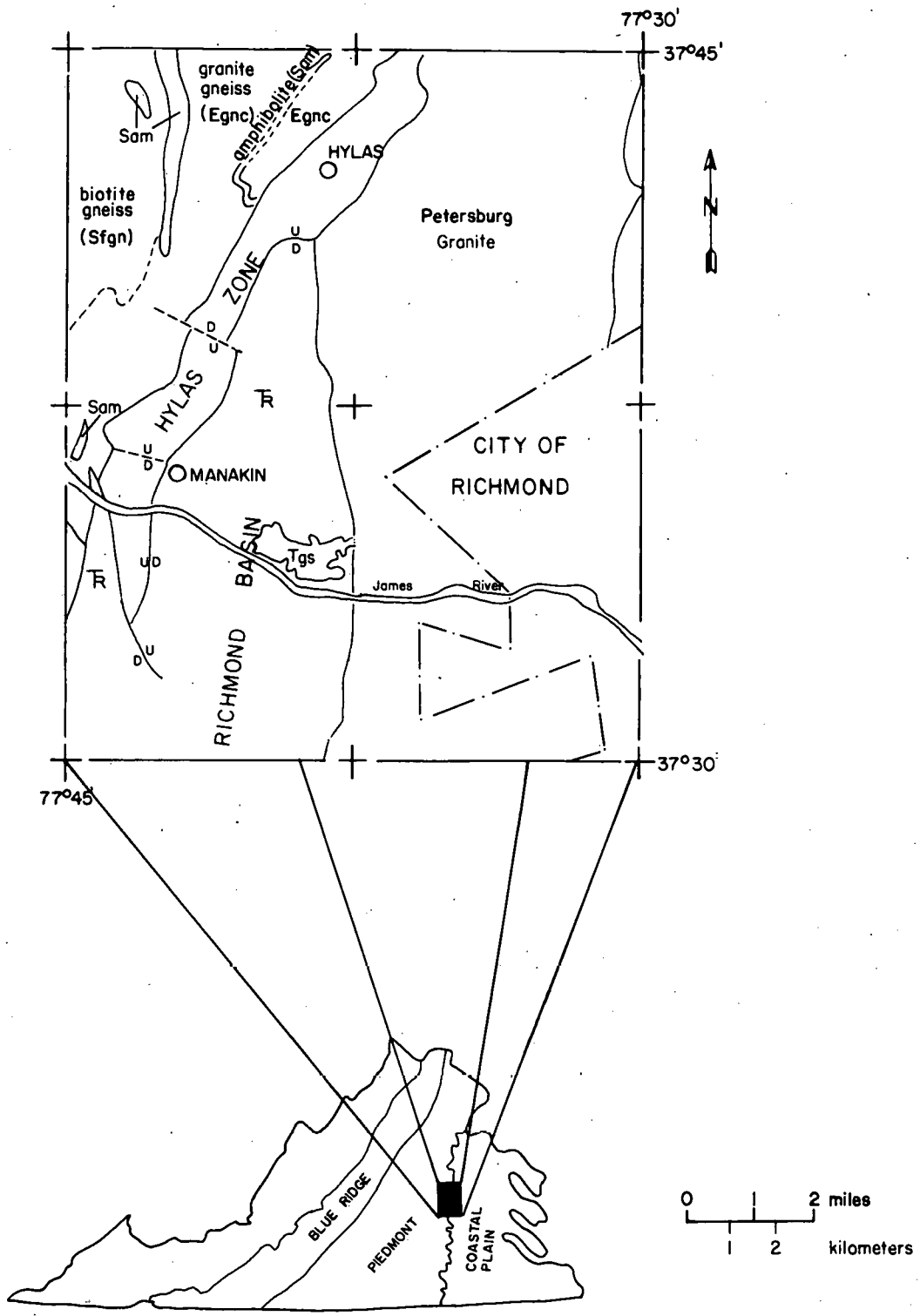

Figure I-1. Location map and general geology of the Hylas Zone/Richmond Basin area. Sfgn = State Farm Gneiss; Egnc = Eastern gneiss complex; Sam = Sabot amphibolite; TR = Triassic rocks of the Richmond Basin; Tgs = Tertiary sands and gravels. Geology simplified from Bobyarchick (1976) and Goodwin (1970).

TABLE I-1. GAMMA-RAY SURVEY *

Location/Description	Total Count (cps)	K (cps)	U (cps)	Th (cps)	K(%)	eU (ppm)	eTh (ppm)	Th/U
LUCK QUARRY								
Mylonite	550.4	17.8	6.5	3.3	3.8	13.7	24.8	1.8
Mylonite	528.0	18.4	5.9	2.5	4.2	13.3	18.4	1.4
Mylonite	527.1	18.5	6.0	2.7	4.2	13.3	20.0	1.5
Breccia	515.3	17.5	5.4	2.4	4.1	12.0	17.7	1.5
BOSCOBEL QUARRY								
Pegmatite	1,606.2	67.6	58.9	5.3	4.0	203.5	30.1	0.15
Pegmatite	1,079.1	43.1	33.7	4.1	5.1	97.0	24.3	0.25
Pegmatite	1,566.0	63.3	53.0	5.4	6.6	154.7	29.8	0.19
Mylonite	631.3	26.3	10.6	3.5	5.5	26.0	25.2	1.0
Mylonite	617.6	25.7	7.8	3.6	6.0	17.1	26.7	1.6
Mylonite contact with tourmaline schist	669.6	25.9	12.7	3.3	4.9	33.0	23.1	0.7
Mylonite contact with tourmaline schist	682.9	26.9	11.5	2.6	5.5	30.6	17.7	0.6
Pegmatite	4,321.5	99.0	89.2	22.1	7.7	235.4	156.6	0.1
Pegmatite	1,963.8	77.1	78.7	5.2	4.7	235.5	21.8	0.1
'Average' pegmatite	1,026.3	39.3	28.7	4.0	5.1	81.6	24.7	0.3
'Average' gray granite	755.4	26.5	15.7	3.2	4.3	42.6	21.6	0.5
TRIASSIC ROCKS**								
Coaly shale	444.8	12.2	2.3	1.7	3.2	3.7	12.9	3.5
Coaly shale	499.4	17.0	5.8	3.1	3.9	9.4	23.6	2.5
Upper gray sandstone	426.6	11.4	3.9	1.6	2.5	8.9	11.8	1.3
Lower gray sandstone/shale	399.4	7.7	2.6	1.5	1.7	5.1	11.4	2.2

*Instrument: Scintrex GAD-6
**Shown in Figure 3

TABLE I-2. GEOCHEMICAL RESULTS OF ROCK SAMPLES: KUT AND CHEMICAL URANIUM

Sample No.	% Potassium K by K40	Uranium (ppm) Equiv. U by Bi214	Thorium (ppm) Equiv. Th by Tl208	U_3O_8 (ppm) Fluorometric	Rock Type
MFT-626	3.74 ± 0.99	15.0 ± 0.3	14.0 ± 1.2	29	Mylonite
MFT-627	4.41 ± 1.18	5.0 ± 0.1	36.0 ± 0.2	3	Mylonite
MFT-628	4.67 ± 1.25	5.0 ± 0.2	26.0 ± 0.7	3	Quartz monzonite porphyry
MFT-653	5.89 ± 0.77	369.0 ± 40.4	7.0 ± 3.3	450	Pegmatite
MFT-654	1.03 ± 0.29	5.0 ± 0.4	17.0 ± 1.1	3	Tourmaline schist
MFT-655	--	--	--	5	Coaly shale
MFT-656	--	--	--	19	Feldspathic wacke
MFT-659	1.50 ± 0.42	3.0 ± 0.7	9.0 ± 1.8	1	Protomylonite granite-breccia

TABLE I-3. EMISSION SPECTROSCOPY SEMIQUANTITATIVE ANALYSIS

Concentration in ppm

Sample No.	Ag	Al	As	B	Ba	Be	Bi	Ca	Cd	CO	Cr	Cu	Fe	K	La	Li	Mg
MFT-626	<5	64,000	<40	5	570	4	<1	12,000	<10	<2	<1	2	11,000	30,000	<40	<10	4,100
MFT-627	<5	62,000	<40	9	660	3	<1	7,000	<10	<2	<1	22	12,000	36,000	<40	<10	3,400
MFT-628	<5	62,000	<40	7	540	7	<1	3,000	<10	<2	<1	26	10,000	37,000	<40	<10	2,900
MFT-653	<5	71,000	<40	52	240	4	<1	19,000	<10	<2	<1	<1	7,700	49,000	<40	<10	3,200
MFT-654	<5	120,000	<40	>20,000	100	5	<1	9,500	<10	36	160	150	69,000	14,000	<40	<10	20,000
MFT-655	<5	62,000	<40	56	420	10	<1	10,000	<10	18	85	66	32,000	42,000	89	210	10,000
MFT-656	<5	69,000	<40	24	410	4	<1	7,600	<10	<2	<1	<1	9,800	34,000	<40	<10	2,900
MFT-659	<5	65,000	<40	120	250	6	<1	3,000	<10	<2	<1	<1	11,000	12,000	<40	<10	4,300

Sample No.	Mn	Mo	Na	Nb	Ni	P	Pb	Sb	Sc	Si	Sn	Sr	Ti	V	W	Y	Zn	Zr
MFT-626	460	<10	16,000	<10	<1	540	36	<200	<1	310,000	<1	200	1,200	<10	<50	<5	<50	39
MFT-627	470	<10	17,000	<10	<1	550	35	<200	<1	330,000	<1	160	1,100	<10	<50	<5	<50	50
MFT-628	280	<10	18,000	<10	<1	530	25	<200	<1	310,000	<1	180	1,000	<10	<50	<5	<50	69
MFT-653	1,200	<10	14,000	<10	<1	5,100	55	<200	<1	300,000	<1	77	<300	<10	<50	51	<50	16
MFT-654	710	52	14,000	18	110	1,500	27	<200	26	190,000	<1	150	9,400	210	<50	29	230	340
MFT-655	970	<10	7,200	52	41	4,200	<10	500	18	240,000	<1	150	5,400	110	200	30	96	100
MFT-656	1,300	<10	20,000	<10	<1	320	55	<200	<1	340,000	<1	100	520	<10	<50	14	<50	<10
MFT-659	110	<10	19,000	<10	4	370	29	<200	<1	350,000	<1	86	1,600	<10	<50	<5	54	87

TABLE I-4. GROUND-WATER SAMPLES

Sample No.	Location		Temperature (°C)	Filtered/ Unfiltered (pH)	Filtered/ Unfiltered Eh(+mV)	Radon (pCi/l)	CO_2 (ppm)
	Lat.	Long.					
MFT-629	37°36'08"	77°42'40"	19	6.9/6.0	158/185	5,280	25.5
MFT-630	37°35'56"	77°42'57"	24	7.2/7.0	155/174	4,015	7.5
MFT-631	37°36'09"	77°42'10"	24	7.5/7.5	110/130	91	21.0
MFT-632	37°36'31"	77°42'10"	22	6.6/6.5	155/155	2,761	53.5
MFT-633	37°36'18"	77°41'45"	20	6.3/5.9	179/177	769	87.5
MFT-634	37°37'19"	77°41'48"	24	7.4/7.3	109/132	290	11.5
MFT-635	37°37'08"	77°41'19"	18	6.2/5.9	161/172	619	61.0
MFT-636	37°37'55"	77°40'50"	17	6.7/6.5	161/155	454	53.5
MFT-637	37°38'34"	77°40'41"	22	6.6/6.5	164/170	2,262	38.0
MFT-638	37°40'00"	77°40'10"	19	7.1/6.9	140/145	1,142	53.5
MFT-639	37°39'59"	77°40'43"	26	6.5/6.4	182/170	1,640	33.5
MFT-640	37°39'51"	77°39'19"	26	8.4/8.1	110/105	280	0
MFT-641	37°40'28"	77°39'58"	20	6.3/6.2	135/141	501	47.0
MFT-642	37°40'42"	77°40'19"	20	7.3/7.0	150/150	452	11.0
MFT-643	37°40'48"	77°39'43"	20	6.6/6.9	139/160	779	90.0
MFT-644	37°41'25"	77°39'54"	18.5	6.2/5.9	168/183	885	72.0
MFT-645	37°42'14"	77°39'01"	18.5	6.1/6.1	175/171	640	40.5
MFT-646	37°42'24"	77°38'58"	17	7.3/7.0	90/ 59	213	30.5
MFT-647	37°41'41"	77°38'27"	25	6.7/6.5	80/ 98	563	79.0
MFT-648	37°40'52"	77°38'26"	21	7.4/7.4	115/118	718	20.0
MFT-649	37°40'42"	77°38'11"	23	6.4/6.3	186/192	525	55.5
MFT-650	37°39'47"	77°38'15"	18	5.8/5.7	191/191	2,458	67.0
MFT-651	37°39'40"	77°38'23"	20	6.4/6.1	160/187	6,505	35.0
MFT-652	37°39'38"	77°38'38"	22	6.8/6.4	170/184	1,077	55.5
MFT-657	37°38'53"	77°38'27"	20	- /6.2	- /158	609	48.5
MFT-658	37°38'07"	77°37'47"	21	- /5.9	- /176	1,377	74.5

TABLE I-4. GROUND-WATER SAMPLES (continued)

Sample No.	U_3O_8 (ppb)	Ca (ppm)	Mg (ppm)	K (ppm)	Na (ppm)	Cl (ppm)	SO_4 (ppm)	PO_4 (ppm)	F (ppm)	NO_3 (ppm)	Si (ppm)	Fe (ppb)	Mn (ppb)	V (ppb)	Al (ppb)	Cu (ppb)	Pb (ppb)	Zn (ppb)	SiO_2 (ppm)
MFT-629	<1	0.8	0.8	2.7	9.5	5	<1	<1	<1	47	15	19	7	<2	23	110	82	135	32
MFT-630	107	16.0	5.9	1.3	20.0	17	<1	2	<1	16	13	27	34	31	7	274	970	100	28
MFT-631	4	27.2	2.2	1.2	34.0	11	30	<1	<1	4	13	8	13	53	8	30	15	1,200	28
MFT-632	<1	0.4	0.6	0.9	6.5	3	2	<1	<1	5	10	31	4	<2	9	114	6	139	21
MFT-633	<1	1.0	0.8	1.0	4.4	3	14	9	<1	15	8	15	19	<2	13	480	26	102	17
MFT-634	<1	25.1	1.1	2.2	36.0	75	8	54	<1	<1	10	31	11	33	3	17	<2	123	21
MFT-635	<1	0.7	0.8	0.4	8.7	11	2	<1	<1	42	7	27	15	<2	7	31	4	81	15
MFT-636	<1	4.4	1.8	1.0	10.2	6	<1	<1	<1	66	16	94	3	4	11	422	5	88	34
MFT-637	<1	1.0	0.9	3.1	6.1	2	<1	<1	<1	19	9	23	20	<2	11	319	11	83	19
MFT-638	<1	18.2	10.0	0.6	28.0	54	15	<1	<1	2	21	23	29	15	6	302	<2	10	45
MFT-639	<1	0.6	0.9	0.9	4.2	4	2	<1	<1	11	8	11	1	<2	5	522	<2	32	17
MFT-640	<1	1.7	3.1	0.2	69.0	24	8	<1	<1	2	5	15	3	3	5	15	<2	5	11
MFT-641	<1	0.4	1.0	0.8	10.3	5	9	5	<1	8	13	115	46	<2	4	179	4	99	28
MFT-642	<1	4.8	2.3	0.7	21.0	14	9	<1	<1	9	4	5	<1	5	4	398	<2	14	8.6
MFT-643	<1	12.5	3.3	0.7	6.0	2	6	<1	<1	<1	8	8	190	23	5	38	<2	144	17
MFT-644	<1	0.7	0.6	2.1	8.4	6	<1	<1	<1	60	9	147	8	<2	4	147	3	58	19
MFT-645	<1	1.7	2.0	2.8	10.5	11	5	3	<1	15	8	16	9	<2	7	155	11	54	17
MFT-646	<1	11.4	6.8	3.8	20.0	2	4	<1	<1	56	22	1,179	230	13	23	13	2	577	47
MFT-647	<1	1.0	6.9	2.3	22.0	16	18	<1	<1	2	18	3,256	166	4	11	15	7	81	38
MFT-648	<1	1.2	3.4	1.5	4.0	1	6	2	<1	2	10	91	27	4	3	11	<2	58	21
MFT-649	<1	1.0	0.3	0.8	3.8	3	7	<1	<1	244	8	46	7	<2	<2	673	<2	276	17
MFT-650	<1	7.3	7.1	4.2	26.0	18	3	<1	<1	94	11	88	41	14	12	142	6	130	23
MFT-651	<1	0.8	0.9	1.0	9.1	6	<1	<1	<1	36	12	38	4	<2	7	32	<2	292	26
MFT-652	<1	2.5	8.4	1.2	31.0	22	25	<1	<1	25	13	78	33	13	9	590	<2	248	28
*MFT-657	<1	0.8	1.8	2.5	6.2	8	6	<1	<1	59	7	125	14	<2	7	268	<2	30	15
*MFT-658	<1	1.3	1.4	1.8	25.0	12	2	<1	<1	17	16	30	17	4	12	1,339	6	23	34

*Not filtered in field.

GEOLOGIC SETTING

Rocks in the study area range in age from Middle Proterozoic to Mesozoic (Pl. 1). Precambrian rocks are highly deformed granite gneiss, biotite gneiss, and amphibolite. A granitic pluton intrusive into gneiss west of the study area has been dated by the Rb-Sr whole rock method at 1 b.y. (Glover and others, 1978).

The northeast-trending Hylas tectonic zone is 21 km long (Fig. I-1) and consists of mylonitized Precambrian rocks. The zone formed during late Paleozoic time as a result of northwesterly directed thrusting. The Petersburg Granite was apparently thrust over felsic gneiss and amphibolite. This resulted in the formation of cataclastic foliations and associated intrafolial folds (Bobyarchick, 1976). Retrograde metamorphism, synchronous with the shearing event, is particularly intense in areas of fracturing and brecciation. Pegmatite is concordant with the cataclastic foliation and appears to have been intruded after the shearing event. The Hylas Zone is covered by Tertiary sediments to the northeast and underlies the Richmond Basin to the southwest. The cataclastic foliation of the zone has an average regional dip of 40° to the east and a zonal thickness of 1.6 km (Bobyarchick, 1976). Because of the fine-grained texture of the mylonite and the low metamorphic grade, early investigators correlated the rocks with metavolcanic units of the Carolina slate belt (Brown, 1937; Goodwin, 1970). A detailed description of the mylonite was given by Bobyarchick (1976).

The Petersburg Granite, which intruded the Precambrian terrane, has a U/Pb zircon date of 330±8 m.y. (Wright and others, 1975) and a Rb/Sr date of 380 m.y. (D. Mose, oral comm.). Although the Petersburg Granite previously was thought to be nearly homogeneous, composed of at most three distinct phases, workers in the past 12 years have shown the granite to be very heterogeneous (Condit, 1970; Dickey, 1970; Huber, 1972; Simpson, 1971; Goodwin, 1969). Textures range from equigranular to porphyritic and from pegmatitic to aplitic. Composition varies from granitic to gabbroic (Goodwin, 1969). The Petersburg Granite near the Hylas Zone is predominantly a coarse-grained, muscovite-biotite granite. Quartz monzonite and quartz monzonite porphyry are present near the northeast end of the Richmond Basin. Granite porphyry is gradational into relatively equigranular or microphaneritic granite (Bobyarchick, 1976). The Petersburg Granite is assumed to have been emplaced during a period of prograde metamorphism. Weak to moderate metamorphic foliation has been developed locally in the granite.

The western boundary of the Richmond Basin is a major northeast-trending normal fault offset by later northwest-trending normal faults. Triassic sedimentary rocks fill the basin, and along the eastern margin of the basin they rest unconformably on the Petersburg Granite. Coarse conglomerate and sandstone are adjacent to the western border fault; minor conglomerate is discontinuous along the eastern basin margin. Basinward, the sediments become finer grained. Coal has been produced from thin seams in the Richmond Basin.

Fracturing and northeast-oriented high-angle faulting began about 221 m.y. ago and was intermittently active throughout deposition of fanglomerate and arkose in the Richmond Basin during Late Triassic time. Northwest-oriented fractures (joints) and faults are thought to be of Jurassic age (Bobyarchick, 1976).

RESULTS OF FIELD INVESTIGATIONS

South of the town of Hylas, several stone quarries are in operation within the mylonite zone. In the Luck and Royal quarries, the mylonite is gray and highly foliated. The cataclastic foliation is deformed into broad, open folds and is locally disrupted along minor faults. Individual layers show a broad range of textures. Coarser grained laminae have augen of feldspar; pyrite is present locally.

One sample of mylonite (MFT-627) was collected less than 0.4 km west of the Hylas Zone-Petersburg Granite contact, and another sample (MFT-626) was collected approximately 0.8 km west of the contact (Pl. 1). Both samples are granitic in composition. The sample closer to the contact has more recrystallization textures, whereas the more distant sample has a very strong fluxion structure. In the cataclastic mortar of MFT-626, traces of uraninite euhedra are found associated with zircon and pyrite, and traces of thorium-calcium phosphate are found associated with galena. In MFT-627, thorium-bearing monazite was detected in trace amounts within the mortar.

In general, the mylonite has a uniform radiometric character; radioactivity is about twice the regional background. Field gamma-ray assays reveal a range of 12 to 14 ppm equivalent uranium (eU) and 18 to 25 ppm equivalent thorium (eTh) (Table I-1).

In the southern part of the Royal quarry (Pl. 1), pieces of gray granite occur as float. In hand specimen, the gray granite consists of quartz, feldspar, muscovite, and minor garnet. This granite is similar in appearance to the gray granite common in the Boscobel quarry (MFT-659; Pl. 1). The "Boscobel" granite is sheared and commonly interlayered with younger pegmatite. Petrographic examination indicates that MFT-659 is a protomylonitic granite with a complex history. At least five distinct events are indicated in thin section: 1) crystallization, 2) metamorphism (cohesive portions contain garnet and display a mosaic-interlock texture), 3) brecciation, 4) cataclasis, and 5) later infilling of open fractures with calcite. Chemical analysis of the protomylonite sample yields 3 ppm eU and 9 ppm eTh. Traces of potassium-uranyl-silicate and pyrite were identified in the mortar.

Pegmatite that intruded the protomylonitic granite is common in the Boscobel quarry. Along the north wall of the quarry, field gamma-ray assays indicate a range of 95 to 200 ppm eU and 25 to 30 ppm eTh within this younger, pink pegmatite. A sample of this pegmatite (MFT-653) yielded 369±40 ppm eU, 450 ppm U_3O_8, and 7±3 ppm eTh. No uranium minerals were identified petrographically. On the south wall of the Boscobel quarry, pegmatite cuts the protomylonitic granite and is exposed over an area of 25 m^2 (Fig. I-2). Overall, the pegmatite displays radioactivity 5 to 10 times background. Spectrometer and scintillometer readings obtained in the field show that most of the pegmatite contains approximately 80 ppm eU and 25 ppm eTh. The most radioactive zone in the pegmatite on this wall contains 235 ppm eU and 156 ppm eTh. Pegmatites (pegmatite zones?) have been mapped by Bobyarchick (1976) and are shown on Plate 1.

An outcrop of Petersburg Granite occurs on the northeast flank of the Richmond Basin. Both foliated and nonfoliated rocks are evident in this

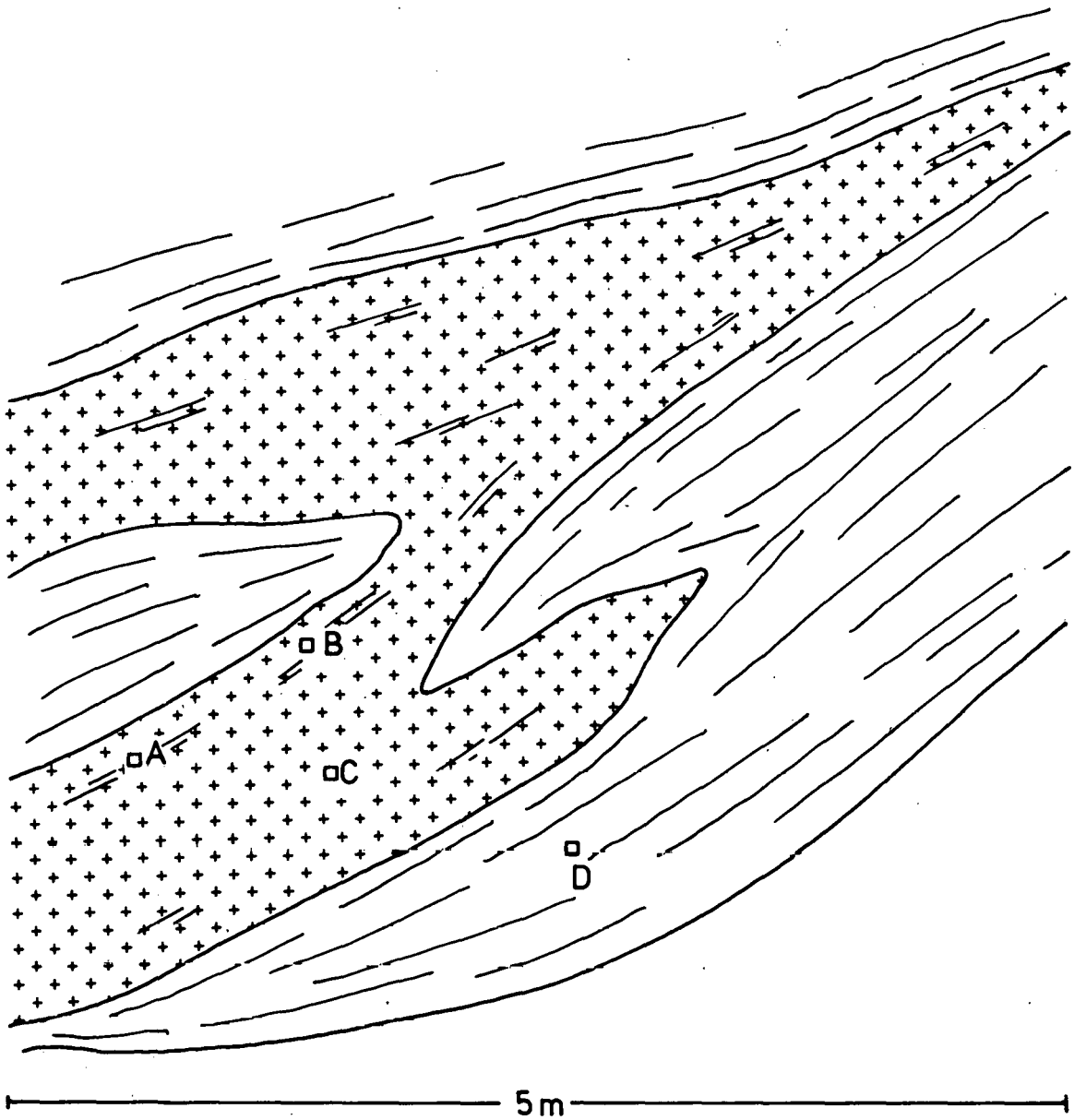

Figure I-2. Pegmatite (pattern) intrusive into protomylonitic granite at the Boscobel quarry. Field measurements are: A) 235 ppm eU, 157 ppm eTh; B) 235 ppm eU, 22 ppm eTh; C) 82 ppm eU, 25 ppm eTh; and D) 43 ppm eU, 22 ppm eTh.

outcrop, and compositional variations have been mapped by Goodwin (1970). A sample of coarse-grained, nonfoliated quartz monzonite porphyry was collected from this outcrop (MFT-628). Thorium-bearing monazite and thorium-silico-phosphate were identified in trace amounts as inclusions in quartz. This sample contained 5 ppm eU and 26 ppm eTh.

Triassic rocks of the Richmond Basin range from coarse boulder conglomerate along the western basin margin to sandstone and shale with interlayered coal toward the basin center. The conglomerate was seen only in a highly weathered exposure. Here, boulders and cobbles of medium-grained Petersburg-type granite are in a highly micaceous, fine-grained matrix. A cut near the Boscobel quarry exposes finer grained Triassic sediments. A seam of coaly shale about 1 m thick lies between two medium-grained, gray sandstones (Fig. I-3). The coaly shale has abundant pyrite. The lower sandstone unit (dominantly feldspathic wacke) contains some carbonaceous shale. Field gamma-ray assays of these rocks show an average of 6.5 ppm eU and an average of 18.5 ppm eTh in the coaly shale and 5 ppm eU and 11 ppm eTh in the lower gray sandstone.

Ground water was collected across the Hylas mylonite zone and the northern portion of the Richmond Basin. Ground waters throughout the area generally display a uniform, slightly acidic-to-neutral pH and an Eh of +100 mV to +190 mV. Dissolved carbonate and radon contents vary considerably but cannot be related to a specific rock type. Radon-gas content ranges from a low of 91 pico-Curies/liter (pCi/l) to a high of 6,505 pCi/l.

Only two well-water samples contained detectable (>1 ppb) uranium: MFT-630 (107 ppb) and MFT-631 (4 ppb). These samples were collected just east of the Boscobel quarry in Triassic sediments.

Ouput from the WATEQF program shows that the saturation index (defined as the ion activity product divided by the true thermodynamic solubility constant) with respect to 12 different uranium minerals is much less than zero for all ground-water samples. This indicates that ground water in the vicinity of sample locations is undersaturated with respect to the 12 uranium minerals and therefore is capable of dissolving these minerals (Bloch, 1979).

CONCLUSIONS

1. Radon values in ground water from the Hylas Zone and the adjacent Richmond Basin are anomalous and may indicate nearby uranium-enriched source rocks.

2. Pegmatites, protomylonitic granite, and the Petersburg Granite can be good sources of uranium for ground water. The pegmatites described in this report appear to be the best source rocks because of uranium values ranging from 82 to 235 ppm eU and corresponding low values of Th as well (average Th/U = 0.18). The protomylonitic granite has an average Th/U ratio of 0.5. Additional evidence for the pegmatites and protomlyonitic granite as a source is the anomalous (107 ppb uranium) ground-water sample collected in Triassic sediments just to the east of the Boscobel quarry (see Pl. 1).

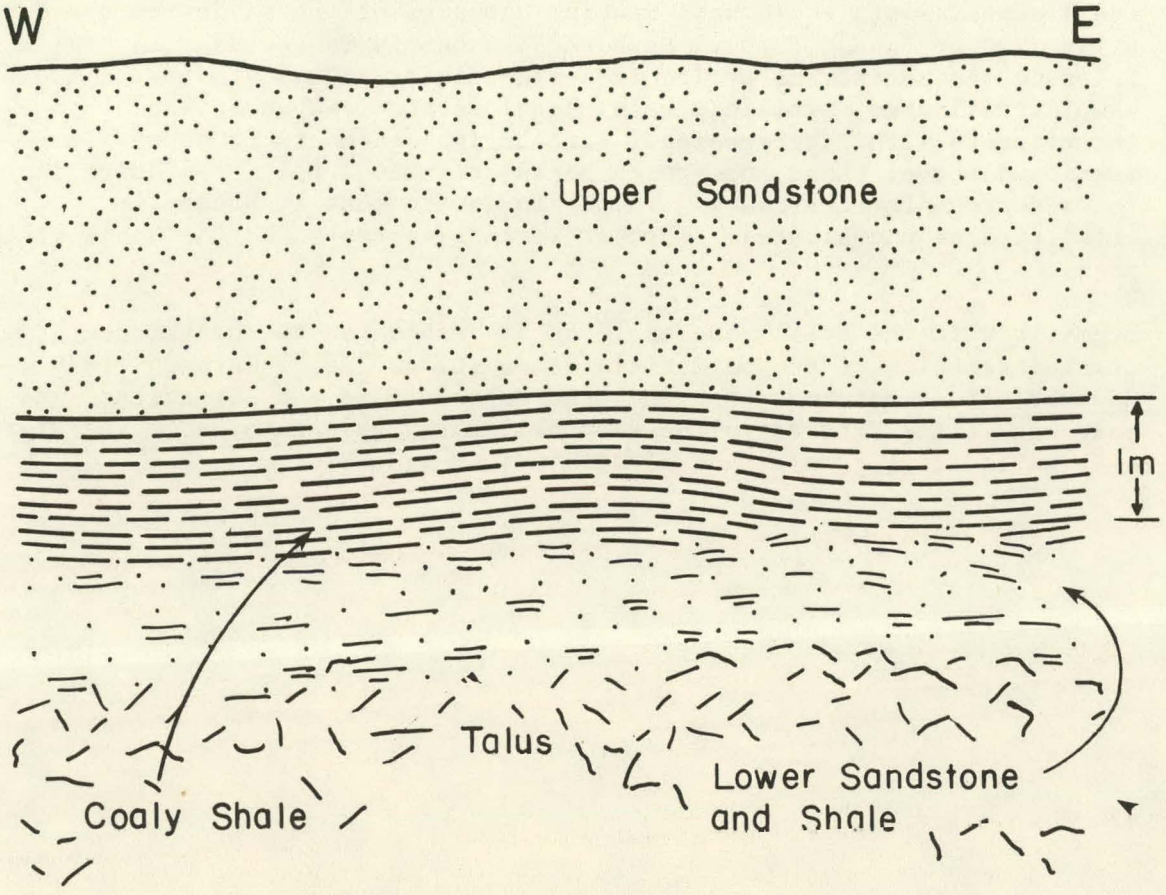

Figure I-3. Triassic sedimentary rocks exposed in a cut adjacent to the Boscobel quarry (MFT-655 was obtained from the lower sandstone and shale unit, and MFT-656 was collected from the coaly shale unit).

Ground-water samples (ranging from 70 to 270 ppb uranium) from southwest Richmond (approximately 19 km southeast of the Hylas Zone) are believed to have originated from a major ground-water system at the contact of the Petersburg Granite and overlying coastal plain sediments (Cook, 1981; Conley, 1978). Thus, the Petersburg Granite may be considered a possible source of uranium available to ground water entering the Richmond Basin.

3. The Richmond Basin could host uranium deposits of the sandstone class (Class 240 of Jones, 1978). Carbonaceous debris is abundant in the Triassic sediments, and pyrite is present in trace amounts in the two samples collected. Triassic basal conglomerate is abundant and interfingers with finer grained, carbon-rich sediments at depth. As mentioned above, there appears to be an adequate supply of uranium in rocks surrounding the basin. The basin environment is presently classified as unevaluated. Further work is warranted on the basis of this study.

4. Pegmatites in the Hylas Zone could be favorable for the occurrence of uranium deposits of the pegmatitic class (Class 320 of Mathews, 1978). However, it is not known how the uranium occurs in the pegmatites, and only pegmatites exposed in the Boscobel quarry were examined. Therefore, this environment remains unevaluated.

REFERENCES

Bobyarchick, A. R., 1976, Tectogenesis of the Hylas Zone and eastern Piedmont near Richmond, Virginia [M.S. thesis]: Blackbury, Virginia Polytechnic Institute, 161 p.

Bloch, Salmon, 1979, Application of WATEQF computer model (Runnels version) to interpretation of hydrogeochemical data from Clinton Quadrangle, west-central Oklahoma: Oklahoma Geology Notes, Oklahoma Geological Survey, v. 39, no. 6, p. 221-228.

Brown, C. B., 1937, Outline of the geology and mineral resources of Goochland County, Virginia: Virginia Geological Survey Bulletin 48, 68 p.

Condit, C. D., 1970, Mineralogy of the Petersburg Granite exposed in the Tidewater Stone Quarry, Richmond, Virginia [abs.]: Virginia Journal of Science, v. 21, no. 3, p. 132.

Conley, J. F., 1978, Geology of the Piedmont in Virginia--Interpretations and problems, in Contributions to Virginia geology--III: Virginia Division of Mineral Resources Publication 7, p. 115-149.

Cook, J. R., 1981, Richmond and northern Eastville 1° x 2° NTMS areas, Virginia, hydrogeochemical and stream sediment reconnaissance: U.S. Department of Energy Open-File Report GJBX-18(81), 17 p. plus microfiche.

Dickey, N., 1970, A preliminary study of mineralogic trends in a portion of the Petersburg Granite, Richmond [abs.]: Virginia Journal of Science, v. 21, no. 3, p. 132.

Geodata International, Inc., 1975, Aerial radiometric and magnetic survey of central Appalachian Triassic basins--parts of Virginia and the Carolinas: U.S. Energy Research and Development Administration Open-File Report GJO-1644, v. I and II.

Glover, Lynn, III, Mose, D. G., Poland, F. B., Bobyarchick, A. R., and Bourland, W. C., 1978, Grenville basement in the eastern Piedmont of Virginia [abs.]: Geological Society of America Abstracts with Programs, v. 10, no. 10, p. 169.

Goodwin, B. W., 1969, The typical(?) Petersburg Granite [abs.]: Virginia Journal of Science, v. 20, no. 3, p. 125.

-----1970, Geology of the Hylas and Midlothian Quadrangles, Virginia: Virginia Division of Mineral Resources Report of Investigations 23, 51 p., 2 plates, scale 1:24,000.

Huber, D. R., 1972, Petrologic aspects of a complex area in the Petersburg Granite at Richmond, Virginia [abs.]: Virginia Journal of Science, v. 23, no. 3, p. 135.

Jones, C. A., 1978, A classification of uranium deposits in sedimentary rocks, in Mickle, D. G., ed., A preliminary classification of uranium deposits: U.S. Department of Energy Open-File Report GJBX-63(78), p. 1-16.

Mathews, G. W., 1978, Uranium occurrences in and related to plutonic igneous rocks, in Mickle, D. G., and Mathews, G. W., eds., Geologic characteristics of environments favorable for uranium deposits: U.S. Department of Energy Open-File Report GJBX-67(78), p. 121-180.

Mickle, D. G., and Mathews, G. W., eds., 1978, Geologic characteristics of environments favorable for uranium deposits: U.S. Department of Energy Open-File Report GJBX-67(78), 250 p.

Simpson, M. C., 1971, Textural variations within the Petersburg Granite in Richmond, Virginia: Virginia Journal of Science, v. 22, no. 3, p. 123.

Wright, J. E., Sinha, A. K., and Glover, L., 1975, Age of zircons from the Petersburg Granite, Virginia, with comments on belts of plutons in the Piedmont: American Journal of Science, v. 275, p. 848-856.

II. EVALUATION OF RADIOACTIVITY ANOMALIES IN THE SISCHU CREEK AREA, CENTRAL ALASKA

W. A. Girdley, J. R. Anderson, and W. G. Farley
Bendix Field Engineering Corporation

and

W. A. Roberts
U.S. Department of Energy

June 1981

BENDIX FIELD ENGINEERING CORPORATION
Grand Junction Operations
Grand Junction, Colorado 81502

INTRODUCTION

BACKGROUND

Aerial gamma-ray spectrometer surveys conducted in 1978 during the field investigation phase of the Mount McKinley Quadrangle evaluation (Hinderman, 1981) indicated uranium and thorium anomalies northwest of Lake Minchumina. These anomalies were traced into the adjacent Kantishna River Quadrangle, where ground followup led to discovery of secondary uranium minerals consisting of disseminated grains and fracture coatings in rhyolitic rocks (VABM Corner occurrence; Hinderman, 1981, p. 13). Selected samples contained from 0.1% to 0.5% U_3O_8.

Reconnaissance and detailed airborne gamma-ray spectrometer and magnetometer surveys conducted in 1979 detected both uranium and thorium anomalies (Western Geophysical, 1980a, 1980b, 1980c, 1980d). A detailed survey centered approximately over the adjoining corners of the Ruby, Kantishna River, Mount McKinley, and Medfra Quadrangles (Fig. II-1) consisted of 24 north-south flight lines at 1-mi spacing and eight east-west tie lines at 3-mi spacing. Equivalent-uranium values derived from this survey are not very large, but poor outcrops, high soil moisture, and moderate-to-heavy vegetation tend to make any anomalous responses significant.

Some of the anomalies from the survey were checked in the field by Anderson, Girdley, and Roberts during a 3-day period in June 1980. This report presents the data resulting from that examination, as well as an interpretation by Farley of radiometric and magnetic data from the detailed survey.

LOCATION

The anomalies are near the common corner of the Ruby, Medfra, Mount McKinley, and Kantishna River 1° x 3° NTMS Quadrangles in the Sischu Creek area approximately 30 km northwest of Lake Minchumina (Fig. II-2). The anomalies lie mainly between the Sethkokna River and North Fork of the Kuskokwim River.

GEOLOGIC SETTING

The anomalous rocks are part of a narrow belt of siliceous volcanic and intrusive rocks of Late Cretaceous and early Tertiary age (Fig. II-2) that extends from the Sischu Mountains in the Medfra Quadrangle northeastward into the western half of the Kantishna River Quadrangle. Available geologic maps (Cass, 1959; Reed, 1961; Chapman and others, 1975; Miller and others, 1980) show this belt to be bordered, and possibly underlain, by an assemblage of Paleozoic metamorphic rocks composed mainly of quartzite, schist, greenstone, and carbonate. Bed rock is mostly reflected by locally derived rubble, and up to 30% of the surface is covered by unconsolidated deposits of Pleistocene and Holocene age.

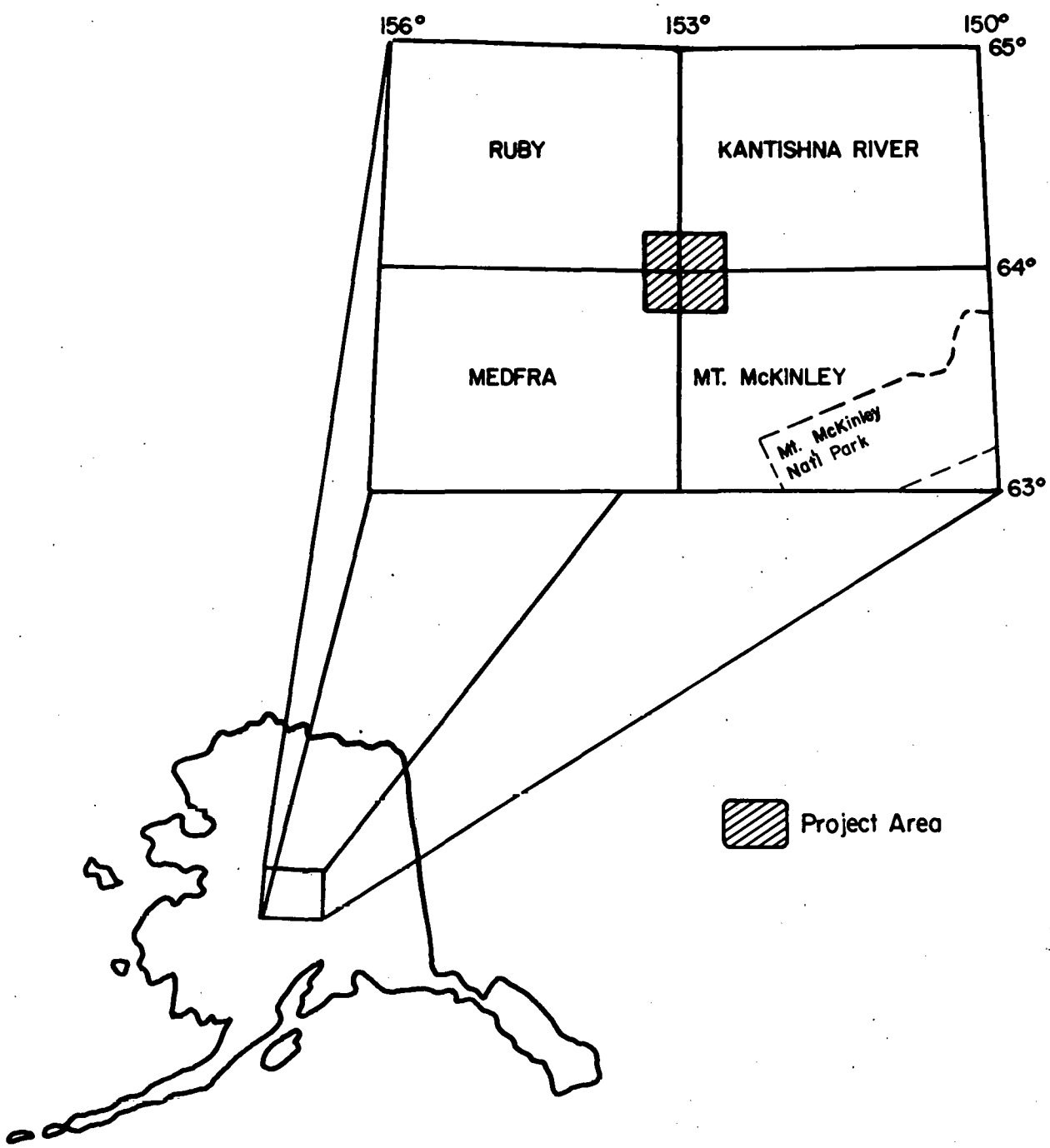

Figure II-1. Project location map showing area of "Four Corners" detailed aerial gamma-ray spectrometer and magnetometer survey.

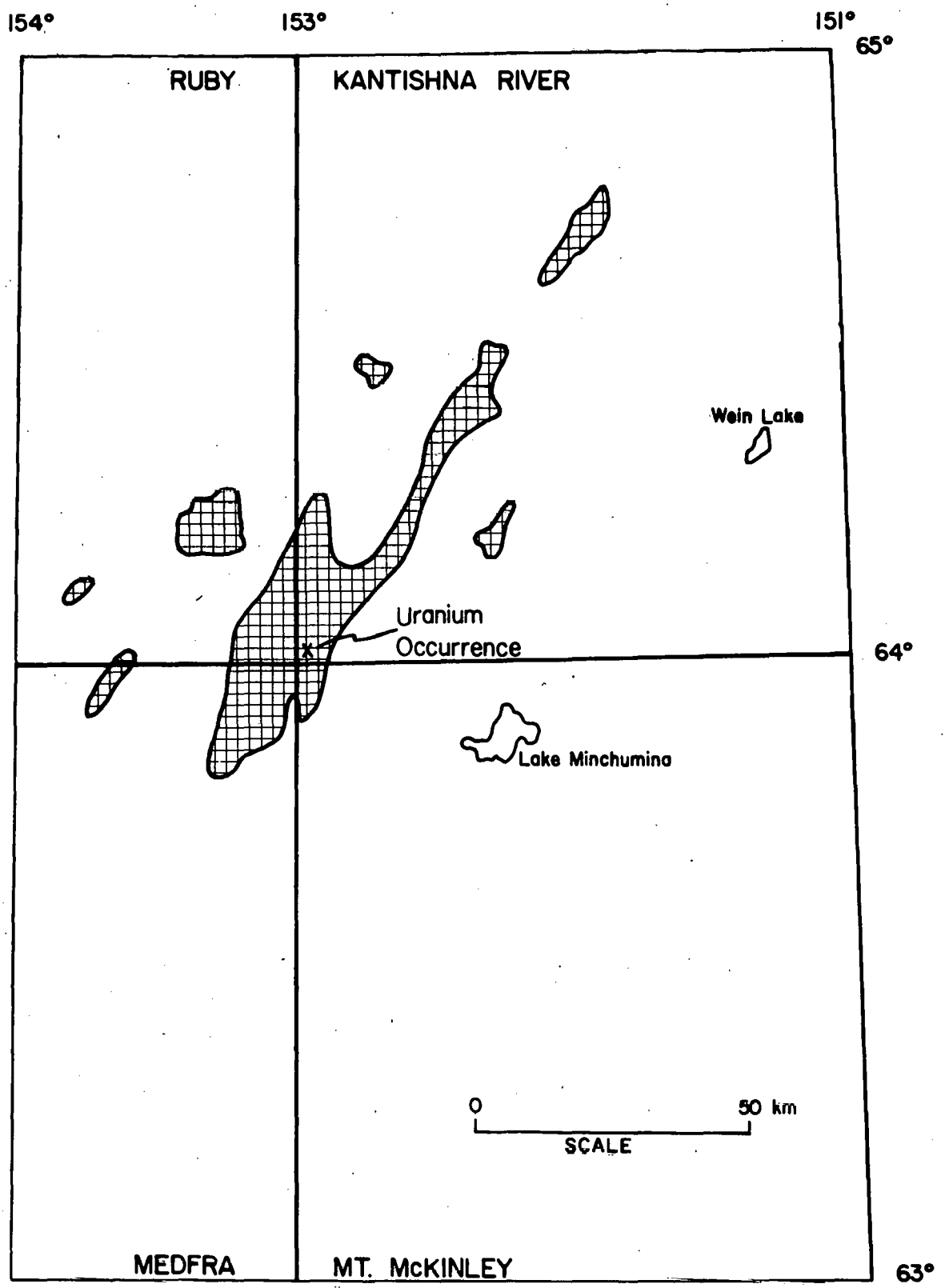

Figure II-2. Areas that include Cretaceous and Tertiary silicic volcanic and related intrusive rocks (generalized from Beikman, 1978).

The Sischu Mountains igneous sequence is part of an extensive, discontinuous volcanic-plutonic terrane that can be traced for almost 800 km from the lower Kuskokwim River to the Arctic Circle (Hinderman, 1981; Miller and others, 1980; Patton and others, 1976). The sequence was found to be strongly radioactive in the Medfra Quadrangle, where it occurs along the axis of a broadly folded syncline mapped by Miller and others (1980). Similar conditions appear to hold where the anomalously radioactive igneous sequence occurs east of Sischu Creek in the Kantishna River Quadrangle.

The Sischu Mountains igneous sequence in the Medfra Quadrangle consists chiefly of rhyolitic and dacitic flows and domes with subordinate tuff, andesite, and basalt (unit Tfv; Miller and others, 1980). Similar rocks are in the southwest corner of the Kantishna River Quadrangle, where the VABM Corner occurrence was found (Unit TKr of Chapman and others, 1975).

The Iditarod-Nixon fault system trends northeast through the adjacent northern corners of the Medfra and Mount McKinley Quadrangles and probably extends into the southwestern Kantishna River Quadrangle. Numerous smaller faults in the area have a similar northeast trend.

METHODS

Anomalies identified from the detailed airborne spectrometer survey were plotted on 1:62,500-scale topographic maps for use in field investigations. Areas selected for field inspection are defined by (1) the principal Bi-214 (eU) and Tl-208 (eTh) anomalies detected in the survey and (or) (2) gross gamma-ray measurements greater than 1,200 counts per second (cps). In addition, priority was given to those anomalies confined mainly to a pronounced magnetic trend (Pl. 2) that appears to define the igneous rock assemblage.

The project area first was reconnoitered by helicopter-borne scintillometer traverses to verify the positions of anomalies defined by the detailed airborne spectrometer survey; subsequently, ground traverses were made in parts of the anomalous areas. Twenty-two specific sites, which consisted largely of rubble crop, were examined and described. Total-count (gross gamma-ray) readings were taken with a hand-held scintillometer (Mt. Sopris 131-A) at each ground station, and spectrometer (geoMetrics 310) measurements for uranium, thorium, and potassium were made at 15 of the 22 sites (Table II-1). Rock samples were collected at seven of the sites (Fig. II-3) for petrographic and geochemical analyses.

Rock samples were submitted to the BFEC laboratory in Grand Junction, Colorado, where the following analyses were performed: petrographic study of thin sections, whole-rock chemistry, fluorometric determination of U_3O_8, and gamma-ray spectroscopic (closed-can) determinations of potassium, uranium, and thorium. Analytical data are presented in Table II-2.

Radiometric and magnetic data collected in the detailed survey were used to produce an interpretative geophysical map (Pl. 2) of the project area. Significance of map features is discussed in the following section.

TABLE II-1. RADIOMETRIC DATA

Station No.	Rock[1] Type	Closed-Can γ-Spec eU(ppm)	eTh(ppm)	K(%)	Th/U	Scintillometer[2] (cps)	Field Spectrometer[3] eU(ppm)	eTh(ppm)	Th/U
M-1	A	25	64	4	2.6	150- 250	15	96	6.4
M-2	A					175- 325	19	104	5.5
M-3	A					200	22	115	5.2
M-4	A					250	25	133	5.3
M-5	A					200	19	96	5.1
M-6	A					100	15	59	3.9
M-7	A	18	105	4	5.8	275	21	129	6.1
M-8	A					400	22	119	5.4
M-9	A	14	96	4	6.8	350	23	130	5.6
M-10	A					350			
M-11	C					100			
K-1	A	30	131	4	4.4	450	32	145	4.5
K-2	A	24	589	2.5	24.5	2,000	37	476	12.8
K-3	B					75	11	60	
K-4	B					75	12	63	
K-5	A	21	127	3.5	6.0	400	30	192	6.4
K-6	A	18	116	3.5	6.4	400	35	168	4.8
K-7	A					400-1,500			
K-8	A								
R-1	C					80			
R-2	D					75			
R-3	D					75			

[1]Field lithologic classification:
A-Rhyolitic rocks
B-Basalt/andesite
C-Tuff
D-Carbonate

[2]Mt. Sopris model 131-A

[3]GeoMetrics model GR-310

Figure II-3. Location map of rock-sample and ground-check sites.

TABLE II-2. ANALYTICAL DATA FROM SELECTED SAMPLES

Station No.	BFEC Sample No.	ppm U_3O_8	% SiO_2	% K_2C	% CaO	% Al_2O_3	% TiO_2	% MgO	% P_2O_5	% FeO	% Fe_2O_3	% Fe	% Na_2O	ppm MnO	Name (Thin-Section)
M-1	MJV 501	42	78.16	5.35	0.11	13.81	0.05	0.06	0.02	<0.10	2.00	1.41	1.05	129	Rhyolite Porphyry
M-7	MJV 502	32	72.59	5.29	0.34	14.68	0.09	0.04	0.02	0.10	2.58	1.88	4.30	232	Rhyolite Porphyry
M-9	MJV 507	19	72.16	5.48	0.31	14.81	0.09	0.04	<0.01	<0.10	2.45	1.72	4.44	129	Rhyolite Porphyry
K-1	MJV 503	29	69.01	5.10	0.27	15.08	0.10	0.03	0.02	<0.10	3.58	2.51	5.63	284	Rhyolite
K-2	MJV 504	20	68.46	3.15	0.07	15.06	0.10	0.03	0.11	<0.10	4.85	3.40	5.92	697	Rhyolite
K-5	MJV 505	27	76.70	4.53	0.04	13.18	0.08	0.03	<0.01	0.37	1.23	1.15	4.09	155	Rhyolite Porphyry
K-6	MJV 506	18	75.03	4.53	0.34	12.74	0.08	0.06	<0.01	0.39	1.35	1.25	3.94	155	Rhyolite Porphyry
K-7	MHX*197	950													Rhyolite Porphyry
K-7	MHX*198	5,000													Rhyolite Porphyry

*C.C. Hawley Project (Hinderman, 1981)

INTERPRETATION OF GEOPHYSICAL DATA

Plate 2 shows a structural and lithologic interpretation of magnetic and radiometric data obtained over the "Four Corners Area" covered in this report. Based on magnetic data, the assemblage of volcanic rocks described earlier appears to occupy a 6.5-mi-wide graben having a N. 25°-30° E. trend. The graben was apparently later sheared by a N. 70° W. wrench fault system that weakened the volcanic rocks and permitted intrusion of a magnetic and anomalously radioactive granite that has a less magnetic, monzonitic core. This zoned intrusion, mapped by Chapman and others (1975), was clearly outlined by the magnetic response, as shown in Plate 2. A close correlation also exists between the 20-cps contour of the uranium channel response and the zoned intrusion as mapped by magnetometer data. A 40-cps contour approximately outlines the monzonite core, and two higher response anomalies (up to 100 cps) occur in volcanic rocks above the southern part of the inferred subsurface position of the intrusion. The uranophane occurrence (VABM Corner occurrence) mentioned previously is at the intersection of the westernmost anomaly with the projected boundary of the granitic intrusion. Two other distinct radiometric uranium anomalies were outlined a few miles southwest of the uranophane occurrence in an area mapped as volcanic rocks (Unit Tfv, Miller and others, 1980), and these appear to be associated with a clearly defined right-lateral wrench fault zone (fault A, Pl. 2). A model of such fault development is shown on Plate 2 and indicates primary compression forces, tension fault direction, and trend of drag fold axes. The two anomalies along fault A may correlate with a drag fold axis.

Fault B (Pl. 2) is also quite distinct and may have influenced the anomalous zone with which the uranophane occurrence is associated. Faults C through G are much more speculative than A and B because of obscuring effects of the zoned pluton.

RESULTS FROM FIELD WORK AND ROCK-SAMPLE ANALYSES

Locations where ground checks were conducted and rock samples were collected are shown in Figure II-3. Anomalous areas shown on Plate 2 were readily verified by scintillometer during low-level helicopter overflights and by subsequent radioactivity measurements (Table II-1) on the ground. Anomalies are associated with rocks that are moderately to strongly enriched in uranium and thorium. Shape and extent of the anomalies may be partly related to stronger gamma-ray response over outcrop or frost-riven rubble in contrast with that over adjacent mantled areas. The anomalies are associated exclusively with rhyolitic flows and (or) hypabyssal rocks, which are part of the Cretaceous and early Tertiary igneous assemblage.

The southernmost east-trending pair of anomalies (Pl. 2) is in the northeastern corner of the Medfra Quadrangle, where Miller and others (1980) found anomalous uranium and thorium concentrations during field mapping in 1979. The anomalous trend in the southwestern Kantishna River Quadrangle, which includes the VABM Corner uranium occurrence described by Hinderman

(1981), appears to have been offset from that in the Medfra Quadrangle. This apparent offset is a basis for part of the structural interpretation in the preceding section.

Based on field observations plus thin-section analyses of seven rock samples (Fig. II-3) collected from rubble boulders, rhyolite porphyry is the dominant lithology associated with the two east-trending anomalous areas. Major mineral constituents in all samples are nearly identical. Samples differ chiefly in the phenocryst-to-groundmass ratio, which ranges widely. Euhedral to subhedral phenocrysts of quartz and K-feldspar (sanidine?) are enclosed in quartzofeldspathic groundmass with minor amounts of muscovite, biotite, and iron oxides. During examination of the VABM Corner uranium occurrence, a northeasterly trend of uranophane-bearing cobble-sized rubble fragments was noted. This zone is roughly 4-in. thick and appeared to be bounded by subparallel fractures. One cobble-size fragment contained a tiny quartz veinlet parallel to a fracture surface coated locally with a secondary uranium mineral. Except for uranophane at the VABM Corner uranium occurrence (site K-7, Fig. II-3), no uranium or thorium minerals were identified in any samples from the radiometrically anomalous areas. Samples K-1 and K-2 (Pl. 2) differ from the others in having a hypidiomorphic-granular texture and extensive argillic alteration of feldspars.

Rock samples from the radiometrically anomalous areas are highly siliceous, averaging 73% SiO_2 by weight (Table II-2) and are slightly potassic (average $K_2O/Na_2O = 1.2$). They can be characterized as subaluminous to peraluminous (agpaitic coefficients average 0.92).

Uranium assays by fluorometry on the seven rhyolite samples range from 18 to 42 ppm U_3O_8 and average 27 ppm, which is above the world average for rhyolites. A plot of uranium concentrations determined by both chemical and radiometric methods indicates a slight tendency toward disequilibrium in favor of chemical uranium. Equivalent-thorium concentrations based on laboratory gamma-ray spectroscopy are also relatively high for rhyolitic rocks. In the same seven samples, equivalent thorium ranges from 64 to 589 ppm (Table II-2). Thorium-to-uranium ratios average approximately 5. The ratios are not significantly different from worldwide averages for rocks of granitic composition (Nishimori and others, 1977). Rocks outside the anomalous areas were not sampled during field check of the detailed survey, but Hinderman (1981) reported that most thorium-to-uranium ratios for rocks elsewhere in the same igneous assemblage are not anomalous for rocks of this composition.

CONCLUSIONS AND RECOMMENDATIONS

Occurrences of secondary uranosilicates, like those at the VABM Corner, are common in rhyolite terranes and by themselves are not diagnostic of favorable areas for uranium deposits. However, the combination of uranophane occurrence, rocks enriched in uranium and thorium, and zones of structural dilation indicated by geophysical data and by the fracture-controlled uranium occurrence at the VABM Corner may indicate favorable conditions for larger deposits. Uranophane occurrences of the type found in the Sischu Mountains igneous assemblage seem to best fit criteria of the hydroauthigenic class or,

less likely, the hydroallogenic class of Pilcher (1978). Such occurrences are not noted for their large size, but they may signal significantly larger concentrations related to remobilization of uranium with subsequent deposition in receptive fracture systems or in sedimentary rocks of adjacent basins.

Because field work reported herein was limited to a brief ground check to verify and determine the cause of radioactivity anomalies, insufficient information was obtained to elaborate on possible favorable environments; however, it is postulated that the highest potential for uranium deposits in the area is at fault intersections, at the contact of the granitic intrusive, and in Tertiary sedimentary rocks in nearby basins. Future work to evaluate the volcanic and intrusive rocks should include aerial electromagnetic surveys in potentially favorable places in order to pinpoint possible breccia or fracture zones for drill targets. Hinderman (1981) reported high lead and molybdenum in samples from the VABM Corner uranium occurrence; therefore, the area may also be prospective for base metals.

REFERENCES

Beikman, Helen, 1978, Preliminary geologic map of Alaska: U.S. Geological Survey Map, scale 1:2,500,000.

Cass, J. T., 1959, Reconnaissance geologic map of the Ruby Quadrangle, Alaska: U.S. Geological Survey Investigation Map I-289, scale 1:250,000.

Chapman, R. M., Yeend, W. E., and Patton, W. W., 1975, Preliminary reconnaissance geologic map of the western half of the Kantishna River Quadrangle, Alaska: U.S. Geological Survey Open-File Report 75-351, scale 1:250,000.

Hinderman, T. K., 1981, Uranium resoure evaluation, Mount McKinley Quadrangle, Alaska: U.S. Department of Energy Open-File Report PGJ-054(81), 60 p.

Miller, T. P., Moll, E. J., and Patton, W. W., Jr., 1980, Uranium- and thorium-rich volcanic rocks of the Sischu Creek area, Medfra Quadrangle, Alaska: U.S. Geological Survey Open-File Report 80-803, 8 p.

Nishimori, R. K., Ragland, P. C., Rogers, J. J. W., and Greenberg, J. K., 1977, Uranium deposits in granitic rocks: U.S. Energy Research and Development Administration Open-File Report GJBX-13(77), 298 p.

Patton, W. W., Jr., Lanphere, M. A., Miller, T. P., and Scott, R. A., 1976, Age and tectonic significance of volcanic rocks on St. Matthew Island, Bering Sea, Alaska: U.S. Geological Survey Journal of Research, v. 4, p. 67-73.

Pilcher, R. C., 1978, Volanogenic uranium occurrences, in Mickle, D. G., and Mathews, G. W., eds., Geologic characteristics of environments favorable for uranium deposits: U.S. Department of Energy Open-File Report GJBX-67(78), p. 181-220.

Reed, J. C., Jr., 1961, Geology of the Mount McKinley Quadrangle, Alaska: U.S. Geological Survey Bulletin 1108-A, 36 p.

Western Geophysical Company of America, Aero Service Division, 1980a, Airborne gamma-ray spectrometer and magnetometer survey, Ruby Quadrangle (Alaska): U.S. Department of Energy Open-File Report GJBX-75(80), 137 p.

-----1980b, Airborne gamma-ray spectrometer and magnetometer survey, Medfra Quadrangle (Alaska): U.S. Department of Energy Open-File Report GJBX-76(80), 169 p.

-----1980c, Airborne gamma-ray spectrometer and magnetometer survey, Kantishna River Quadrangle (Alaska): U.S. Department of Energy Open-File Report GJBX-94(80), 159 p.

-----1980d, Airborne gamma-ray spectrometer and magnetometer survey, Four Corners detail area, portions of Kantishna River, Mount McKinley, Medfra, and Ruby Quadrangles (Alaska): U.S. Department of Energy Open-File Report GJBX-116(80), 216 p.

III. EVALUATION OF URANIUM ANOMALIES IN THE GOODMAN-DUNBAR AREA, NORTHEASTERN WISCONSIN

Geoffrey W. Mathews
William H. Blackburn

May 1982

BENDIX FIELD ENGINEERING CORPORATION
Grand Junction Operations
Grand Junction, Colorado 81502

INTRODUCTION

This brief uranium anomaly investigation was carried out in conjunction with a similar reconnaissance study 35 km to the southwest at McCaslin Syncline. Analysis of a rock sample taken near Dunbar, Wisconsin, in 1962 indicated 0.09% U_3O_8 (Kinnaman and Illsley, 1962). Recent information, including HSSR and ARMS data, corroborate the apparent favorability of the area for the occurrence of uranium deposits.

The objective of this investigation was to undertake a short-term field reconnaissance of the indicated anomalies and to make a recommendation regarding the advisability of further detailed work in the area.

LOCATION

The Goodman-Dunbar area is in the east-central portion of the Iron Mountain NTMS 1° x 2° Quadrangle (Fig. III-1). The area encompasses approximately 45 km^2 and is in Marinette County along the line separating T. 37 N. and T. 36 N. and between R. 16 E. and R. 18 E. (Fig. III-2). The western half of the area includes HSSR and ARMS anomalies but is covered by glacial drift in excess of 30 m thick, which makes outcrop reconnaissance virtually impossible. Therefore, the majority of the work for this study was concentrated in the eastern half of the area near the town of Dunbar (Fig. III-2).

BACKGROUND

The Iron Mountain Quadrangle was scheduled to be evaluated in 1978 by BFEC for the NURE program. Because quadrangle evaluation priorities were rearranged, evaluation of the Iron Mountain Quadrangle was cancelled. However, the ARMS and HSSR surveys were completed. Examination of these surveys and corroborative information (Kinnaman and Illsley, 1962) indicate that an area with anomalous uranium content is near the towns of Goodman and Dunbar, Wisconsin.

Very little work has been done in this area specifically regarding uranium. The results of a stream-water sampling program by Kinnaman and Illsley (1962) for the U.S. Atomic Energy Commission indicated that the North and South Branches of the Pike River contain anomalous uranium concentrations and high uranium-to-conductivity ratios. The Pike River drains a slight highland between Goodman and Dunbar.

A sample of gray, coarsely crystalline granite that contains abundant sulfides and altered biotite was taken about 2 km southwest of Dunbar. Analysis of the sample showed the rock contained 920 ppm U_3O_8. An autoradiograph of the same sample showed the uranium occurred as small blebs at the junction of crystal surfaces (Kinnaman and Illsley, 1962).

Surveys done for NURE by Union Carbide (HSSR) and geoMetrics (ARMS) indicate overlapping stream-water and aerial uranium anomalies. Sulfide exploration in the area also supports the general mineralization favorability.

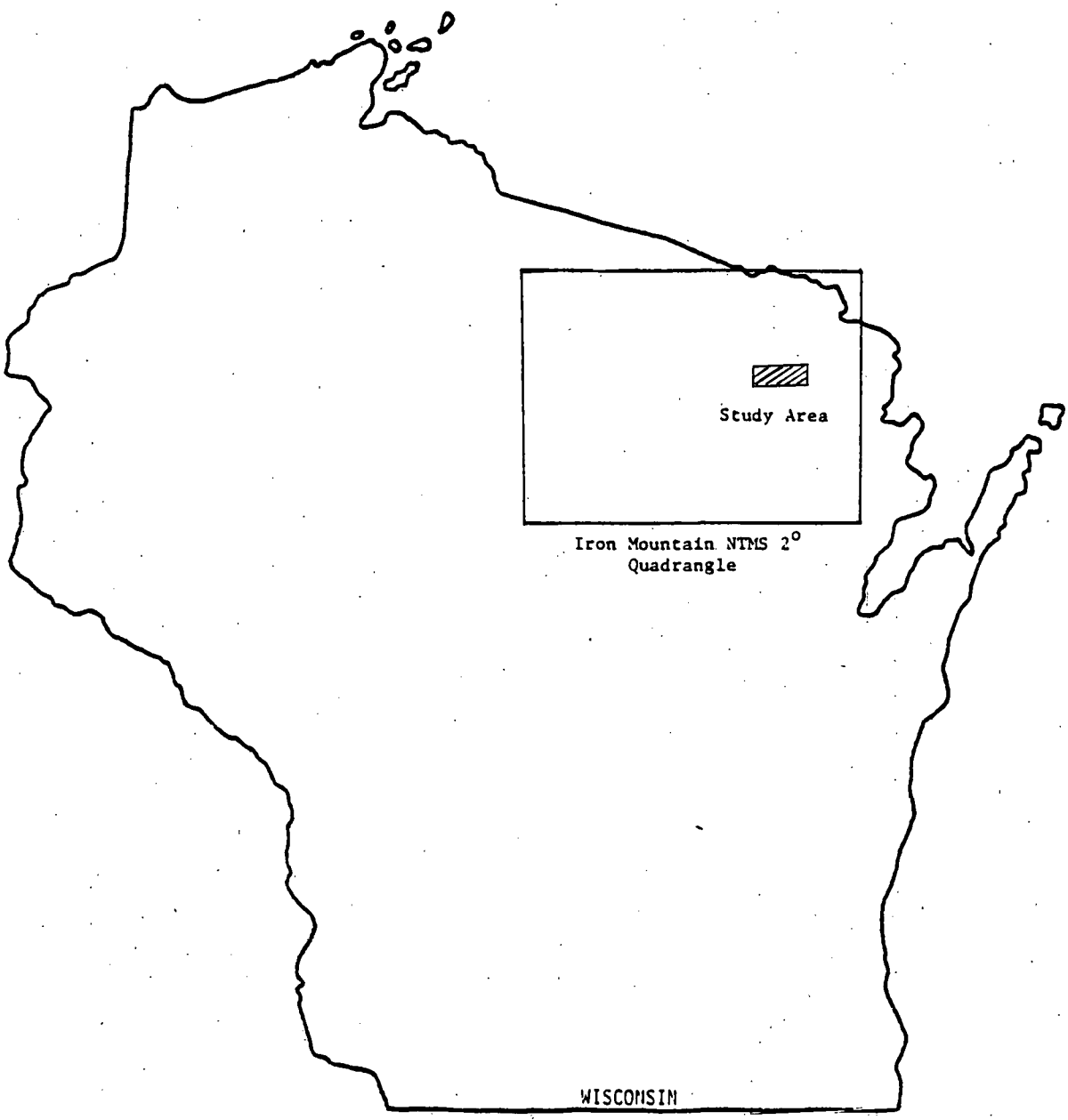

Figure III-1. Location map.

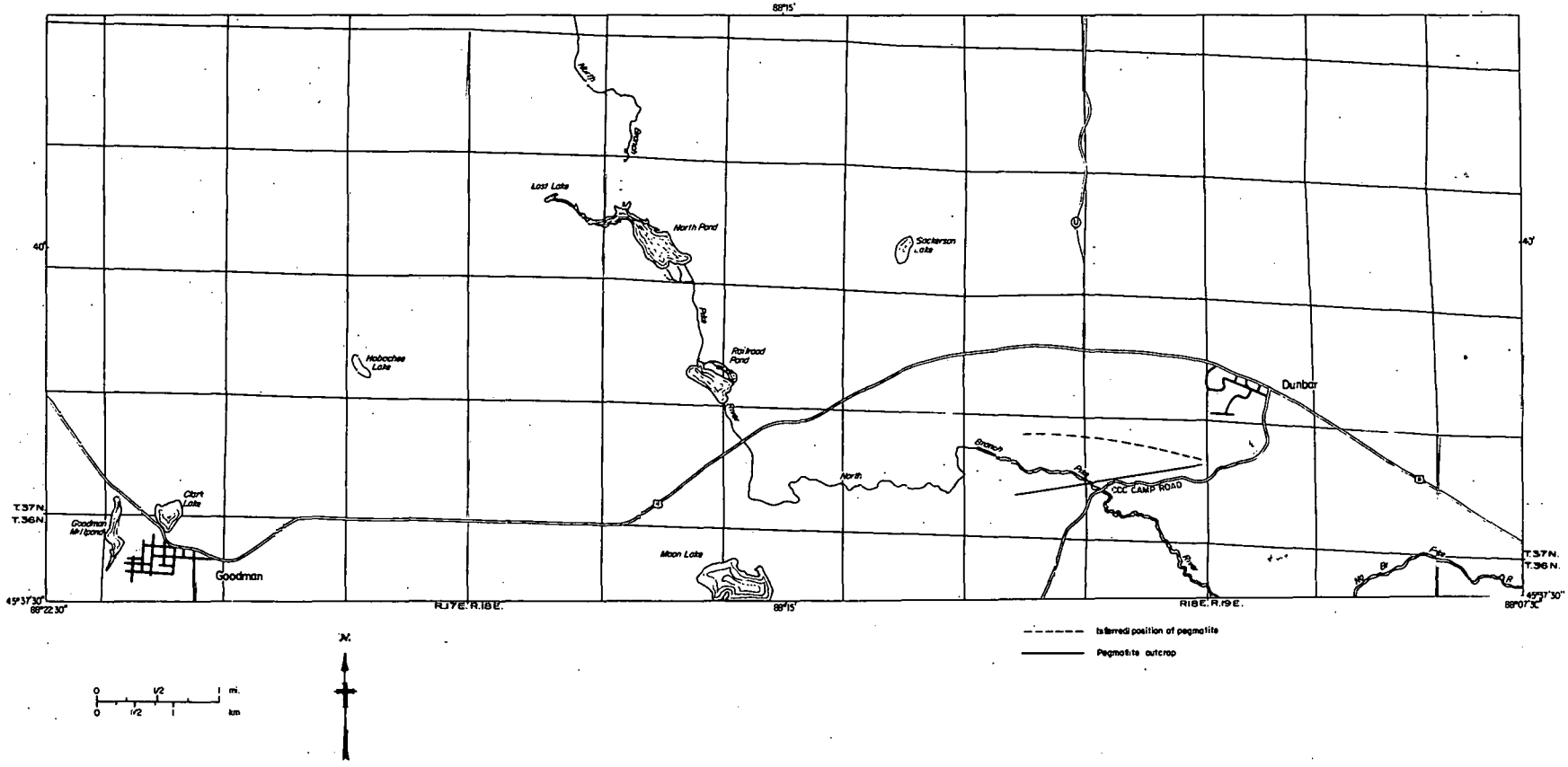

Figure III-2. Map of the Goodman-Dunbar study area showing location of pegmatite bodies.

Previous works that pertain to this area include those by Cain (1961), Wadsworth (1962), Prinz (1965), Banks and Rebello (1969), and VanSchmus and others (1975).

GEOLOGIC SETTING

Bedrock exposures in this part of Wisconsin are often restricted to isolated, glacially abraded knobs of limited areal extent. The glacial drift is very thick just a few kilometers west of Dunbar and makes geologic correlations and contact relationships difficult to discern.

The Goodman-Dunbar area lies south of a major east-southeast-trending fault system that passes through the town of Iron Mountain, Michigan (Fig. III-3). The geology north of the fault system has been studied extensively in conjunction with exploration for iron in the Menominee Range.

The rocks north of the fault system consist primarily of metasedimentary and metavolcanic units of the Marquette Range Supergroup. The Carney Lake Gneiss is the southernmost exposure of Precambrian W rocks near east-central Wisconsin. In general, as one proceeds southward from the Precambrian Carney Lake Gneiss, the rocks become younger. For detailed descriptions of the area north of the fault system, see Bayley and others (1966) and James and others (1961).

The rocks south of the fault system include the Quinnesec Formation, intrusive plutonic units, and associated gneisses. The plutonic units include the Hoskin Lake Granite, Marinette Quartz Diorite, Athelstane Quartz Monzonite, Amberg Quartz Monzonite, Dunbar Gneiss, Newingham Grandiorite, and the Twelve-Foot Falls Quartz Diorite.

The rock unit of primary interest in this report is the Dunbar Gneiss in the vicinity of Dunbar, Wisconsin. This area was studied by Cain (1961) and Wadsworth (1962). Cain's dissertation dealt mainly with the Pembine vicinity, whereas Wadsworth's thesis was directed at the Twelve-Foot Falls Quartz Diorite (Fig. III-4).

Cain (1961) subdivided the Dunbar Gneiss into two dominant gneisses, a coarse-grained banded gneiss and a fine-grained migmatitic gneiss. The following descriptions are from Cain (1961):

> The banded gneiss is commonly uncontorted and locally resembles foliated granitic rock. The alternating leucocratic and mafic (mainly biotite) bands range from 1/2 in. to 2 ft wide. The feldspar is subhedral, gray, and rarely shows twinning in hand specimen. Biotite is abundant and occurs in elongated aggregates. Locally, the gneiss exhibits augen texture with gray feldspar ovoids 5 cm long. Typically, however, the gneiss is medium-grained and is characterized by regular bands up to 4 or 5 cm wide.

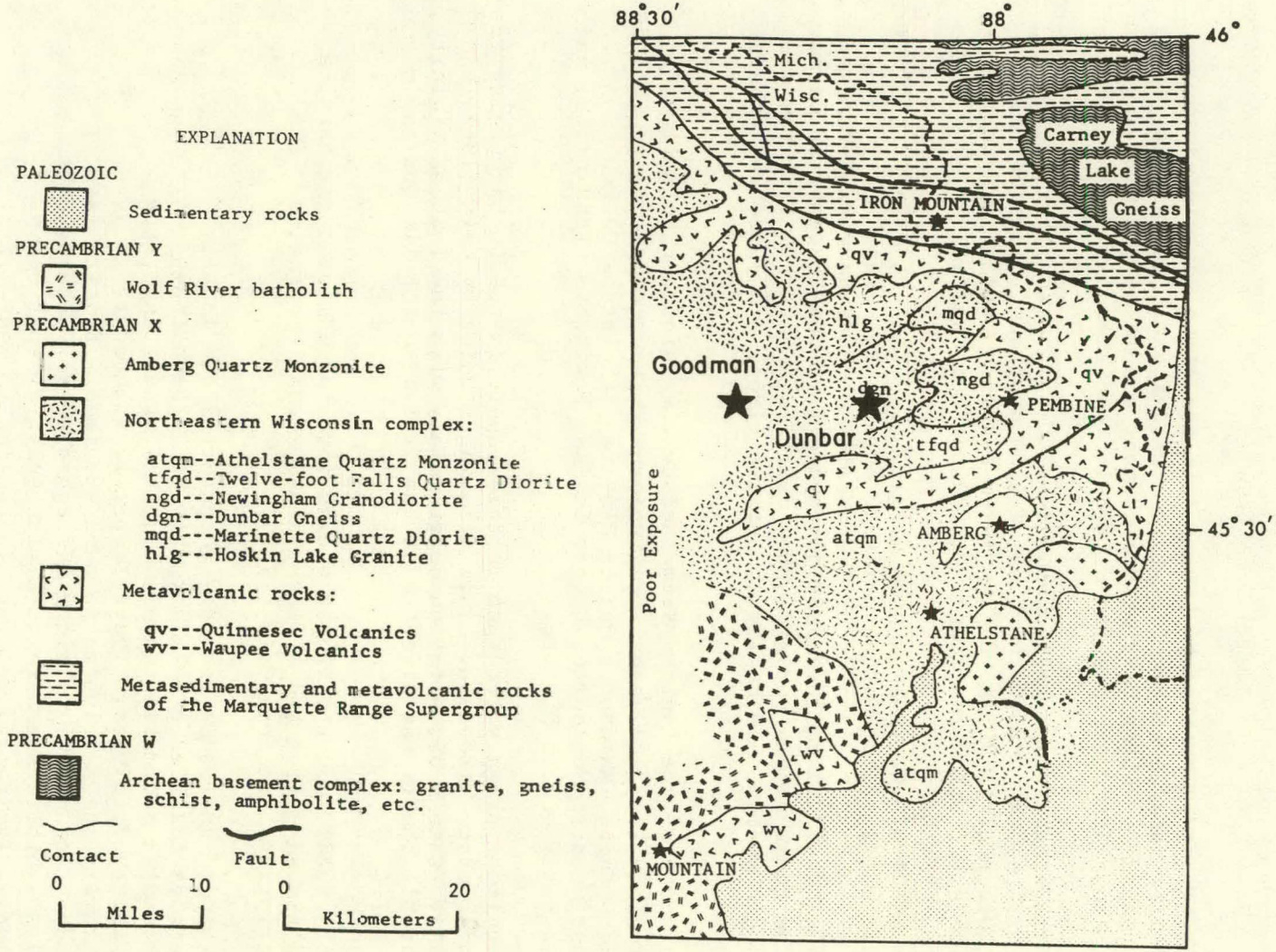

Figure III-3. Generalized geologic map of part of northeastern Wisconsin and upper Michigan (from VanSchmus and others, 1975).

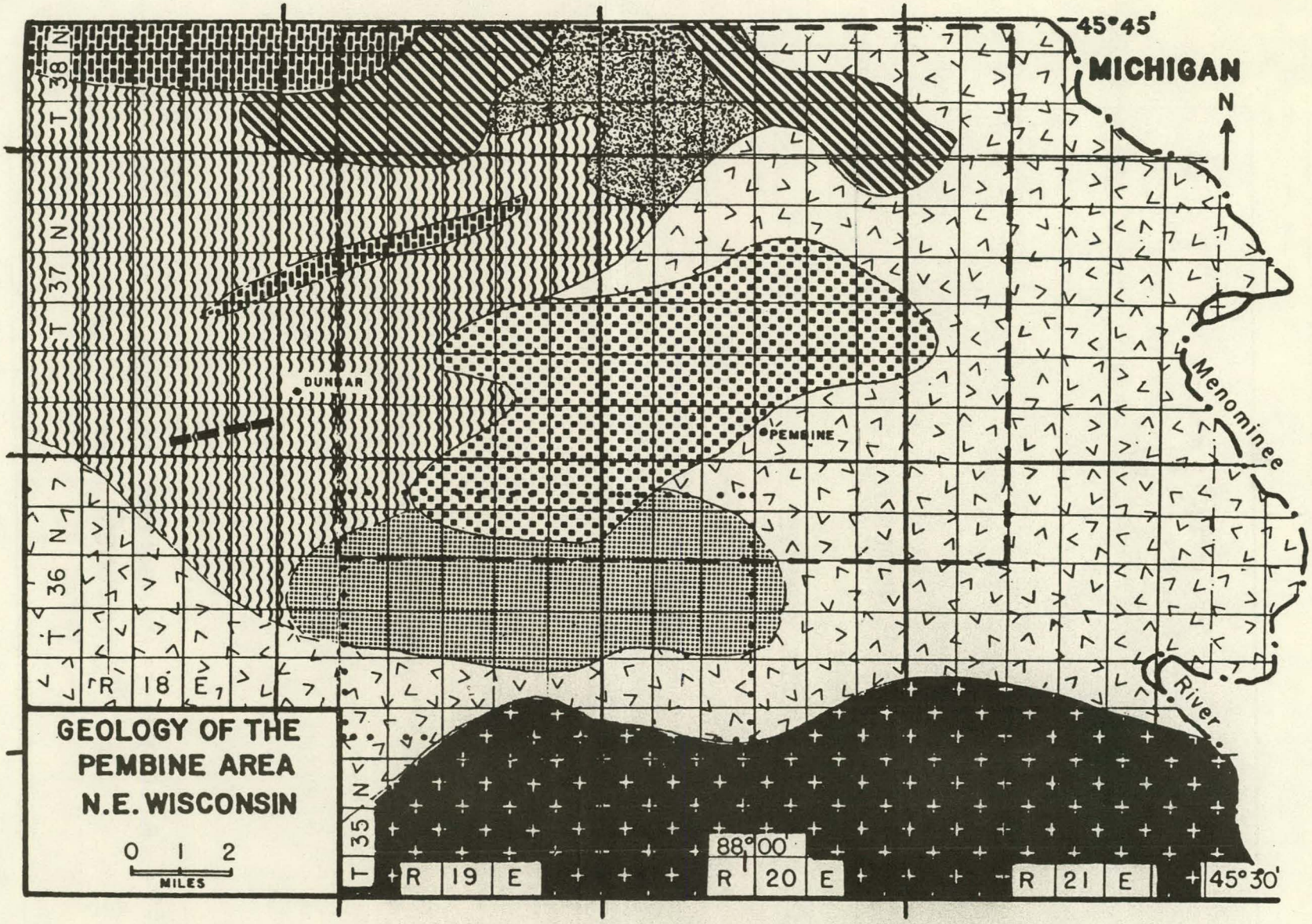

Figure III-4. Geology of the Pembine area, northeast Wisconsin (from Cain, 1961).

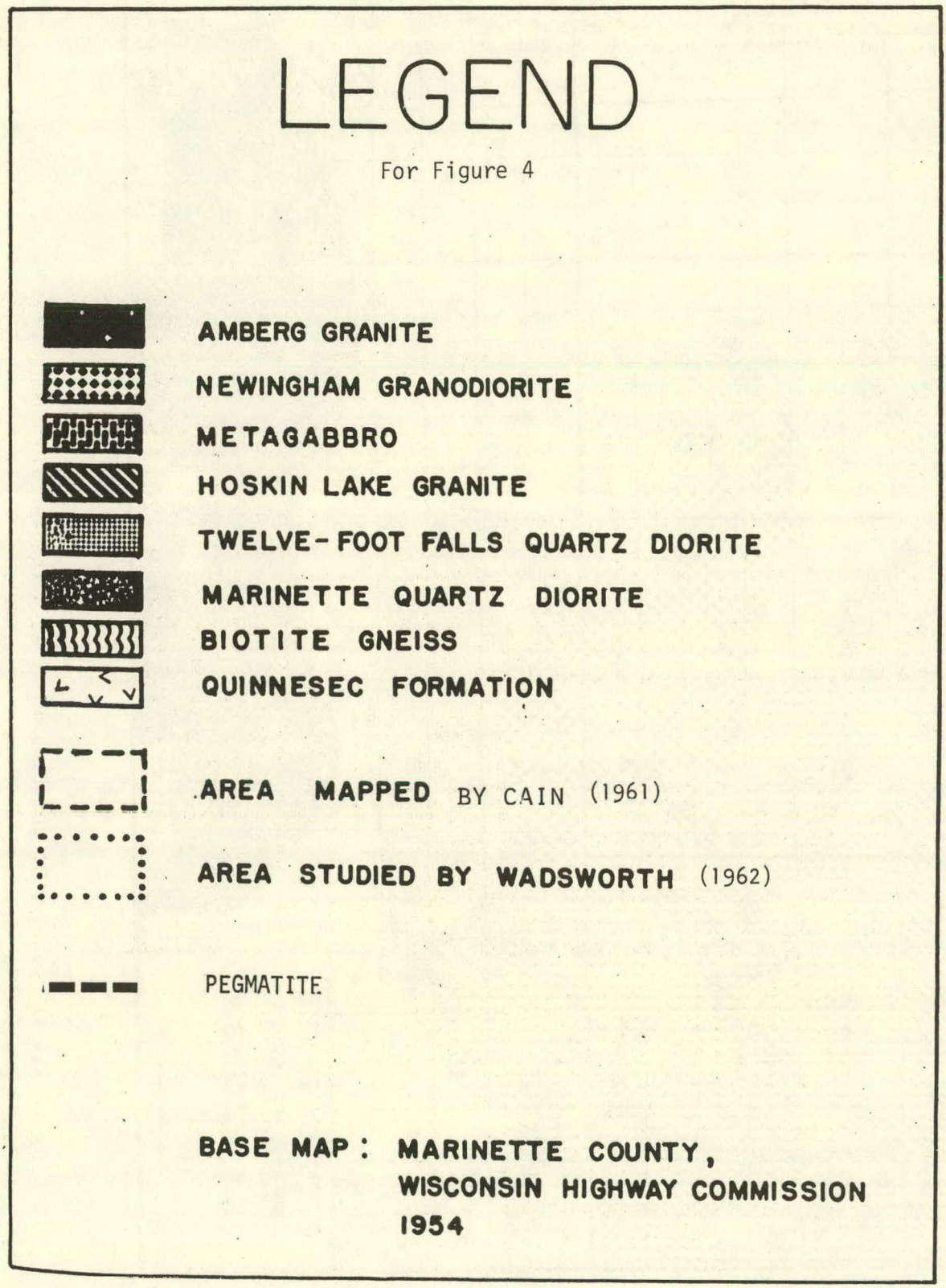

Figure III-4. Geology of the Pembine area, northeast Wisconsin (from Cain, 1961) (continued).

The migmatitic gneiss is fine-grained and appears, in hand specimen, to consist almost entirely of biotite. Leucocratic bands and stringers extend through the rock, locally forming agmatites. The migmatitic gneiss occurs only as zenoliths up to 6 ft long within the banded gneiss.

By contrast, outcrops of the Dunbar Gneiss in T. 37 N., R. 18 E., have numerous alaskitic and granitic pegmatites that exceed the 0.6-m maximum width of "gneissic banding" described by Cain (1961). Along Marinette County Road 'U' northwest of Dunbar (Fig. III-2), the Dunbar Gneiss is cut by at least two generations of pegmatites. The pegmatites are discordant and in some instances contain what appear to be xenoliths of partially assimilated Dunbar Gneiss. Radiation levels of these pegmatites are not above the background levels of their gneissic host.

A large alaskitic pegmatite/aplite complex occurs southwest of Dunbar along the north side of CCC Camp Road. The pegmatite at this location averages 15 m in width and is traceable over a distance of 2.0 km from SE 1/4 SW 1/4 NE 1/4, sec. 36 to SE 1/4 NE 1/4 SW 1/4, sec. 35, T. 36 N., R. 18 E. (Fig. III-2).

The pegmatite is generally very coarse grained but contains small masses of aplitic material and darker "gneissic inclusions." It is leucocratic and contains white feldspars, quartz, and little or no ferromagnesian material. R. Gebhardt (BFEC field notes, 1978) reported small (3 mm) almandine garnets near the CCC Camp Road locality. It is difficult to ascertain from Gebhardt's notes the precise host of the garnets. They were not found in the alaskites during this investigation. Fractures in the alaskites are limonite stained and tend to be slightly more radioactive than the rest of the rock. Characteristically, the adjacent Dunbar Gneiss showed count rates of 80 to 150 cps, whereas the coarser alaskites had count rates of 200 to 800 cps.

The origin of the pegmatite, whether an intrusive body or an anatectic derivative, is not known. Relict structures were not apparent, and any contact margins were obscured by vegetation or were so indistinct as to be inconclusive. However, the strike of the pegmatite (N. 85° E.) is consistent with the overall structural trend of metasedimentary units found to the south in the McCaslin district. The pegmatite is somewhat more resistant than surrounding units and forms a slight topographic high. A similar subparallel topographic feature to the north (Fig. III-2) was not investigated because of access problems and time constraints.

METHODS

Ground surveys were conducted using Mount Sopris SC-132 scintillometers and Scintrex GAD-6 spectrometers. Carborne surveys were run on all access roads. Scintillometer and spectrometer measurements were taken on outcrops of all rock types encountered in the area.

RESULTS

Data from the spectrometer surveys are presented in Appendix III-A. The average KUT, Th/U, and cps values for the units near Dunbar are summarized in Table III-1.

Table III-1. SUMMARY OF RADIOMETRIC SURVEYS

		K%	eU ppm	eTh ppm	eTh/eU	Avg. cps
Dunbar Gneiss and pegmatites County Road U	n = 12					
	x	3.5	5.4	16.3	3.0	80-150
	S. Dev.	1.2	1.6	6.8		
Pegmatites CCC Camp Road	n = 4					
	x	4.0	49.3	39.8	0.8	200-800
	S. Dev.	0.6	28.3	12.6		

The 0.8 Th/U value for the alaskite southwest of Dunbar suggests uranium enrichment. However, the maximum observed eU value was only 88 ppm over a single square meter. The average equivalent-uranium values for the remainder of the Dunbar Gneiss are not significantly elevated. The reported prospect pits (Kinnaman and Illsley, 1962) containing uranium concentrations of up to 920 ppm could not be located. They are presumed not to have been associated with leucocratic pegmatites.

CONCLUSIONS

Based on this investigation, the Goodman-Dunbar area is considered not to be favorable for the occurrence of uranium deposits of economic potential. Whether one adopts an anatectic or igneous intrusive model for the pegmatites, the area does not meet NURE favorability criteria guidelines (Mickle and Mathews, 1978) because:

- The apparent average grade of the alaskites will not meet or exceed the 100-ppm minimum cutoff grade.
- Even if the grade requirements were met, the alaskite is not extensive enough to provide a sufficient volume of endowed rock.

It is reasonable to assume that similar alaskites may exist west of this study area, beneath the glacial drift. If the uranium is located in interstitial sites (Kinnaman and Illsley, 1962) and (or) along fractures, as postulated in this investigation, then it would be readily available for leaching into local surface- and ground-water regimes. This alaskite and

other possible alaskites are probably the cause of local stream-water anomalies. The contrasting uranium contents of the alaskites and Dunbar Gneiss also are probable causes for anomalous airborne measurements.

The area near Dunbar, Wisconsin, warrants no further study in terms of uranium potential.

REFERENCES

Arendt, J. W., project manager, 1978, Hydrogeochemical and stream-sediment reconnaissance basic data for Iron Mountain NTMS Quadrangle, Michigan, Wisconsin: U.S. Department of Energy Open-File Report GJBX-97(78), 36 p.

Banks, P. O., and Rebello, D. P., 1969, Zircon age of a Precambrian rhyolite, northern Wisconsin: Geological Society of America Bulletin, v. 80, p. 907-910.

Bayley, R. W., Dutton, C. E., and Lamey, C. A., 1966, Geology of the Menominee iron-bearing district, Dickinson County, Michigan, and Florence and Marinette Counties, Wisconsin: U.S. Geological Survey Professional Paper 513, 95 p.

Cain, J. A., 1961, The geology of the Pembine area, northeastern Wisconsin: Evanston, Illinois, Northwestern University, Ph.D. dissertation.

GeoMetrics, 1978, Aerial gamma-ray and magnetic survey, Rice Lake Quadrangle, Wisconsin, Iron Mountain Quadrangle, Wisconsin/Michigan, Green Bay Quadrangle, Wisconsin: U.S. Department of Energy Open-File Report GJBX-26(78), p. 1-70.

James, H. L., Clark, L. D., Lamey, C. A., and Pettijohn, F. J., 1961, Geology of central Dickinson County, Michigan: U.S. Geological Survey Professional Paper 310, 176 p.

Kinnaman, R. L., and Illsley, C. T., 1962, Geochemical and geophysical reconnaissance in northern peninsula, Michigan and northeastern Wisconsin: U.S. Atomic Energy Commission Open-File Report RME-1099, 136 p.

Medaris, L. G., and Anderson, J. L., 1973, Preliminary geologic map or Iron Mountain sheet: University of Wisconsin-Extension, Wisconsin Geologic and Natural History Survey.

Mickle, D. G., and Mathews, G. W., eds., 1978, Geologic characteristics of environments favorable for uranium deposits: U.S. Department of Energy Open-File Report GJBX-67(78), 250 p.

Prinz, W. C., 1965, Marinette Quartz Diorite and Hoskin Lake Granite of northeastern Wisconsin, in Changes in stratigraphic nomenclature by the U.S. Geological Survey, 1964: U.S. Geological Survey Bulletin 1224-A, p. A53-A55.

VanSchmus, W. R., Thurman, E. M., and Peterman, Z. E., 1975, Geology and Rb-Sr chronology of middle Precambrian rocks in eastern and central Wisconsin: Geological Society of America Bulletin, v. 86, no. 9, p. 1255-1265.

Wadsworth, W. B., 1962, The Twelve-foot Falls Quartz Diorite, northeastern Wisconsin: Evanston, Illinois, Northwestern University, M.S. thesis.

APPENDIX III-A. GAMMA SPECTROMETRY DATA

Formation	Locale	Location ¼ Sec.	Sec.	Twp. (N)	Rng. (E)	K (%)	eU (ppm)	eTh (ppm)	Th/U	Remarks
Dunbar Gneiss	Co. Road U	NESE	26	37	18	2.6	3.5	16.5	4.7	Finely foliated qtz-biotite-feldspar
Pegmatite	Co. Road U	NESE	26	37	18	5.4	4.8	11.7	2.4	
Pegmatite	Co. Road U	SENE	23	37	18	5.9	5.8	17.2	3.0	Well-foliated biotite-gneiss
Pegmatite	Co. Road U	SENE	23	37	18	4.7	5.1	14.5	2.8	
Granodiorite	Co. Road U	SESE	14	37	18	2.4	6.3	36.2	5.7	
Granodiorite	Co. Road U	NESE	14	37	18	3.4	3.9	12.3	3.2	Two generations of pegmatites
Pegmatite	Co. Road U	NESE	14	37	18	2.9	4.6	16.0	3.5	
Pegmatite	Co. Road U	NESE	14	37	18	3.2	6.5	10.1	1.5	
Dunbar Gneiss(?)	Spur Lake Road	NWSE	15	37	18	3.0	6.1	16.1	2.6	Well foliated biotite-gneiss
Dunbar Gneiss(?)	Spur Lake Road	NWSE	15	37	18	2.6	6.3	15.9	2.5	
Dunbar Gneiss(?)	U.S. Hwy 8	SENW	27	37	18	3.8	4.5	20.3	4.5	
Pegmatite	U.S. Hwy 8	SENW	27	37	18	3.4	7.0	15.3	2.2	
Dunbar Gneiss(?)	CCC Camp Road	NESW	36	37	18	1.6	2.3	7.1	3.1	
Pegmatite	CCC Camp Road	NESW	36	37	18	3.4	8.6	18.6	2.2	
Gneiss	Pike River Bridge	SENE	6	37	19	1.7	4.1	3.6	0.9	Twelve-Foot Falls Quartz Diorite (?)
Aplite	CCC Camp Road	SWNE	36	37	18	4.6	46.2	48.8	1.1	Dike in Dunbar Gneiss(?)
Pegmatite	CCC Camp Road	SWNE	36	37	18	4.4	21.1	26.2	1.2	
Pegmatite	CCC Camp Road	SWNE	36	37	18	3.8	41.3	32.0	0.8	Limonitic staining
Pegmatite	CCC Camp Road	SWNE	36	36	18	3.2	88.4	52.1	0.6	Very small hot spot
Norway Lake Granite Gneiss	Dickinson Co., MI	SESW	5	42	28(W)	4.0	25.0	10.7	0.43	Basement
Norway Lake Granite Gneiss	Dickinson Co., MI	SESW	5	42	28(W)	3.7	20.6	9.3	0.45	Basement
East Branch Arkose	Dickinson Co., MI	SESW	8	42	28(W)	4.1	3.4	52.6	15.0	Stretched pebble conglomerate
East Branch Arkose	Dickinson Co., MI	SESW	8	42	28(W)	3.8	1.6	34.0	21.0	Stretched pebble conglomerate

THIS PAGE

WAS INTENTIONALLY

LEFT BLANK

IV. EVALUATION OF URANIUM ANOMALIES IN THE McCASLIN SYNCLINE, NORTHEASTERN WISCONSIN

William H. Blackburn
Geoffrey W. Mathews

January 1982

BENDIX FIELD ENGINEERING CORPORATION
Grand Junction Operations
Grand Junction, Colorado 81502

INTRODUCTION

Samples of Elliot Lake-type quartz-pebble conglomerate were found in 1955 in float in northeastern Wisconsin along the northern limb on the McCaslin syncline (Kalliokoski, 1976). Since then, this structure has been a uranium exploration target. More recent information, including HSSR and ARMS data, corroborate the apparent favorability of the area.

Previous workers (Kalliokoski, 1976; Kinnaman and Illsley, 1962) suggested the possibility of the occurrence of Elliot Lake-type or unconformity-related uranium deposits in the area. The objective of this investigation was to undertake a short field reconnaissance of the indicated HSSR and airborne radiometric anomalies and to make a recommendation regarding the advisability of further detailed work in the area.

LOCATION

The McCaslin syncline underlies about 500 km^2 in the east-central portion of the Iron Mountain, Wisconsin, NTMS 1° x 2° Quadrangle (Fig. IV-1). This investigation was confined to the limbs of the syncline and particularly to those rocks near the base of the McCaslin Quartzite.

BACKGROUND

The Iron Mountain Quadrangle was scheduled to be evaluated in 1978 by BFEC for the NURE program. As a result of the rearrangement of priorities the evaluation of the Iron Mountain Quadrangle was cancelled. However, the ARMS and HSSR surveys were completed. Examination of these surveys shows an area with anomalous uranium in the McCaslin district.

Kalliokoski (1976) described float blocks of Elliot Lake-type quartz-pebble conglomerates from near the Carter fire tower hill on the northern limb of the syncline. The samples were first reported in 1955 and again in 1972 with respective grades of 0.17% and 0.33% U_3O_8. In a brief inspection of the Carter tower area, Kalliokoski reported the occurrence of very minor amounts of pyrite (<0.1%) in the basal quartz-pebble conglomerate of the McCaslin Quartzite. Kalliokoski and others (1978) later discounted the applicability of the Elliot Lake model due to age considerations and suggested that an Athabascan unconformity-related model might be more appropriate.

The results of a stream-water sampling program for the U.S. Atomic Energy Commission indicated that waters in the McCaslin district contain amounts of dissolved uranium that approach the maximum values found in the State of Wisconsin (Kinnaman and Illsley, 1962). Anomalous uranium concentrations were found in the Rat River, Otter Creek, North Branch Oconto River, and Forbes Creek, all of which drain the McCaslin structure (Kinnaman and Illsley, 1962).

Surveys done for NURE by Union Carbide (HSSR) and geoMetrics (ARMS) indicate overlapping stream-water uranium and aerial uranium anomalies. Industry activity in the McCaslin district and nearby occurrences of molybdenite and other sulfides support the general favorability of the area.

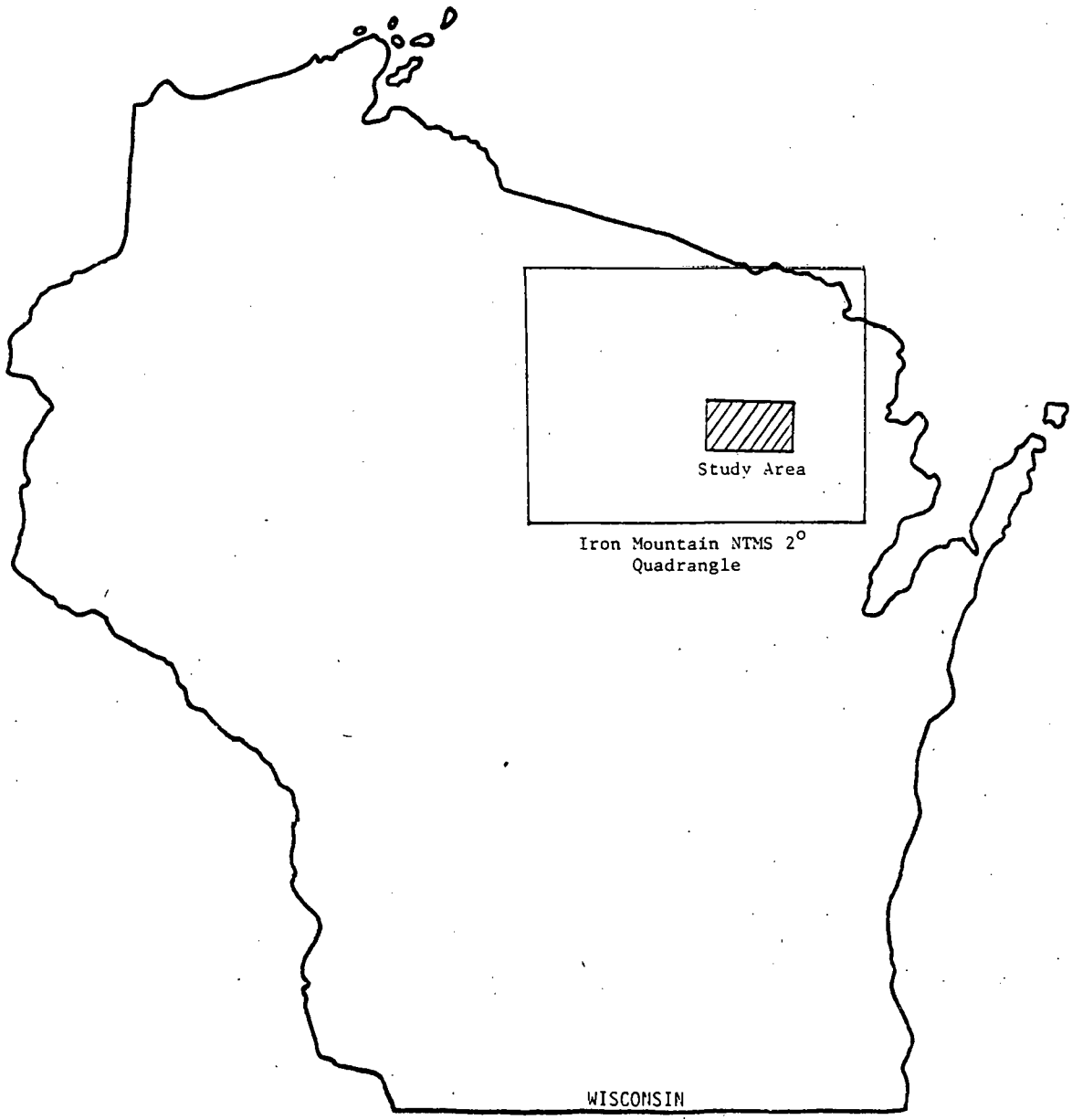

Figure IV-1. Location map.

GEOLOGIC SETTING

The McCaslin syncline is the major structural feature in northeastern Wisconsin. It is an elongate east-trending syncline that has steeply dipping limbs and plunges a few degrees to the west. The eastern end has been disrupted by the intrusion of the High Falls Granite, which is a member of the Wolf River batholith (Fig. IV-2).

The Waupee Volcanics, a thick sequence of metamorphosed volcanogenic rocks that form a greenstone belt, are the oldest rocks in the district. These rocks have been tentatively correlated by Mancuso (1960) with the Quinnesec Formation of southern Dickinson and Iron Counties, Michigan. The Quinnesec Formation and the Waupee Volcanics are thought to be correlative with the Marquette Range Supergroup, dated at approximately 1.9 b.y. (Banks and Rebello, 1969). Correlation of the Quinnesec Formation and the Waupee Volcanics is very tenuous because the units do not occur within less than 25 or 30 km of each other. However, if they are correlative, then the favorability of the area for the formation of quartz-pebble conglomerate uranium deposits may be diminished because an extensive greenstone belt would not be a good source for uranium-enriched granites and subsequent detrital uranium (Houston and Karlstrom, 1980).

The Waupee Volcanics are intruded by the Macauley Granite Gneiss. Both of these units are unconformably overlain by the McCaslin Quartzite. The resistant quartzites of the McCaslin Formation are the major ridge formers.

The McCaslin Quartzite is overlain and (or) intruded by the Hager Rhyolite (Mancuso, 1960; Medaris and Anderson, 1973). The Hager has been dated at about 1.5 b.y. (Kalliokoski and others, 1978) and is contemporaneous with other units of the Wolf River batholith. The youngest rock in the area is the High Falls Granite; it has intruded and disrupted the eastern nose of the McCaslin structure.

WAUPEE VOLCANICS

The Waupee Volcanics include a wide variety of rock types. They have been described by Mancuso (1960) near Mountain, Wisconsin, as a thick (>1,500 m) succession of rhyolitic tuffs, andesites, rhyolites, agglomerates, basalts, amphibolites, and porphyritic basalts. The Waupee Volcanics also include dark-gray to black, fine-grained and finely bedded amphibolitic rocks. The bedding(?) is only a few millimeters thick, but it can be traced over distances of several meters. Near the eastern nose of the McCaslin syncline, in the vicinity of Thunder Mountain, the Waupee Volcanics have a somewhat different character. Motten (1972) described the Waupee in this vicinity as a thick sequence of water-laid, felsic crystal tuffs. Quartz, oligoclase, biotite, and muscovite compose the bulk of the rock. Motten (1972) also reported relict glass shards and rounded to subrounded allochthonous plagioclase aggregates.

The Waupee Volcanics are exposed in various localities along the north limb of the syncline. Near Carter, Wisconsin, they include igneous rocks of granitic to dioritic composition, as well as banded lithologies similar to those found on the southern limb. Thin sections of two samples of the Waupee

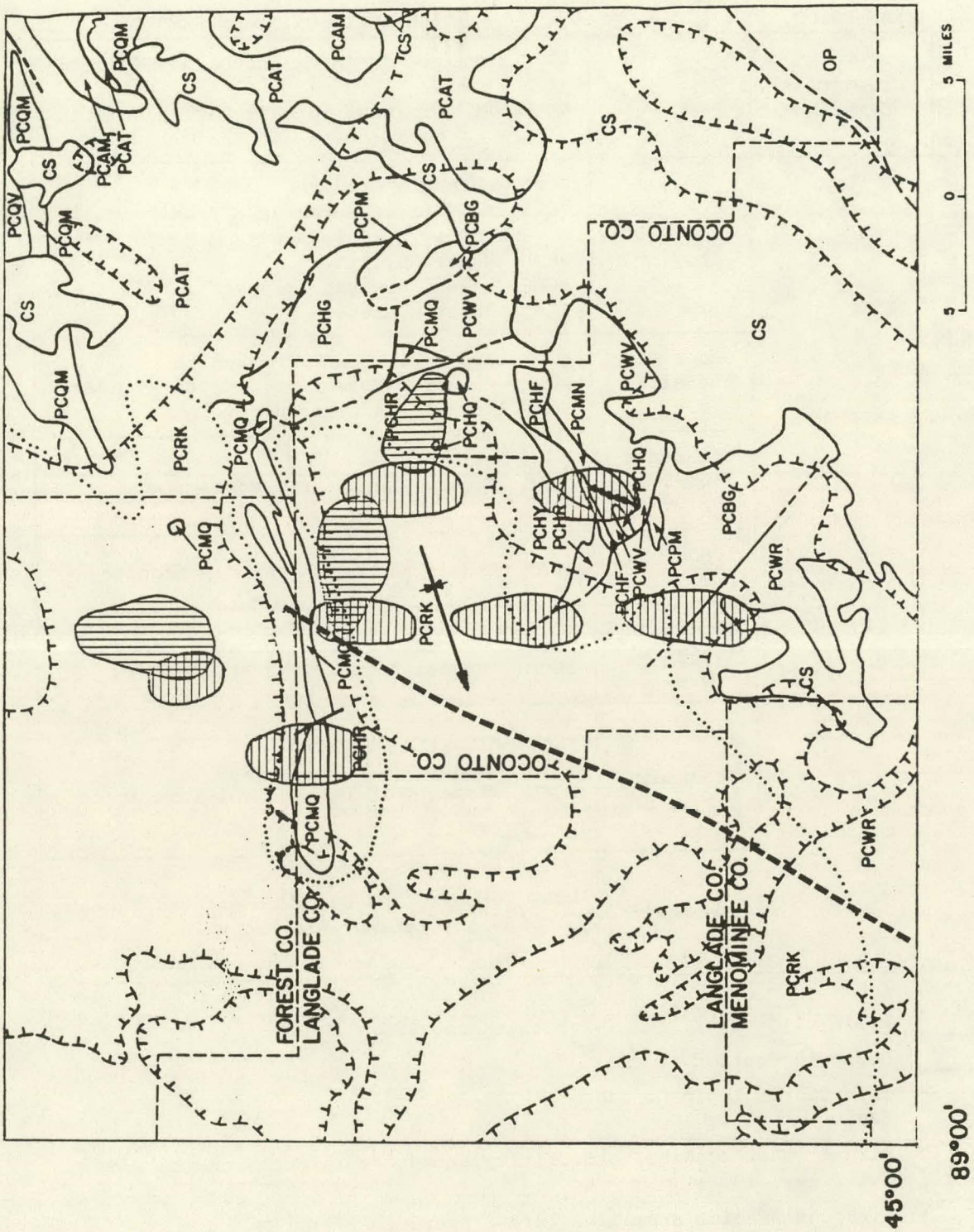

Figure IV-2. Generalized geologic map (after Medaris and Anderson, 1973).

EXPLANATION FOR MAP SYMBOLS

ERA/PERIOD	AGE	LITHOLOGIC UNIT AND SYMBOL
PALEOZOIC — Ordovician Cambrian		OP Prairie du Chien Group, mainly dolomite CS St. Croixan, largely sandstone with some dolomite and shale
PRECAMBRIAN	1.45-1.50 b.y.	PCBG Belongia Granite PCWR Wolf River Hornblende Granite and Quartz Monzonite PCHR Hager Rhyolite PCHF Hager Feldspar Porphyry PCHY Hager Syenite
	Uncertain 1.45-1.50 b.y.	PCHQ Hay Creek Quartz Monzonite PCPM Peshtigo Monzonite and Trachyandesite PCHG High Falls Granite
	Uncertain 1.64-1.67 b.y.	PCAM Amberg Gray Quartz Monzonite
	1.85-1.91 b.y.	PCAT Athelstane Pink Quartz Monzonite
	Uncertain 1.85-1.91 b.y.	PCQV Quinnesec Felsic Volcanic Rocks PCQM Quinnesec Mafic Volcanic Rocks
	Uncertain	PCMQ McCaslin Quartzite PCMN Macauley Granite Gneiss PCWV Waupee Volcanic and Volcaniclastic Rocks
	Uncertain	PCRK Granite and Undifferentiated Igneous and Metamorphic Rocks

$>_{30}$

$\perp\perp\perp$ $<_{30}$ Limit of glacial till (with thickness >30 m)

Geologic Contact

Inferred Geologic Contact

Fault

Stream water uranium/conductivity anomalies (after Kinnaman and Illsley, 1962)

Airborne uranium anomalies (after Arendt, 1978)

Inferred magnetic fault (after Arendt, 1978)

Figure IV-2. Generalized geologic map (after Medaris and Anderson, 1973) (continued).

Volcanics, one from the Thunder Mountain area (MFQ-201) and one from the Mountain, Wisconsin, area (MFQ-202), were analyzed petrographically by M. Dixon (BFEC/Petrology Lab, App. IV-C).

McCASLIN QUARTZITE

The McCaslin Quartzite is the major ridge-forming unit in the McCaslin district. Rock units that have been correlated with the McCaslin Quartzite by Mancuso (1960) are known locally near Mountain, Wisconsin, as the Baldwin Conglomerate and the Thunder Mountain Quartzite.

The McCaslin Quartzite consists of two distinct lithologies: quartzite and metaconglomerate. Most of the rock unit is well-indurated, vitreous quartzite. It ranges from white through gray and purple to red. The red color is caused by disseminated hematite. The texture differs from locality to locality and appears to be related to the amount of recrystallization caused by the High Falls Granite thermal event. Recrystallization is most complete near the eastern end of the McCaslin structure.

Pronounced bedding is common in most outcrops of McCaslin Quartzite. Bedding is accentuated by variations in grain size and hematitic staining along bedding planes. Cross-bedding and oscillation ripple marks are present in several outcrops.

The quartzite has been disrupted, brecciated, and recemented by secondary white quartz along fault zones. The brecciation is especially prominent near the base of the Carter fire tower hill, where open spaces in the brecciated McCaslin are incompletely filled.

The basal conglomeratic facies of the McCaslin occurs in several localities around the perimeter of the syncline. Near Mountain, the conglomeratic facies (locally called the Baldwin Conglomerate) is exposed within a hundred meters of the underlying Waupee Volcanics. At this locality, the McCaslin is a dark-gray, poorly sorted, polymictic conglomerate that contains large angular clasts (up to 25 cm) of rocks similar to the Waupee Volcanics and Macauley Granite Gneiss. At Thunder Mountain, the conglomeratic facies of the McCaslin is finer grained, mineralogically more mature, and better sorted than is the Baldwin Conglomerate. The color of the conglomerate ranges from light gray to red. Close to the High Falls Granite, the hematitic staining is more pervasive. The conglomerate strikes due north and dips about 45° to the west.

Near Carter, Wisconsin, the pebbles in the conglomerate attain their maximum observed size (20 cm). Nearly 50% of the pebbles are either quartzite or white vein quartz. Several clasts of banded iron formation and other lithologies were found within the conglomerate. No grains of detrital pyrite were found in the rocks at Carter, in contrast to the Elliot Lake model. The coarsest conglomerates grade rapidly upward over a distance of a few meters into fine-grained, gray, vitreous quartzite.

HAGER RHYOLITE

The Hager Rhyolite is confined to the inside of the McCaslin syncline with the exception of a few outcrops east of the disrupted nose of the structure and north of the structure along the North Branch of the Oconto River. It has been described by Cochran (1966), Read and Weiss (1962), and Mancuso (1960) as having a "light" and a "dark" phase. The dark phase is characterized by large feldspar phenocrysts, inconspicuous quartz, and a gray, aphanitic groundmass. The light phase contains rounded, resorbed quartz phenocrysts in a pinkish, fine-grained phaneritic groundmass.

The Hager Rhyolite is undoubtedly younger than the McCaslin Quartzite, though the precise structural and stratigraphic relationship between the two is not known. Mancuso (1960) found no dikes of Hager Rhyolite in the McCaslin Quartzite. He suggested that the Hager was extruded into the structural depression created by folding of the McCaslin and Waupee units. Outcrops of Hager outside the limits of the McCaslin syncline are thought to have formed by flows that breached the structure. Whether the Hager is intrusive into the McCaslin or extrusive onto an erosional surface on the McCaslin, it is, nonetheless, younger than the McCaslin. This places the younger limit of the McCaslin at more that 1.5 b.y.

METHODS

Ground surveys were conducted using Mount Sopris SC-132 scintillometers, Scintrex GAD-6 spectrometers, and TSA RE-350 radon emanometers. Carborne surveys were run on the access roads. Scintillometer and spectrometer measurements were taken on outcrops of all rock types associated with the McCaslin structure.

Soil-gas samples were taken from two east-west traverses across a north-trending fault in the western end of the northern limb of the syncline (Fig. IV-3). It was anticipated that radon values would be higher than background if the fault intersected a concentration of uranium in any underlying rock unit. Five east-west traverses were originally planned; however, only two were completed because of equipment problems. Two north-south traverses were run farther to the east across the same limb of the structure. It was anticipated that comparative measures of radon emanating from the individual units and their contacts would be obtained by stepping outward (down section) across the northern limb of the structure.

The glacial drift thins to zero near the limbs of the syncline. All radon measurements were made where the thickness of drift was no greater than 30 m.

RESULTS

Data from the spectrometer surveys are grouped by formation and are presented in Appendix IV-A. The mean KUT and Th/U values for the major formations associated with the McCaslin syncline are summarized in Table IV-1.

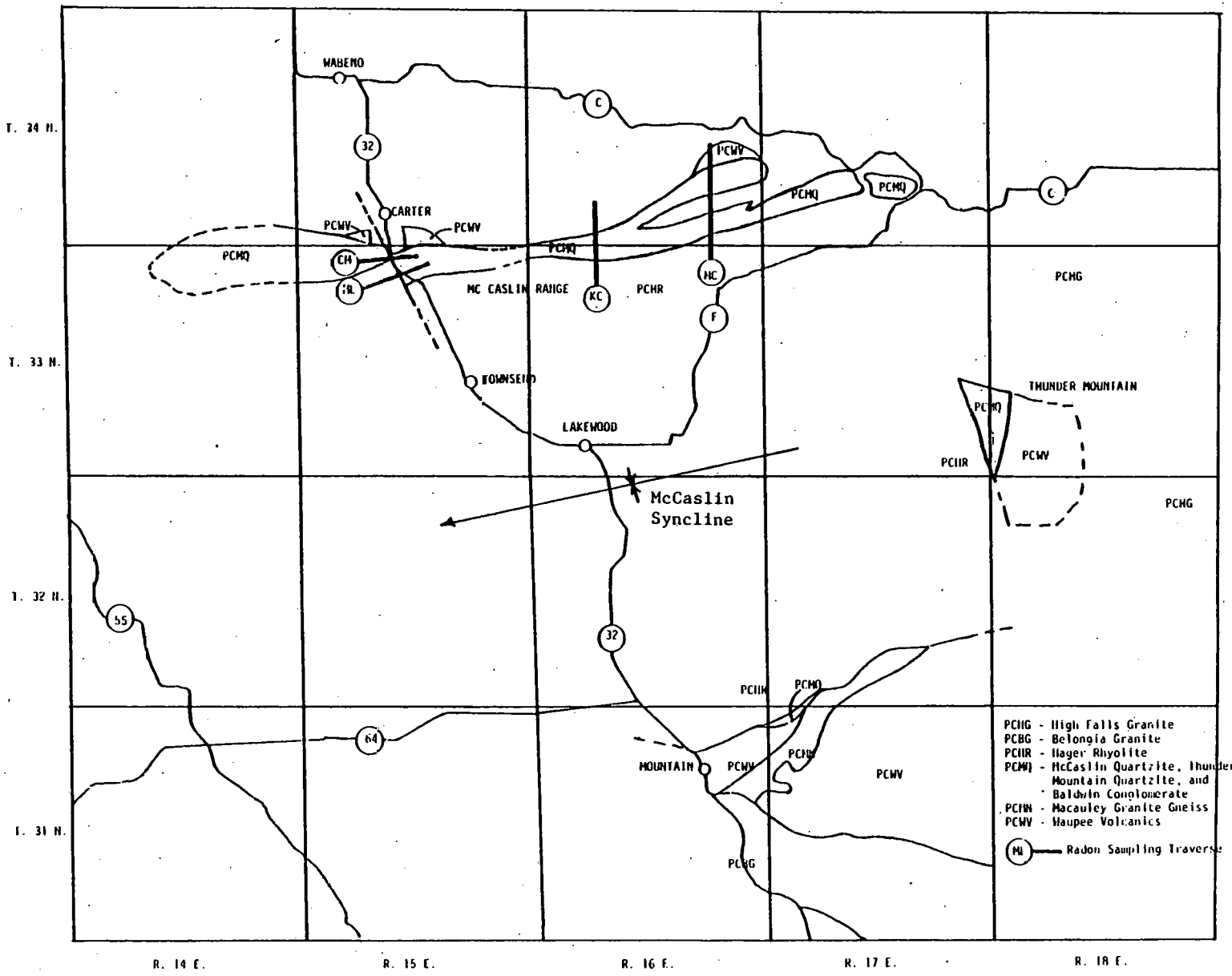

Figure IV-3. Geology of McCaslin syncline (after Mancuso, 1960).

Whereas the targeted basal portions of the McCaslin Quartzite exhibited elevated thorium concentrations (maximum 60 ppm), no significant increase in uranium values was found.

The Hager Rhyolite had a uniform background count of 200 to 250 cps. This was consistently higher than other formations in the district. The Hager is a probable source for the local stream-water and airborne uranium anomalies.

The Waupee Volcanics show no noteworthy concentration or depletion of uranium.

TABLE IV-1. SUMMARY OF RADIOMETRIC SURVEYS

		K%	eU ppm	eTh ppm	eTh/eU	$\bar{x}$ cps
Hager Rhyolite	$\bar{x}$	5.1	14.1	34.7	2.5	200-250
	S. Dev	1.1	2.9	6.7		
McCaslin Quartzite	$\bar{x}$	0.8	2.8	11.9	4.3	60-70
	S. Dev	1.1	1.9	13.7		
Waupee Volcanics	$\bar{x}$	3.5	6.1	11.1	1.8	50-100
	S. Dev	1.8	2.0	5.9		

The results of the soil-gas surveys are in Appendix IV-B. These are raw data. They demonstrate the difficulties encountered in using this particular soil-gas radon detection technique in the McCaslin area. Approximately 75 emanometer readings (including replication tests) were taken. The efficiency of the TSA RE-350 soil-gas extraction system depends on the soil type. It is difficult to obtain the volume of gas from fine-grained glacial sediments needed to perform an analysis. This problem might be overcome by increasing the capacity of the pump and (or) modifying the probe. At the very least, a flow meter should be used in conjunction with the emanometer when sampling in heterogeneous glacial sediments. The measurement of residual ^{210}Po in soils might be a viable alternative for investigation in this glacial drift.

CONCLUSIONS

On the basis of this investigation, the McCaslin area does not demonstrate sufficient recognition criteria to be considered favorable for the occurrence of uranium deposits that are analogous to quartz-pebble conglomerate deposits or unconformity-related deposits (Mickle and Mathews, 1978). Neither model is applicable because:

- More often than not the conglomeratic lenses of the McCaslin Quartzite are polymictic; they contain clasts of granites, banded iron formation, and various dark rocks.

- Pyrite and chlorite are essentially lacking. Instead of a consistent greenish or grayish color, the McCaslin often has a pink to purplish tint from disseminated hematite.

- Pervasive chloritic and hematitic alteration are not present in the McCaslin district. The major fault through the northern limb shows only minor, local hematitic staining.

- The maximum estimated age of the McCaslin is 1.9 b.y. This is younger than the ages for known quartz-pebble conglomerate uranium deposits.

- The presence or absence of uranium is not, in itself, a definitive criterion for classifying an environment favorable for the occurrence of uranium deposits. However, the notable absence of anomalous uranium values in the basal McCaslin Quartzite, and especially where known faulting intersects the McCaslin, suggests that a process for concentrating uranium has not been effective in the area.

- The Waupee Volcanics are not known to contain any extensive graphitic or chloritic schists, nor do they have more than normal amounts of uranium.

- Uranium anomalies in stream-water, stream-sediment, and aerial surveys may be explained by uranium derived from the relatively uraniferous Hager Rhyolite, or other granitic intrusives related to the Wolf River batholith.

The McCaslin area warrants no further investigation; it will not contribute any significant new potential to the NURE resource base.

REFERENCES

Arendt, J. W., project manager, 1978, Hydrogeochemical and stream-sediment reconnaissance basic data for Iron Mountain NTMS Quadrangle, Michigan-Wisconsin: U.S. Department of Energy Open-File Report GJBX-97(78), 36 p.

Banks, P. O., and Rebello, D. P., 1969, Zircon age of a Precambrian rhyolite, northern Wisconsin: Geological Society of America Bulletin 80, p. 907-910.

Cochran, M. D., 1966, A re-evaluation of the Hager Rhyolite Porphyry: Bowling Green, Ohio, Bowling Green State University, M.A. thesis.

geoMetrics, 1978, Aerial gamma-ray and magnetic survey, Rice Lake Quadrangle, Wisconsin, Iron Mountain Quadrangle, Wisconsin/Michigan, Green Bay Quadrangle, Wisconsin: U.S. Department of Energy Open-File Report GJBX-26(78), p. 1-70.

Houston, R. S., and Karlstrom, K. E., 1980, Uranium-bearing quartz-pebble conglomerate: Exploration model and United States resource potential: U.S. Department of Energy Open-File Report GJBX-1(80), 510 p.

Kalliokoski, J., 1976, Uranium and thorium occurrences in Precambrian rocks, upper peninsula of Michigan and northern Wisconsin, with thoughts on other possible settings: U.S. Energy Research and Development Administration Open-File Report GJBX-48(76), 294 p.

Kalliokoski, J., Langford, F. F., and Ojakangas, R. W., 1978, Criteria for uranium occurrences in Saskatchewan and Australia as guides to favorability for similar deposits in the United States: U.S. Department of Energy Open-File Report GJBX-114(78), 479 p.

Kinnaman, R. L., and Illsley, C. T., 1962, Geochemical and geophysical reconnaissance in northern peninsula, Michigan and northeastern Wisconsin: U.S. Atomic Energy Commission Open-File Report RME-1099, 136 p.

Mancuso, J. J., 1960, Stratigraphic and structure of the McCaslin district, Wisconsin: Lansing, Michigan State University, Ph.D. dissertation, 101 p.

Medaris, L. G., and Anderson, J. L., 1973, Preliminary geologic map of Iron Mountain sheet: University of Wisconsin-Extension, Wisconsin Geologic and Natural History Survey.

Mickle, D. G., and Mathews, G. W., eds., 1978, Geologic characteristics of environments favorable for uranium deposits: U.S. Department of Energy Open-File Report GJBX-67(78), 250 p.

Motten, R. J., III, 1972, The bedrock geology of the Thunder Mountain area, Wisconsin: Bowling Green, Ohio, Bowling Green State University, M.S. thesis, 59 p.

Read, W. F., and Weiss, L. W., 1962, Geology of the McCaslin syncline: Tri-State Geological Society Guidebook, 26th Annual Field Conference, p. 1-13.

APPENDIX IV-A. GAMMA SPECTROMETRY DATA

Formation	Locale	Location ¼ Sec.	Sec.	Twp. (N)	Rng. (E)	K (%)	eU (ppm)	eTh (ppm)	Th/U	Remarks
McCaslin	Carter Tower	NENE	5	33	15	0.1	4.0	60.2	15.0	Conglomerate
McCaslin	Carter Tower	NENE	5	33	15	0.2	2.3	35.7	15.5	Conglomerate
McCaslin	Carter Tower	NENE	5	33	15	0.3	1.7	4.2	2.5	Coarse quartzite
McCaslin	Carter Tower	NENE	5	33	15	0.2	2.5	6.0	2.4	Basal conglomerate
McCaslin	Carter Tower	NENE	5	33	15	0.3	1.9	13.4	7.1	Conglomerate
McCaslin	Carter Tower	NWSE	4	33	15	1.1	2.1	8.0	3.0	Fault breccia
McCaslin	Thunder Mtn.	SWSE	30	33	18	0.5	1.6	6.6	3.9	Fine to medium quartzite
McCaslin	Thunder Mtn.	SWSE	30	33	18	0.5	1.2	7.5	6.2	Fine to medium quartzite
McCaslin	Thunder Mtn.	SESW	30	33	18	0.3	1.6	7.5	4.8	Coarse quartzite
McCaslin	Thunder Mtn.	SESW	30	33	18	0.1	1.7	10.7	6.2	Fine quartzite
McCaslin	Thunder Mtn.	SESW	30	33	18	0.3	2.7	5.4	2.0	Coarse quartzite
McCaslin	Thunder Mtn.	SESW	30	33	18	0.4	2.4	5.4	2.3	Coarse quartzite
McCaslin	Thunder Mtn.	SESW	25	33	18	0.3	1.6	8.0	5.0	Near High Falls contact
McCaslin	Thunder Mtn.	SENW	25	33	18	0.4	1.6	4.5	2.7	Near High Falls contact
McCaslin	Thunder Mtn.	SESW	25	33	18	0.2	2.0	4.2	2.1	Near High Falls contact
McCaslin	Thunder Mtn.	SESW	36	33	17	0.3	1.5	3.4	2.2	Near High Falls contact
McCaslin	Mountain	SWNW	5	31	17	3.2	6.5	9.1	1.4	Baldwin conglomerate
McCaslin	Mountain	SWNW	5	31	17	2.9	5.1	9.5	1.9	Baldwin conglomerate
McCaslin	Mountain	SWNW	5	31	17	3.5	8.4	16.0	1.9	Baldwin conglomerate
Waupee	Thunder Mtn.	SESE	30	33	18	6.4	8.4	20.0	2.4	Gneissic
Waupee	Thunder Mtn.	SESE	30	33	18	4.9	6.6	17.8	2.7	Pegmatite
Waupee	Thunder Mtn.	SESE	30	33	18	5.7	8.9	13.5	1.5	Gneissic
Waupee	Thunder Mtn.	SESE	30	33	18	3.6	6.7	19.5	2.9	Arkosic conglomerate

APPENDIX IV-A. GAMMA SPECTROMETRY DATA (continued)

Formation	Locale	Location ¼ Sec.	Sec.	Twp. (N)	Rng. (E)	K (%)	eU (ppm)	eTh (ppm)	Th/U	Remarks
Waupee	Thunder Mtn.	SESE	30	33	18	3.4	6.9	17.5	2.5	Stretch pebble conglomerate
Waupee	Thunder Mtn.	NENE	31	33	18	5.7	6.8	14.7	2.2	
Waupee	Thunder Mtn.	NENE	31	33	18	4.2	5.5	14.0	2.5	Gneissic
Waupee	Thunder Mtn.	NENE	31	33	18	1.5	2.1	4.1	1.9	Gneissic
Waupee	Thunder Mtn.	NENE	31	33	18	4.4	4.2	16.9	4.0	Very fine grained
Waupee	Thunder Mtn.	NESE	31	33	18	4.8	8.7	4.2	0.5	Schistose
Waupee	Hatchery	NWNW	5	32	18	2.0	5.8	5.7	1.0	Garnetiferous breccia
Waupee	Hatchery	NWNW	5	32	18	2.8	6.0	9.5	1.6	Staurolite pseudomorphs
Waupee	Hatchery	NWNW	5	32	18	3.4	7.2	8.3	1.2	Diabase
Waupee	Hatchery	NWNW	5	32	18	0.3	6.7	7.7	1.1	Fine-grained
Waupee	Hatchery	NWNW	5	32	18	4.0	7.5	8.5	1.1	Pegmatite
Waupee	Mountain	SWNW	5	31	17	1.7	3.3	3.5	1.1	Finely laminated
Waupee	Mountain	SWNW	5	31	17	1.1	2.9	3.4	1.2	Finely laminated
Macauley Gneiss	Mountain	NWSE	5	31	17	1.7	4.2	9.0	2.1	Granite gneiss
Macauley Gneiss	Mountain	NWSE	5	31	17	2.4	9.5	11.1	1.2	Aplite
Macauley Gneiss	Mountain	NWSE	5	31	17	0.6	3.6	3.8	1.1	Diabase
Hager Rhyolite	Mountain	SWNW	6	31	17	4.4	15.5	34.1	2.2	Rhyolite porphyry
Hager Rhyolite	Mountain	SWNW	6	31	17	6.8	16.2	44.0	2.6	On McCaslin contact
Hager Rhyolite	Mountain	SWNW	6	31	17	4.5	14.7	32.7	2.2	On McCaslin contact
Hager Rhyolite	Thunder Mtn.	SENE	36	33	17	4.7	9.9	28.0	2.9	Granite

APPENDIX IV-A. GAMMA SPECTROMETRY DATA (continued)

Formation	Locale	Location ¼ Sec.	Sec.	Twp. (N)	Rng. (E)	K (%)	eU (ppm)	eTh (ppm)	Th/U	Remarks
High Falls Granite	Thunder Mtn.	NWNE	19	33	18	4.6	7.0	11.7	1.7	Granite
Unknown Diorite	Carter Tower	NWNE	4	33	15	5.9	14.0	21.5	1.5	In Waupee
Unknown Diorite	Carter Tower	NWNE	4	33	15	6.9	12.2	24.0	2.0	In Waupee

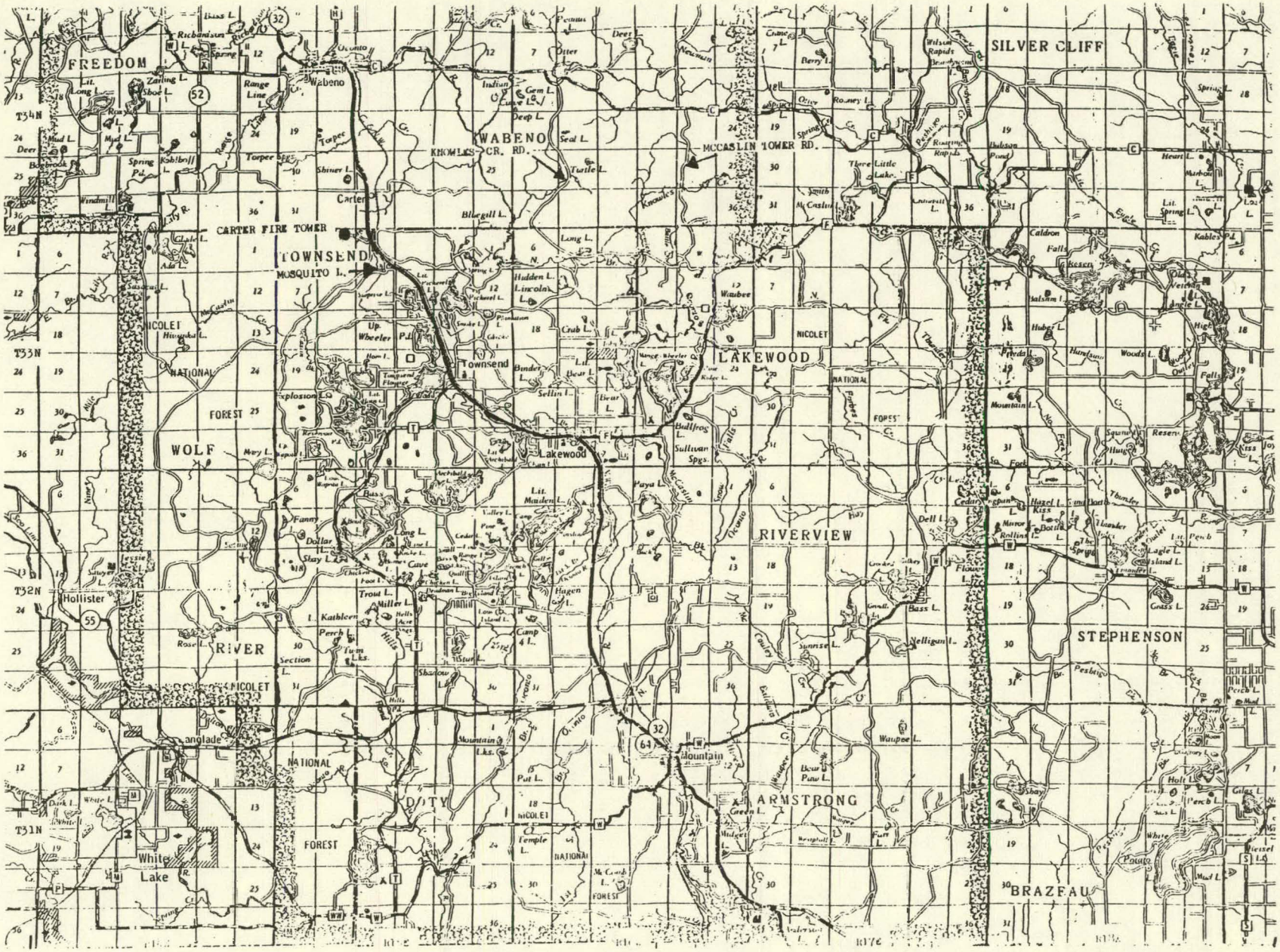

APPENDIX IV-A. GAMMA SPECTROMETRY DATA (continued)--SAMPLE LOCATION MAP

APPENDIX IV-B. RADON EMANOMETRY DATA

Traverse	Station	pCi/ℓ	*	*
Mosquito Lake[1]	ML01	363	--	
	ML02	544	--	
	ML03	304	--	355
	ML04	11	--	3
	ML05	2	779	1558
	ML06	--	--	1025
	ML07	--		525
Carter Mtn.[2]	CM01	178		
	CM02	1273		
	CM03	--		
	CM04	798		
	CM05	--		
	CM06	--		
Knowles Creek[3]	KC01	1		
	KC02	1		
	KC03	72		
	KC04	--		
	KC05	3		
	KC06	2		
	KC07	--		
	KC08	451		
	KC09	417		
	KC10	4		
McCaslin Tower[4]	MC01	5		
	MC02	789		
	MC03	3		
	MC04	629		
	MC05	--		
	MC06	8		
	MC07	--		
	MC08	1		
	MC09	4		
	MC10	1		

1 and 2: Traverses normal to N-S fault near Carter fire tower station spacing 300 m. E-W in ascending order.

3 and 4: Traverses normal to E-W north limb along Knowles Creek Road and McCaslin Tower Road. Station spacing approximately 300 m. N-S in ascending order.

* Repeated Samples

--Sample values less than or equal to background.

APPENDIX IV-C.

PETROGRAPHIC REPORTS

Request # 103500
Project # 1A0955

September 8, 1981

To: W. H. Blackburn, DIG

From: M. L. Dixon, Petrology Lab

McCASLIN SITE,
WISCONSIN

Procedures:

Thin sections of the two samples submitted were examined with a petrographic microscope. Bulk X-ray diffraction analyses of these samples were also performed. The results of these analyses are presented on petrographic description sheets. If you have any questions concerning these results, feel free to contact me.

Summary of Results:

Evidence, in the petrographic microscope, suggesting these rocks are of volcanic origin is not very conclusive. The remnant "volcanic" material that was observed in these samples has been totally altered, with the resultant textures being poorly defined. The "relict glass shards and allochthonous plagioclase aggregates", observed in other studies, were not observed in either of these samples.

Michael L. Dixon
Sr. Petrologist

PETROGRAPHIC DESCRIPTION

PROJECT: McCaslin Site 1A0955 REQUEST: 103500 SAMPLE TICKET NO.: MFQ-201

ROCK NAME: Sillimanite-bearing Sericite-Plagioclase-Quartz Hornfels PETROLOGIST: MLD

MINERAL/COMPONENT	%	COMMENTS
Quartz/Feldspar	70	Microcrystalline to medium-grained anhedra occurring in irregular bands. Quartz and feldspar grains are not differentiated, due to their fine grain size. K-feldspar and plagioclase show slight to strong argillic and sericitic alteration. Bulk X-ray diffraction identified quartz (dominant) and feldspar (subdominant). Coarser quartz grains show inclusions of feldspar, muscovite, sillimanite, and opaques.
Sericite/Muscovite	27	Sericite occurs in irregular bands or in blocky, prismatic patches. Coarsely recrystallized muscovite grains are found in sericite patches and commonly contain sillimanite inclusions.
Biotite	2	Medium- to fine-grained; subhedral. Associated with sericite.
Opaques	tr	Finely disseminated grains which follow banding in rock.
Sillimanite	tr	Fibrous aggregates usually included in coarser grains of quartz and muscovite.
(CONTINUED)		

General Features:

Irregular bands of predominantly microcrystalline quartz, feldspar, and sericite. Sericite occasionally occurs as isolated blocky or prismatic patches. Minor constituents include opaques, biotite, sillimanite, and andalusite(?).

It is believed that this is a metamorphosed sediment or tuffaceous sediment.

The thin section contains a large (10 mm wide) lens-shaped structure believed to be a remnant clast, possibly a sandstone. Recrystallization makes positive identification difficult.

Relatively impure sericite bands occasionally show a "spongy" texture, or other textures which could be interpreted as remnant pyroclastic material.

PETROGRAPHIC DESCRIPTION (CONTINUED)

PROJECT: McCaslin Site 1A0955 REQUEST: 103500 SAMPLE TICKET NO.: MFQ-201

ROCK NAME: Sillimanite-bearing Sericite-Plagioclase-Quartz Hornfels PETROLOGIST: MLD

MINERAL/COMPONENT	%	COMMENTS
Andalusite(?)	tr	Fine equidimensional subhedral to anhedral inclusions in muscovite. Biaxial (-). Fractures contain muscovite.

PHOTOMICROGEAPHS OF SAMPLE MFQ-201

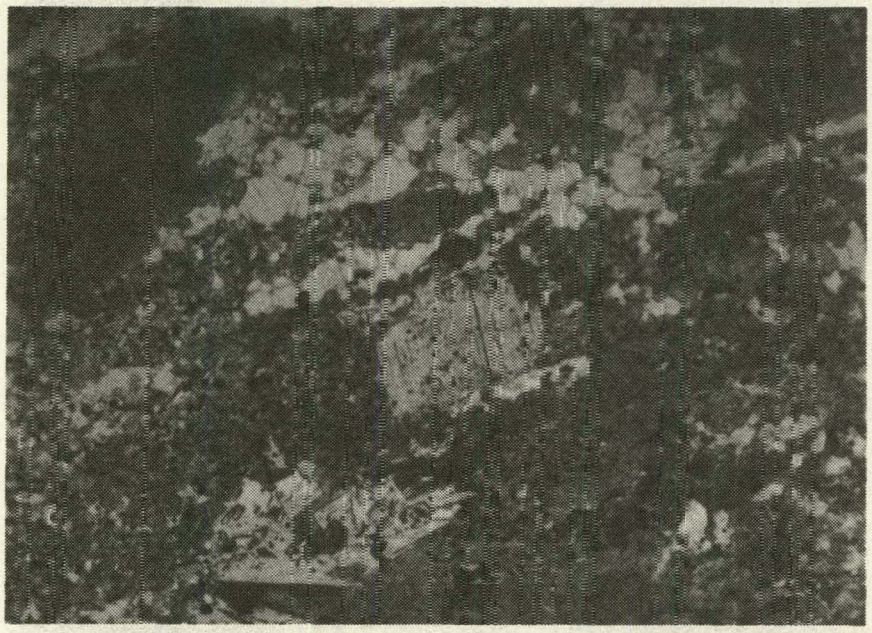

A.

Microcrystalline quartz, feldspar, sericite, biotite, and coarsely recrystallized muscovite; A) plane polarized light, 16x; B) crossed polarizers, 16x.

B.

PETROGRAPHIC DESCRIPTION

PROJECT: McCaslin Site 1A0955 REQUEST: 103500 SAMPLE TICKET NO.: MFQ-202

ROCK NAME: Scapolite-bearing Albite(?)-Epidote Hornfels PETROLOGIST: MLD

MINERAL/COMPONENT	%	COMMENTS
Feldspar/Quartz	46	Discontinuous bands and patches of microcrystalline feldspar (largely plagioclase) and lesser quartz. Bulk X-ray diffraction identified feldspar (dominant) and quartz (tr?). Fine albite(?) and microcline anhedra are scattered throughout the sample with plagioclase showing strong alteration to clay, sericite, and epidote, especially at cores.
Epidote	53	Fine-grained anhedra and microcrystalline material in alternating bands with feldspar/quartz, or in massive patches or lenses. Light green color. Scattered cloudy patches (leucoxene?) in epidote are common.
Scapolite	tr	Anhedral patches (with intergrown feldspar and epidote) showing uniform optical extinction. Uniaxial (-) low relief.
Apatite	tr	Scattered fine anhedral grains.
Opaques	tr	Scattered fine anhedral grains.
(CONTINUED)		

General Features:

Irregular and discontinuous bands of microcrystalline feldspar and quartz with alternating bands, lenses or patches of epidote. Feldspar, largely plagioclase (albite?), shows strong argillic and sericitic alteration.

Possible remnant banding structures suggest volcanic origin. The blocks or patches of altered irregularly banded material could represent pumice fragments.

PETROGRAPHIC DESCRIPTION (CONTINUED)

PROJECT: McCaslin Site 1A0955 REQUEST: 103500 SAMPLE TICKET NO.: MFQ-202

ROCK NAME: Scapolite-bearing Albite(?)-Epidote Hornfels PETROLOGIST: MLD

MINERAL/COMPONENT	%	COMMENTS
Chlorite	tr	Patches or lenses in epidote masses.
Sphene	tr	Fine anhedral to subhedral aggregates.

PHOTOMICROGRAPH OF SAMPLE MFQ-202

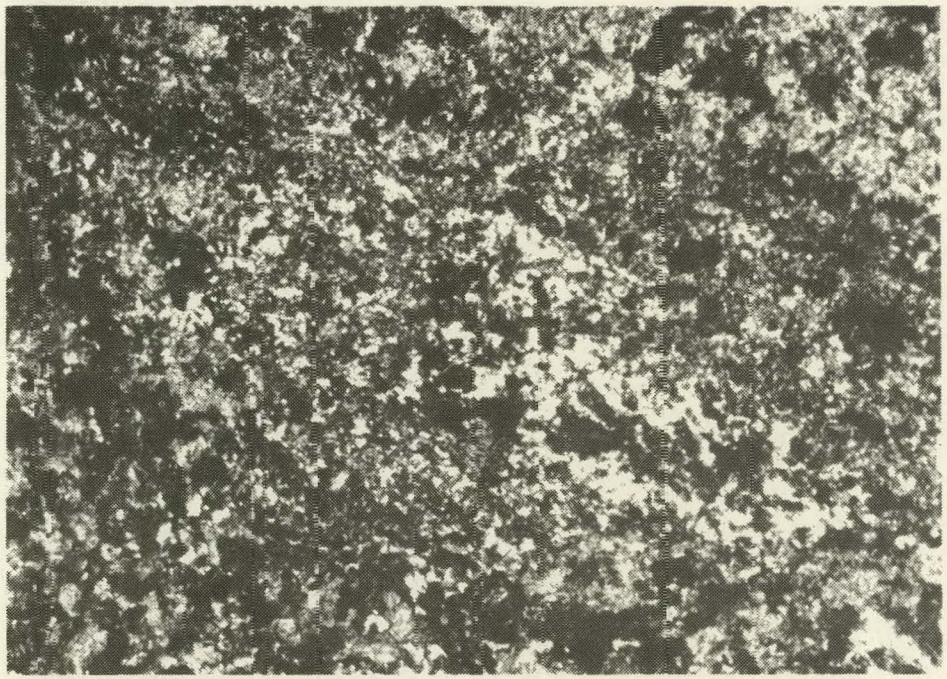

Epidote with patchy feldspar and quartz; crossed polarizers, 16x.

THIS PAGE
WAS INTENTIONALLY
LEFT BLANK

V. URANIUM FAVORABILITY EVALUATION OF THE MT. WITHINGTON CAULDRON, SOCORRO COUNTY, NEW MEXICO

R. E. Dickson and R. D. Dayvault

September 1982

BENDIX FIELD ENGINEERING CORPORATION
Grand Junction Operations
Grand Junction, Colorado 81502

INTRODUCTION

The Mt. Withington cauldron (Fig. V-1) is one of two cauldrons documented in the San Mateo Mountains (Deal and Rhodes, 1976). The presence of thick, silicic alkali-rhyolite ash-flow tuff, ash-fall tuff, domes, lava flows, volcaniclastic sedimentary rocks, and numerous faults suggests that there might be favorable uranium source rocks and environments associated with the cauldron. Berry and others (1981) concluded that the margin of the Nogal Canyon cauldron (Fig. V-1), in the southern part of the San Mateo Mountains, is favorable for uranium deposits but that the Mt. Withington cauldron is unfavorable because of "ore-tonnage and -grade considerations." Berry and others (1981) stated, however, that the cauldron margin has many favorable features. The purpose of the present reconnaissance project was to augment the data base sufficiently to permit more definitive evaluation of the favorability of the rocks in the Mt. Withington cauldron for volcanogenic uranium deposits.

GEOLOGIC SETTING

The San Mateo Mountains are a north-northwest-trending, eastward-tilted, isolated fault block about 75 km long and about 30 km wide. The block is surrounded by sediment-filled troughs. These mountains are part of the Mogollon Plateau volcanic field, which is inferred to be underlain by a composite pluton (Elston and others, 1976).

The San Mateo Mountains consist mainly of mid-Tertiary andesitic to rhyolitic rocks, which lie upon Paleozoic sedimentary rocks. Two cauldrons have been documented in the mountains--the Nogal Canyon cauldron in the southern part of the range and the Mt. Withington cauldron in the northern part (Fig. V-1). Most of the information on the igneous and volcanic rocks presented in this section is from Deal and Rhodes (1976).

The Mt. Withington cauldron formed on a basement of rhyolitic ash-flow tuff that is about 32 m.y. old. Cauldron development occurred from approximately 32 m.y. to 28 m.y. ago. The cauldron, which is some 30 km to 40 km in diameter, has a large resurgent dome and was the source of high-silica alkali-rhyolite ash-flow tuff. The tuff attained thicknesses of more than 2000 m in the area of cauldron depression. It comprises, in ascending order, the A-L Peak Rhyolite, the Potato Canyon Rhyolite, and part of the Beartrap Canyon Formation.

The A-L Peak Rhyolite is a gray to purple, moderately to densely welded, crystal-poor, multiple-flow, composite ash-flow tuff that is 600 m to 700 m thick. Pumice-fragment lineation and the distribution and thicknesses of the formation indicate that its components came from the Mt. Withington cauldron. Sparse phenocrysts, mainly of sanidine, quartz, and plagioclase, are enclosed in a glassy to devitrified groundmass. Finely disseminated opaques, iron oxides, and zircon may be present in trace amounts. Eutaxitic structures are common.

The Potato Canyon Rhyolite is mainly a red to reddish-brown, slightly to densely welded, crystal-rich ash-flow tuff that commonly contains many lithic

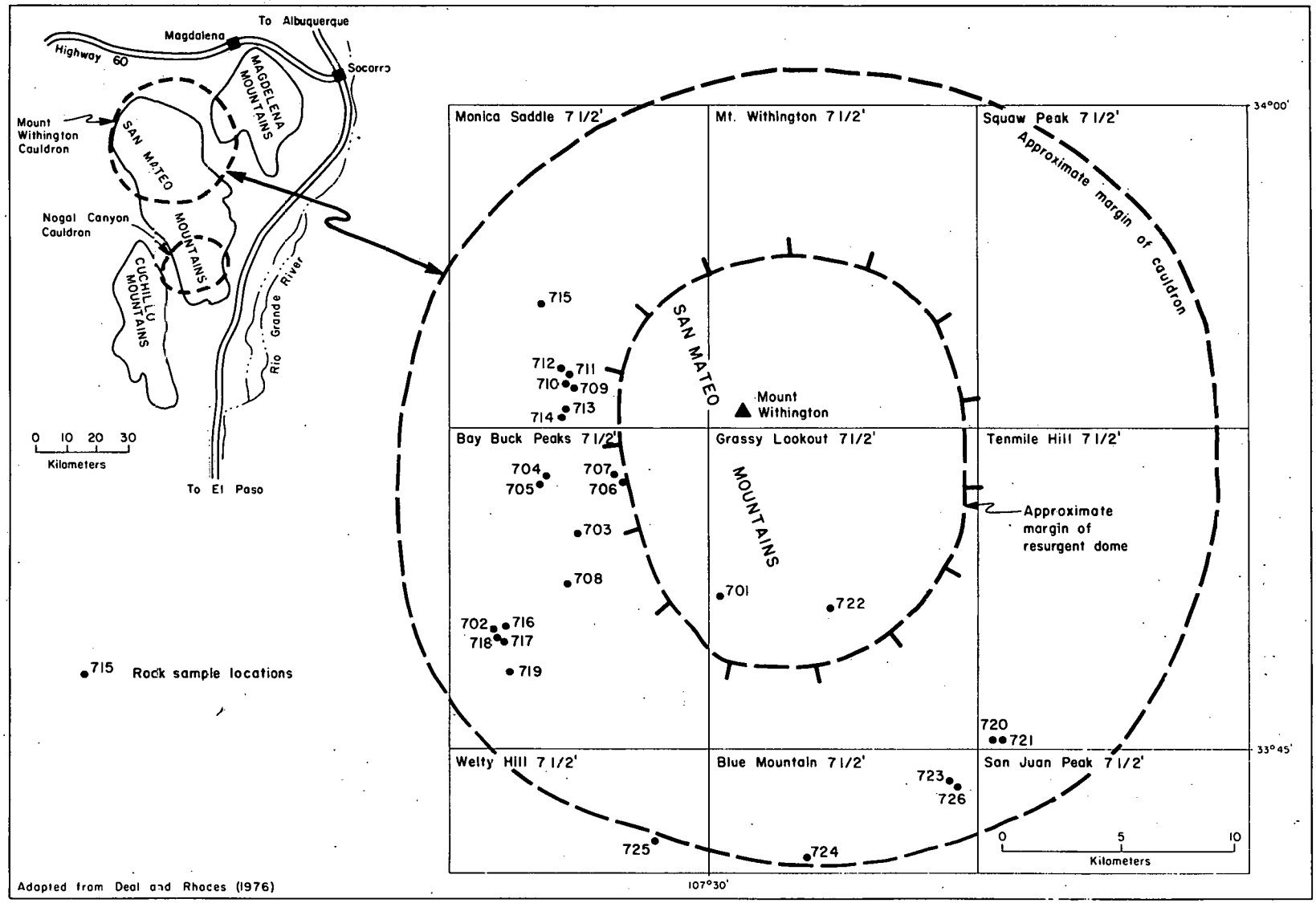

Figure V-1. Location of the Mt. Withington Cauldron.

fragments. It is about 1500 m to 1700 m thick within the cauldron. Phenocrysts, predominantly of sanidine, quartz, plagioclase, and biotite, are in a glassy to devitrified groundmass that consists mainly of quartz and feldspar. Minor constituents include opaques and zircon.

The Beartrap Canyon Formation comprises moat deposits and ring-fracture domes and intrusive rocks. It is absent in the central part of the cauldron. It is locally more than 250 m thick and consists of thin, interbedded, poorly welded, pumiceous tuffs and volcaniclastic rocks, as well as rhyolitic domes and lava flows. The tuffs have a groundmass of quartz and feldspars. Sparse phenocrysts consist mainly of potassium feldspar and quartz. Small amounts of sphene, opaques, and zircon are present. The domes and flows are crystal-poor rhyolite. Rocks in the Beartrap Canyon Formation are pervasively altered in many places.

Post-cauldron rhyolite domes and flows are aligned along ring fractures. Small quartz latite stocks of uncertain age are present in the western part of the San Mateo Mountains.

A basaltic andesite lava flow is present on the north side of Mt. Withington. The flow is about 23.8 m.y. old and probably was erupted from a local vent.

The area was affected by post-cauldron, late Tertiary Basin and Range deformation. The San Mateo Mountain block was isolated structurally and tilted eastward. A large part of the Mt. Withington cauldron margin is now obscured to the north and east by Quaternary sediments.

METHODS

Field methods consisted of radiometric reconnaissance with Mt. Sopris SC-132 scintillometers and gamma-ray spectrometric measurements of rock exposures with two Urtec UG-140 gamma-ray spectrometers. Particular attention during reconnaissance traverses was given to fault zones in the cauldron moat area and to ring-fracture zones. Gamma-ray spectrometer readings were taken at 53 sites (Table V-1). Potassium values are reported in percentage; all other values are ppm. Twenty-six rock samples were collected for analysis.

Most of the rock samples were analyzed for potassium and equivalent uranium and thorium by laboratory gamma-ray spectrometry (closed-can KUT) and for chemical uranium by fluorometry. Some samples were analyzed for trace elements that might indicate metalliferous-solution passage (Table V-1). Six samples (five vitrophyres and a spherulitic flow) were analyzed for major oxides in order to gain information about magmatic differentiation (Table V-2). Petrographic and mineralogic analyses were performed on 13 selected samples by Michael L. Dixon, BFEC Petrology Laboratory.

TABLE V-1. TABLE OF ANALYSES, MT. WITHINGTON CAULDRON

A-L PEAK RHYOLITE	Lat./Long.	7½' Quadrangle	Rock Descriptions	Field KUT %K	Field KUT eU	Field KUT eTh	Field KUT Th/U	Laboratory KUT %K	Laboratory KUT eU	Laboratory KUT eTh	Laboratory KUT Th/U	U_3O_8	As	B[3]	Be	Cs	F	Hg	Li	Mo	Rb	Sn[3]	
K[1]-102	33 50 58 107 28 47	Grassy Lookout	Densely welded tuff	5.7	4.0	33.8	11.1	-	-	-	-	-	-	-	-	-	-	-	-	-	-	-	-
K-103, MFQ[2]-701	33 48 38 107 28 50	Grassy Lookout	Densely welded crystal-poor tuff	6.5	7.3	49.0	13.6	4.2	5.0	29.0	5.8	3	8	-	4	9	397	<0.5	23	3	311	-	123
K-117, MFQ-713	33 52 51 107 34 25	Monica Saddle	Vitric tuff	4.8	13.4	33.6	2.5	-	-	-	-	-	-	-	-	-	-	-	-	-	-	-	-
K-118, MFQ-714	33 52 45 107 34 32	Monica Saddle	Porphyritic rhyolite(?)	6.1	3.8	50.7	16.0	-	-	-	-	-	-	-	-	-	-	-	-	-	-	-	-
K-123	33 54 42 107 32 07	Monica Saddle	Tuff with eutaxitic structure	5.8	4.0	42.7	11.9	-	-	-	-	-	-	-	-	-	-	-	-	-	-	-	-
K-134, MFQ-722	33 48 13 107 26 43	Grassy Lookout	Spherulitic, rhyolitic vitrophyre	5.4	8.7	47.8	5.6	3.6	8.0	28.0	5.6	6	3	-	5	9	1091	<0.5	22	6	263	-	112
K-140	33 44 22 107 23 27	Blue Mountain	Rhyolitic tuff	4.4	12.1	45.4	3.9	-	-	-	-	-	-	-	-	-	-	-	-	-	-	-	-
POTATO CANYON RHYOLITE																							
K-101	33 52 35 107 29 12	Mt. Withington	Densely welded tuff	5.8	5.8	39.9	11.8	-	-	-	-	-	-	-	-	-	-	-	-	-	-	-	-
K-107, MFQ-704	33 51 21 107 54 57	Bay Buck Peaks	Densely welded crystal-rich tuff	7.3	11.5	21.5	1.9	5.6	6.0	16.0	2.7	6	5	-	2	5	324	<0.5	16	4	173	-	484
K-113, MFQ-710	33 53 40 107 34 18	Monica Saddle	Basal vitrophyre	4.5	12.4	28.0	2.4	1.5	5.0	12.0	2.4	6	3	-	5	11	835	<0.5	21	6	279	-	133
K-121	33 54 34 107 32 23	Monica Saddle	Tuff	4.8	13.0	23.5	1.8	-	-	-	-	-	-	-	-	-	-	-	-	-	-	-	-
K-122	33 54 30 107 32 16	Monica Saddle	Dense, brecciated tuff	5.5	9.3	35.1	3.9	-	-	-	-	-	-	-	-	-	-	-	-	-	-	-	-
MFQ-717	33 47 24 107 36 06	Bay Buck Peaks	Crystal-rich vitric tuff	-	-	-	-	2.3	5.0	20.0	4.0	4	3	-	6	11	671	<0.5	97	6	548	-	107
MFQ-718	33 47 29 107 36 13	Bay Buck Peaks	Altered vitric tuff(?)	-	-	-	-	-	-	-	-	-	-	-	-	-	-	-	-	-	-	-	-
K-129	33 46 43 107 21 52	Tenmile Hill	Rhyolitic tuff	7.1	10.1	26.8	2.7	-	-	-	-	-	-	-	-	-	-	-	-	-	-	-	-
K-131	33 45 51 107 24 47	Grassy Lookout	Moderately welded tuff	6.4	5.3	44.5	8.8	-	-	-	-	-	-	-	-	-	-	-	-	-	-	-	-
K-135	33 48 33 107 24 22	Grassy Lookout	Silicified tuff with quartz veinlets	5.1	7.3	20.4	2.9	-	-	-	-	-	-	-	-	-	-	-	-	-	-	-	-
K-136	33 48 34 107 24 27	Grassy Lookout	Silicified tuff	7.2	11.1	24.4	2.3	-	-	-	-	-	-	-	-	-	-	-	-	-	-	-	-
K-138	33 48 07 107 25 10	Grassy Lookout	Silicified tuff	9.6	7.5	51.3	9.3	-	-	-	-	-	-	-	-	-	-	-	-	-	-	-	-
K-142	33 43 58 107 28 25	Blue Mountain	Silicified tuff	4.4	8.5	31.0	3.7	-	-	-	-	-	-	-	-	-	-	-	-	-	-	-	-

[1]K- denotes a field gamma-ray spectrometric measurement site.
[2]MFQ- denotes a rock sample. (The MFQ- prefix has been omitted from Figure 1).
[3]Boron and tin analyses not received.

TABLE V-1. TABLE OF ANALYSES, MT. WITHINGTON CAULDRON (continued)

POTATO CANYON RHYOLITE (con't.)	Lat./Long.	7½' Quadrangle	Rock Descriptions	Field KUT %K	Field KUT eU	Field KUT eTh	Field KUT Th/U	Laboratory KUT %K	Laboratory KUT eU	Laboratory KUT eTh	Laboratory KUT Th/U	U_3O_8	As	B^3	Be	Cs	F	Hg	Li	Mo	Rb	Sn^3	Zr
K-143	33 44 01 107 28 22	Blue Mountain	Dense ash-flow tuff	4.8	9.2	25.5	3.0	-	-	-	-	-	-	-	-	-	-	-	-	-	-	-	-
K-144	33 44 33 107 28 26	Blue Mountain	Crystal-rich tuff	6.2	9.2	50.1	13.5	-	-	-	-	-	-	-	-	-	-	-	-	-	-	-	-
K-146	33 55 19 107 31 01	Monica Saddle	Dense, crystal-rich ash-flow tuff	4.3	9.3	39.6	4.5	-	-	-	-	-	-	-	-	-	-	-	-	-	-	-	-
K-147	33 55 20 107 31 00	Monica Saddle	Densely welded tuff	5.6	8.0	44.9	5.6	-	-	-	-	-	-	-	-	-	-	-	-	-	-	-	-
K-150	33 43 37 107 29 45	Blue Mountain	Dense ash-flow tuff	5.9	2.9	40.3	14.0	-	-	-	-	-	-	-	-	-	-	-	-	-	-	-	-
K-124	33 56 23 107 34 11	Monica Saddle	Brecciated tuff	-	-	-	-	-	-	-	-	-	-	-	-	-	-	-	-	-	-	-	-
K-137	33 48 29 107 24 23	Grassy Lookout	Silicified, hematite-stained tuff	-	-	-	-	-	-	-	-	-	-	-	-	-	-	-	-	-	-	-	-
BEARTRAP CANYON FM.																							
K-104, MFQ-702 (U occur. no. 8)	33 47 34 107 36 18	Bay Buck Peaks	Altered tuffaceous sediment	7.0	37.9	40.1	1.0	2.2	10.0	17.0	1.7	8	-	-	-	-	-	-	-	-	-	-	-
K-105	33 50 10 107 34 09	Bay Buck Peaks	Silicified ash-flow tuff?	5.2	9.1	34.1	3.7	-	-	-	-	-	-	-	-	-	-	-	-	-	-	-	-
K-108, MFQ-705	33 51 19 107 34 58	Bay Buck Peaks	Welded ash-flow tuff	4.1	4.7	27.1	6.3	2.4	4.0	22.0	5.5	4	3	-	4	9	170	<0.5	9	2	177	-	178
K-119, MFQ-715	33 55 14 107 34 37	Monica Saddle	Altered rhyolite (?)	6.7	9.5	36.5	3.8	-	-	-	-	-	-	-	-	-	-	-	-	-	-	-	-
K-120	33 54 31 107 32 24	Monica Saddle	Tuff near fault	3.7	5.7	27.0	5.0	-	-	-	-	-	-	-	-	-	-	-	-	-	-	-	-
K-125, MFQ-716	33 47 44 107 36 02	Bay Buck Peaks	Devitrified, brecciated, rhyolitic tuff(?)	5.6	17.9	58.1	3.3	2.2	11.0	25.0	2.3	16	4	-	9	11	728	<0.5	27	4	429	-	102
K-126	33 47 38 107 35 57	Bay Buck Peaks	Vitric tuff	5.3	14.3	48.0	3.4	-	-	-	-	-	-	-	-	-	-	-	-	-	-	-	-
K-127	33 47 33 107 36 22	Bay Buck Peaks	Indurated tuff with pumice fragments	4.2	15.2	27.1	1.8	-	-	-	-	-	-	-	-	-	-	-	-	-	-	-	-
K-130	33 45 54 107 25 11	Grassy Lookout	Dense, silicified ash-flow tuff	4.9	11.2	27.7	2.5	-	-	-	-	-	-	-	-	-	-	-	-	-	-	-	-
K-139	33 44 40 107 25 46	Blue Mountain	Lithic-rich tuff	8.7	5.6	70.6	12.7	-	-	-	-	-	-	-	-	-	-	-	-	-	-	-	-
K-152	33 42 58 107 31 17	Welty Hill	Tuff with lithic fragments	6.6	3.0	36.1	12.0	-	-	-	-	-	-	-	-	-	-	-	-	-	-	-	-

TABLE V-1. TABLE OF ANALYSES, MT. WITHINGTON CAULDRON (continued)

BEARTRAP CANYON FM. (con't.)	Lat./Long.	7½' Quadrangle	Rock Descriptions	Field KUT				Laboratory KUT				U_3O_8	As	B[3]	Be	Cs	F	Hg	Li	Mo	Rb	Sn[3]	Zr
				%K	eU	eTh	Th/U	%K	eU	eTh	Th/U												
K-103, MFQ-725	33 43 30 107 31 21	Welty Hill	Mordenite in Beartrap Canyon Tuff	3.6	9.6	42.4	4.5	0.6	4.0	19.0	4.8	5	-	-	-	-	-	-	-	-	-	-	-
MFQ-719	33 46 43 107 35 57	Bay Buck Peaks	Ash-flow tuff	-	-	-	-	3.3	3.0	22.0	7.3	2	-	-	-	-	-	-	-	-	-	-	-
K-106, MFQ-703	33 50 09 107 34 44	Bay Buck Peaks	Vitric tuff	4.4	10.5	26.6	2.6	1.9	5.0	13.0	2.6	5	2	-	4	5	891	<0.5	28	4	292	-	123
K-114, MFQ-711	33 53 44 107 34 16	Monica Saddle	Altered rhyolite (?)	6.3	4.7	49.1	10.7	-	-	-	-	-	-	-	-	-	-	-	-	-	-	-	-
K-128	33 46 17 107 21 46	Tenmile Hill	Dense rhyolitic dome	4.4	9.3	26.6	2.9	-	-	-	-	-	-	-	-	-	-	-	-	-	-	-	-
K-132	33 45 58 107 22 58	Grassy Lookout	Ash-flow tuff	5.4	8.8	30.1	3.5	-	-	-	-	-	-	-	-	-	-	-	-	-	-	-	-
K-133, MFQ-720	33 46 27 107 21 37	Tenmile Hill	Welded vitric tuff	4.5	13.8	29.9	2.2	3.8	8.0	29.0	3.6	6	3	-	4	13	891	<0.5	10	6	338	-	205
MFQ-721	33 46 27 107 21 34	Tenmile Hill	Altered porphyritic rhyolite(?) equivalent of 720	-	-	-	-	2.4	4.0	18.0	4.5	6	3	-	4	6	170	<0.5	18	3	293	-	150
K-141, MFQ-723	33 44 15 107 23 13	Blue Mountain	Marginal vitrophyre in dome	6.1	12.0	42.4	3.5	3.4	8.0	27.0	3.4	6	1	-	4	12	728	<0.5	10	4	279	-	118
MFQ-724	33 42 52 107 27 19	Blue Mountain	Pseudobrookite and bixbyite in Beartrap Canyon rhyolite dome	-	-	-	-	2.1	7.0	17.0	2.4	6	-	-	-	-	-	-	-	-	-	-	-
MFQ-726	33 44 11 107 23 07	Blue Mountain	Devitrified equivalent of 723	-	-	-	-	2.4	5.0	19.0	3.8	6	2	-	4	6	299	<0.5	19	6	311	-	142
K-148	33 43 05 107 29 07	Blue Mountain	Agglomerate	7.7	8.6	65.9	7.7	-	-	-	-	-	-	-	-	-	-	-	-	-	-	-	-
K-149	33 43 13 107 29 45	Blue Mountain	Dense lithic-rich tuff	5.5	10.0	34.6	3.5	-	-	-	-	-	-	-	-	-	-	-	-	-	-	-	-
K-151	33 42 56 107 31 21	Blue Mountain	Flow-banded rhyolite	8.4	9.4	24.1	2.2	-	-	-	-	-	-	-	-	-	-	-	-	-	-	-	-
K-145	33 43 27 107 28 57	Blue Mountain	Tuff in fault	7.6	6.9	40.5	5.8	-	-	-	-	-	-	-	-	-	-	-	-	-	-	-	-
TERTIARY INTRUSIVES																							
K-109, MFQ-706	33 51 18 107 32 50	Bay Buck Peaks	Porphyritic rhyolite(?) dome	6.4	10.1	42.4	4.3	2.0	4.0	13.0	3.2	6	3	-	4	5	216	<0.5	13	8	272	-	126
K-110	33 51 37 107 32 41	Bay Buck Peaks	Quartz latite (?)	4.4	9.8	22.6	2.3	-	-	-	-	-	-	-	-	-	-	-	-	-	-	-	-

TABLE V-1. TABLE OF ANALYSES, MT. WITHINGTON CAULDRON (continued)

TERTIARY INTRUSIVES (con't.)	Lat./Long.	7½' Quadrangle	Rock Descriptions	Field KUT				Laboratory KUT				U_3O_3	As	B^3	Be	Cs	F	Hg	Li	Mo	Rb	Sn^3	Zr
				%K	eU	eTh	Th/U	%K	eU	eTh	Th/U												
K-111, MFQ-707	33 51 22 107 33 02	Bay Buck Peaks	Partially devitrified selvage from dome of 70€	5.7	7.5	41.8	5.7	3.8	7.0	25.0	3.6	8	4	-	3	6	486	<0.5	7	6	276	-	97
K-112, MFQ-709	33 53 28 107 34 08	Monica Saddle	Trachyte porphyry(?) intrusive	5.4	4.5	18.1	4.3	-	-	-	-	-	-	-	-	-	-	-	-	-	-	-	-
K-115, MFQ-712	33 53 48 107 34 28	Monica Saddle	Dacitic(?) or rhyolitic(?) dome	8.2	4.6	48.5	10.9	3.4	4.0	16.0	4.0	4	4	-	4	3	130	<0.5	37	4	285	-	173
K-116	33 52 38 107 33 50	Monica Saddle	Quartz latite(?) porphyry	6.3	1.6	28.5	21.2	-	-	-	-	-	-	-	-	-	-	-	-	-	-	-	-
MFQ-708	33 48 40 107 34 22	Bay Buck Peaks	"Pegmatitic" tuff(?) in rhyolite intrusive(?)	-	-	-	-	2.4	2.0	9.0	4.5	2	3	-	2	2	4308	<0.5	8	4	132	-	248

RESULTS

Vitrophyric samples collected from the Mt. Withington cauldron have, for the most part, major-oxide compositions similar to those given by Nockolds (1954) for alkali rhyolites. Exceptions are low Al_2O_3 (11.41% vs. 12.58%), low Fe_2O_3 (0.60% vs. 1.30%), low FeO (0.24% vs. 1.02%), and high MnO (0.07% vs. 0.05%). Agpaitic coefficients (Table V-2) indicate that two samples are peralkaline and that four are almost peralkaline. However, thin-section studies do not reveal any definite sodic-pyroxenes or sodic-amphiboles, which are typically associated with peralkaline rocks. [Small crystals reminiscent of sodic femic minerals proved to be pseudobrookite (Fe_2TiO_5, in sample MFQ-724). Bixbyite, $(Mn,Fe)_2O_3$, was also present in sample MFQ-724].

Trace elements associated with uranium in favorable volcanic rocks include Be, Li, Mo, and Hg. Beryllium contents of the Mt. Withington samples average 4.25 ppm Be, within the averages for acidic rocks. Lithium contents are relatively low. The reason is not known, although it may relate to the low contents of Mg^{+2} and Fe^{+2} ions for which Li may substitute. Molybdenum contents are high; they average about 4.8 ppm Mo compared to average contents in felsic rocks of about 2 ppm (Levinson, 1980). (Mercury contents are all below the analytical threshold of 0.5 ppm Hg.)

The agpaitic coefficients and the contents of beryllium and molybdenum, which ordinarily concentrate in residual melts, indicate that magmatic differentiation has proceeded relatively far. The rocks in the Mt. Withington cauldron could, therefore, be expected to constitute good uranium source rocks.

Fluorometric analyses of 20 samples indicate the uranium content of the rocks to be low. Analyses of 14 devitrified samples range from 2 ppm to 16 ppm U_3O_8 and average 5.9 ppm U_3O_8. Uranium contents of the six vitrophyric samples range from 4 ppm to 6 ppm U_3O_8 and average 5.5 ppm U_3O_8. Thus, the average uranium content of the rock samples is about that of felsic rocks in the western United States, which is about 5 ppm U (Coats, 1956). Neither concentration nor loss of uranium in significant amounts is indicated by these data.

Laboratory KUT analyses indicate that eTh/eU ratios range from 1.7 to 7.3 and average 3.9 overall. Individual eTh/eU ratios average 4.5 for the A-L Peak Rhyolite, 3.0 for the Potato Canyon Rhyolite, 3.8 for the Beartrap Canyon Formation, and 3.6 for the post-cauldron intrusives. The average eTh/eU ratio for the vitrophyric samples is 3.3, about normal for rocks of rhyolitic composition. These data also suggest that little uranium mobilization has occurred.

Fluorine contents of the Mt. Withington samples range from 130 ppm to 1,091 ppm (except for sample MFQ-708, a "pegmatitic" phase in a rhyolite, which contains 4,308 ppm F) and average 535 ppm F. The 535-ppm F average is within the averages reported for rhyolitic extrusive rocks by Koritnig (1972), which range from 260 ppm to 1,080 ppm F, but is considerably less than average fluorine contents of peralkaline rocks, which commonly exceed 3,000 ppm F. Moreover, no fluorite was found during this project. The evidence suggests that the overall fluorine content of the effusive rocks was too low to help

TABLE V-2. MAJOR OXIDE ANALYSES, MT. WITHINGTON CAULDRON

Sample no.	Formation	Rock Type	SiO_2 %	TiO_2 ppm	Al_2O_3 %	Fe_2O_3 %	FeO %	MnO ppm	MgO %	CaO %	Na_2O %	K_2O %	P_2O_5 %	LOI	Totals %	Agpaitic Coef-ficients
MFQ-722	A-L Peak	Vitrophyre	71.52	1329	11.71	0.41	0.21	758	0.07	0.52	3.99	4.11	0.10	4.71	98.72	0.94
MFQ-710	Potato Canyon	Vitrophyre	72.93	1876	10.98	0.73	0.25	960	0.19	0.56	4.34	3.76	<0.01	3.37	98.35	1.02
MFQ-703	Beartrap Canyon	Vitrophyre	74.10	1407	11.15	0.71	0.31	597	0.07	0.49	4.02	4.34	0.01	3.62	97.37	1.01
MFQ-720	Beartrap Canyon	Vitrophyre	73.93	1720	12.05	0.73	0.28	688	0.14	0.40	4.52	4.08	<0.01	3.60	99.80	0.98
MFQ-723	Beartrap Canyon	Vitrophyre	72.94	1642	11.44	0.52	0.28	581	0.10	0.62	3.92	3.92	0.01	4.06	97.67	0.93
MFQ-706	Tertiary Intrusives	Porphyritic Rhyolite(?)	75.97	1564	11.49	0.48	0.09	549	0.09	0.38	3.73	4.92	<0.01	0.73	98.00	1.00

effect significant uranium transport after ash-flow eruption. The fact that the only pegmatitic material found contained 4,308 ppm F but only 2 ppm U_3O_8 (Th/U = 4.5) does not support the existence of a fluorine transporting mechanism.

Calcite cement was not found in any of the rocks. That fact and the low P_2O_5 contents of the vitrophyres suggest that neither carbonate-bicarbonate nor phosphate complexes were available to aid in uranium transport.

Miarolitic cavities and lithophysae are two other indicators of high volatile content. Miarolitic cavities are rare in the Mt. Withington rocks. Lithophysae are sparse, although small lithophysae were seen in places. Evidently, either volatile contents were not high or volatiles were well dissipated during eruption.

Alteration is pervasive in many areas, but the alteration products consist mainly of quartz, feldspar, and clay. Silicification is common, and argillization is evident in places. Quartz veins and veinlets and silicified zones are evident in the Rosedale gold mine area, in the eastern margin of the cauldron, but no radioactivity above background was found there. Hematitic staining is seen in one probable fault (at the location of sample MFQ-719), but no anomalously high radioactivity was found nor is the staining pervasive. Zeolitization evidently is rare; one sample (MFQ-725) contained mordenite $(Ca, Na_2, K_2)(Al_2Si_{10})O_{24}\cdot 7H_2O$, and minor clinoptilolite was identified by bulk X-ray diffraction analysis (sample MFQ-702). Evidence of sericitization, albitization, and hematitic alteration is scarce.

The precipitation of uranium from hot aqueous solutions requires the loss of pressure and temperature and the presence of void spaces in which uranium may accumulate. Such pressure loss before rock consolidation should result in the loss of volatiles, which could be expected to cause the formation of voids. Although spherulitic textures are common in the vitrophyres, lithophysae are rare in the rocks in the Mt. Withington cauldron. Porous textures and structures are sparse in the A-L Peak and the Potato Canyon Rhyolites and in the Beartrap Canyon lava flows and domes. Overall porosity (and permeability) is relatively low, therefore, in the central ash-flow tuffs and in the domes and lava flows.

The concentration of uranium from hot solutions after rock consolidation commonly occurs along fractures, faults, or other porous zones. Faults, fault intersections, and fractures are abundant in the cauldron, but none surveyed are anomalously radioactive nor do they contain anomalous amounts of uranium. Open spaces are rare except in the volcaniclastic moat facies in the Beartrap Canyon Formation. No indication of significant uranium precipitation was found.

Volcaniclastic rocks in the Beartrap Canyon Formation moat facies are very porous. Lateral and vertical lithologic changes within short distances indicate that there is differential permeability, a favorable feature. The volcaniclastic rocks of the Beartrap Canyon Formation would seem to be potentially favorable uranium host rocks for hydroallogenic deposits if reductants were present. Neither carbonaceous trash nor pyrite were seen, however. Nor was uraniferous opal, which is characteristic of hydroallogenic

deposits, found. Only very small amounts of fluorescent chalcedony were noted. (The fluorescence may indicate slight uranium content.)

The Beartrap Canyon uranium occurrence consists of slight uranium enrichment in an agglomerate bed. The bed is reported to contain 120 ppm uranium (Berry and others, 1982). The overlying bed, possibly an altered tuffaceous sediment, contains 8 ppm U_3O_8 (sample MFQ-702). Its eTh/eU ratio of 1.7 indicates slight uranium enrichment. The occurrence appears to be a minor, localized, downward enrichment of uranium, perhaps by adsorption on clay particles. No uranium minerals were found.

CONCLUSIONS

The Mt. Withington cauldron is unfavorable for initial-magmatic, pneumatogenic, hydroauthigenic, and hydroallogenic uranium deposits (Classes 510, 520, 530, and 540; Pilcher, 1978). Despite their favorable major-oxide chemistry, the rocks in the cauldron are relatively poor uranium source rocks; evidence for significant uranium mobilization and transport is lacking; the ash-flow tuffs and the domes and lava flows do not have porous structures adequate to accommodate uranium precipitated by pressure-temperature mechanisms in amounts large enough to constitute uranium deposits; and the lack of reductants signifies that uranium precipitation in adequate amounts by reduction is not probable. It is concluded that no further uranium favorability work in the Mt. Withington cauldron is warranted.

REFERENCES

Berry, V. P., Nagy, P. A., Spreng, W. C., 1982, National Uranium Resource Evaluation, Tularosa Quadrangle, New Mexico: U.S. Department of Energy Open-File Report GJQ-014(82), 22 p.

Coats, R. R., 1956, Uranium and certain other trace elements in felsic volcanic rocks of Cenozoic age in Western United States: U.S. Geological Survey Professional Paper 300, p. 75-78.

Deal, E. G., 1973, Geology of the northern part of the San Mateo Mountains; a study of a rhyolite ash-flow tuff cauldron, and the role of laminar flow in ash-flow tuffs: Albuquerque, University of New Mexico, Ph.D. dissertation.

Deal, E. G., and Rhodes, R. C., 1976, Volcano-tectonic structures in the San Mateo Mountains, Socorro County, New Mexico: New Mexico Geological Society Special Publication 5, p. 51-56.

Elston, W. E., Rhodes, R. C., Coney, P. J., and Deal, E. G., 1976, Progress report on the Mogollon Plateau volcanic field, southwestern New Mexico--Surface expression of a pluton (no. 3), in Cenozoic volcanism in southwestern New Mexico: New Mexico Geological Society Special Publication 5, p. 3-28.

Koritnig, S., 1972, Fluorine abundance in common igneous rocks, in Handbook of geochemistry: New York, Springer-Verlag, p. 9-E-2.

Nockolds, S. R., 1954, Average chemical compositions of some igneous rocks: Geological Society of America Bulletin, v. 65, p. 1007-1032.

Levinson, A. A., 1980, Introduction to exploration geochemistry: Wilmett, Illinois, Applied Publishing Ltd., 874 p.

Pilcher, R. C., 1978, Volcanogenic uranium occurrences, in Mickle, D. G., and Mathews, G. W., eds., Geologic characteristics of environments favorable for uranium deposits: U.S. Department of Energy Open-File Report GJBX-67(78), p. 181-220.

THIS PAGE

WAS INTENTIONALLY

LEFT BLANK

VI. REEVALUATION OF POSSIBLE DIAGENETIC URANIUM CONCENTRATIONS IN PLEISTOCENE LAKE TECOPA, INYO COUNTY, CALIFORNIA

Susan F. Marshall

September 1981

BENDIX FIELD ENGINEERING CORPORATION
Grand Junction Operations
Grand Junction, Colorado 81502

INTRODUCTION

Pleistocene Lake Tecopa was identified as favorable for the occurrence of hydroallogenic uranium deposits during evaluation of the Trona 1° x 2° Quadrangle for the NURE program (Bushnell and Morton, 1980). Bushnell and Morton recognized an apparent correlation between uranium content and different diagenetic facies in the lakebed deposits. An effort was initiated to study this apparent correlation in hope of understanding the processes responsible for uranium concentration in Pleistocene Lake Tecopa. Because uranium deposits have not been reported for Pleistocene closed basins, Lake Tecopa represents a previously unrecognized environment for uranium concentration. This study was therefore undertaken as a first step in the development of a genetic model useful in the identification and evaluation of uraniferous closed-basin sediments.

LOCATION

Pleistocene Lake Tecopa is in southeastern Inyo County, California, approximately 30 km east of Death Valley National Monument (Fig. VI-1) in T. 20, 21, and 22 N., and R. 6 and 7 E. The towns of Shoshone and Tecopa are within the former lake basin.

The Tecopa Lake beds encompass approximately 400 km^2 within an intermontane basin of the Basin and Range physiographic province. The basin is flanked on the east by the southern Resting Spring Range and the Nopah Range. It is bounded on the west and northwest by the Dublin Hills, Ibex Hills, and the southern Greenwater Range and on the south by the Sperry Hills.

GEOLOGIC SETTING

Mason (1948) divided the rocks of the Tecopa area into three main groups: (1) Proterozoic through Cambrian metasedimentary rocks and minor Archean gneiss, (2) Tertiary volcanic rocks, and (3) Quaternary lakebed and alluvial-fan deposits and basalt.

The mountain ranges bordering Lake Tecopa consist primarily of Cambrian metasedimentary rocks overlain by Tertiary volcanic rocks. The Cambrian sequence comprises mildly metamorphosed quartzite, shales, and carbonates, which are disrupted by large-scale, west-directed Laramide thrust faults. The Tertiary volcanic and pyroclastic rocks are mostly tuff, tuff breccia, dacite, and rhyolite. The entire sequence is broken by Basin and Range normal faults (Mason, 1948).

Lake Tecopa formed during the Pleistocene when alluvial-fan deposits south of the present town of Tecopa dammed the Amargosa River. The lake eventually filled with sediments and spilled over the fanglomerate barrier. The Amargosa River cut down through the barrier, drained the lake, and subsequently dissected the lakebed sediments (Noble, 1926; Sheppard and Gude, 1968). These deposits presently form mesas and badlands within the basin.

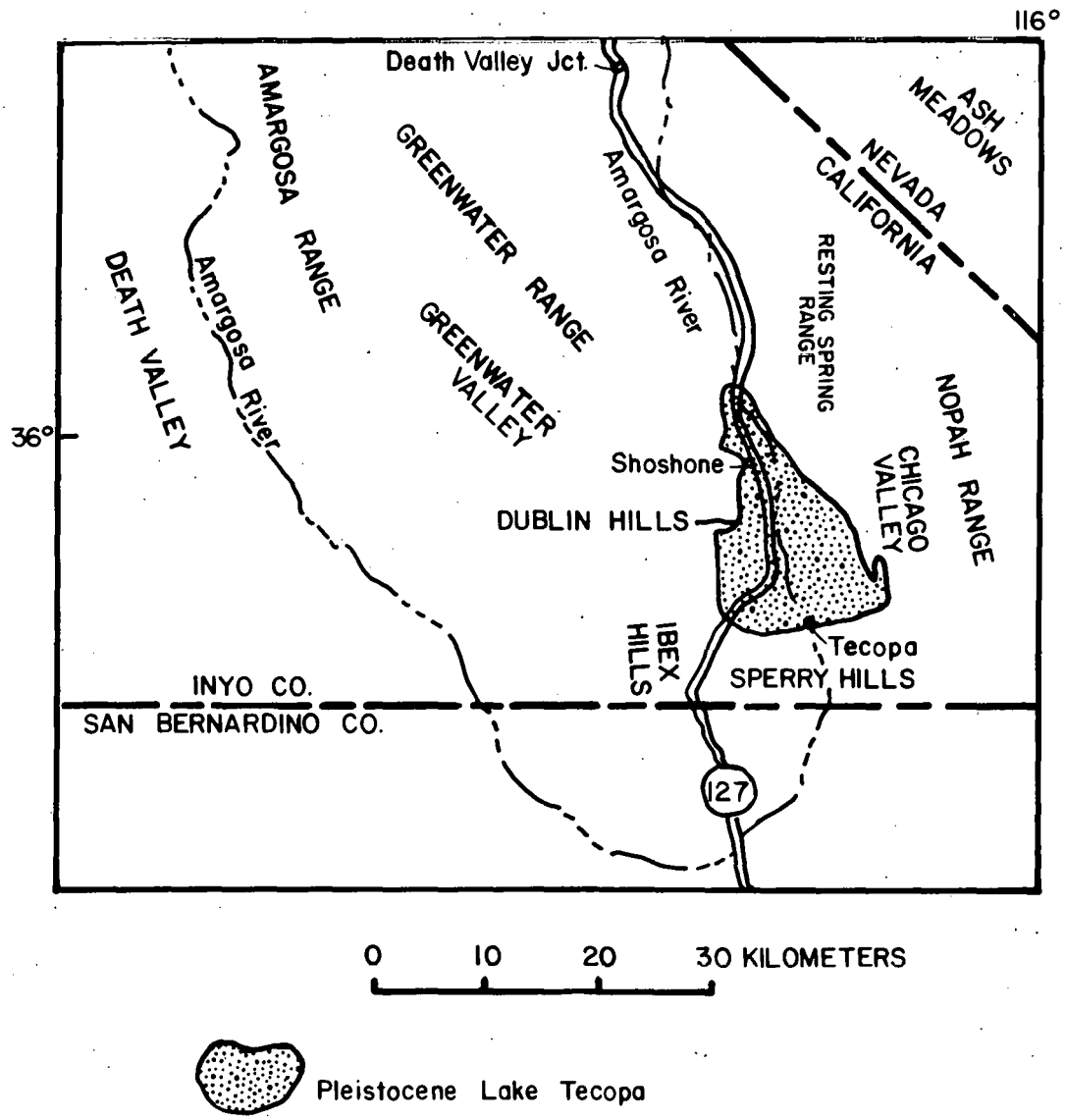

Figure VI-1. Location map (after Starkey and Blackman, 1979).

Sheppard and Gude (1968) defined the lakebed stratigraphy (Fig. VI-2). The deposits consist primarily of mudstone and thin interbeds of rhyolitic tuff. Alluvial conglomerate, sandstone, and siltstone, exposed along the lake margins, pinch out toward the center of the basin. The lakebed sequence also contains calcareous rocks and thin beds of dolomite.

Rhyolitic tuff constitutes 8% to 12% of the exposed stratigraphic section (Sheppard and Gude, 1968). Three thick tuff beds (Fig. VI-2) can be traced throughout the basin. Most of the tuff is ash fall. Sheppard and Gude (1968) delineated three approximately concentric diagenetic facies in the thick tuff beds on the basis of thin-section mineralogy (Fig. VI-3). An outermost zone of fresh glass is found along the former lake margins. This facies grades basinward into a zone of zeolitized tuff. Phillipsite is the predominant zeolite and occurs alone or in association with authigenic clinoptilolite, chabazite, erionite, clay minerals, opal, potassium feldspar, or searlesite. Although the transition is not recognizable in the field, the zeolite facies grades into a zone characterized by authigenic potassium feldspar, which occurs alone or in association with searlesite.

The development of the three diagenetic facies is thought to be a result of variations in the pore-water chemistry (Sheppard and Gude, 1968). The pore water ranged from fresh at the lake margins to saline, alkaline water at the center of the lake. Sheppard and Gude (1968) attributed chemical zonation of the pore water to original zonation of the lake water at the time of deposition. They also suggested the possibility that the lake water was chemically uniform, and zonation in the pore-water chemistry was caused by postdepositional introduction of fresh water at the lake margins.

The authigenic silicate mineralogy directly reflects increasing salinity toward the center of the basin. The fresh glass facies is represented by glass shards in the tuff that have been in contact with relatively fresh pore water. Where salinity increased toward the center of the basin, fresh glass shards were dissolved and replaced by zeolites, forming the zeolite diagenetic facies. Where salinity was highest, zeolites reacted with the pore water to form authigenic potassium feldspar. Nowhere in the potassium feldspar facies is there evidence that potassium feldspar formed directly from glass (Sheppard and Gude, 1968).

STATEMENT OF THE PROBLEM

Bushnell and Morton (1980) sampled the lacustrine sequence for uranium. During the uranium assessment for the Trona Quadrangle, Bushnell suggested in a meeting with the writer that, although tuffs of the fresh glass facies have normal uranium contents for rhyolitic rocks, the zeolite facies rocks are relatively enriched in uranium and the potassium feldspar facies rocks are relatively depleted in uranium. Uranium is particularly concentrated in clay and carbonate-bearing beds within the zeolite facies, where suitable reductants or adsorbants are assumed to be present. Bushnell and Morton (1980) also observed uraniferous caliche at the surface within the potassium feldspar facies.

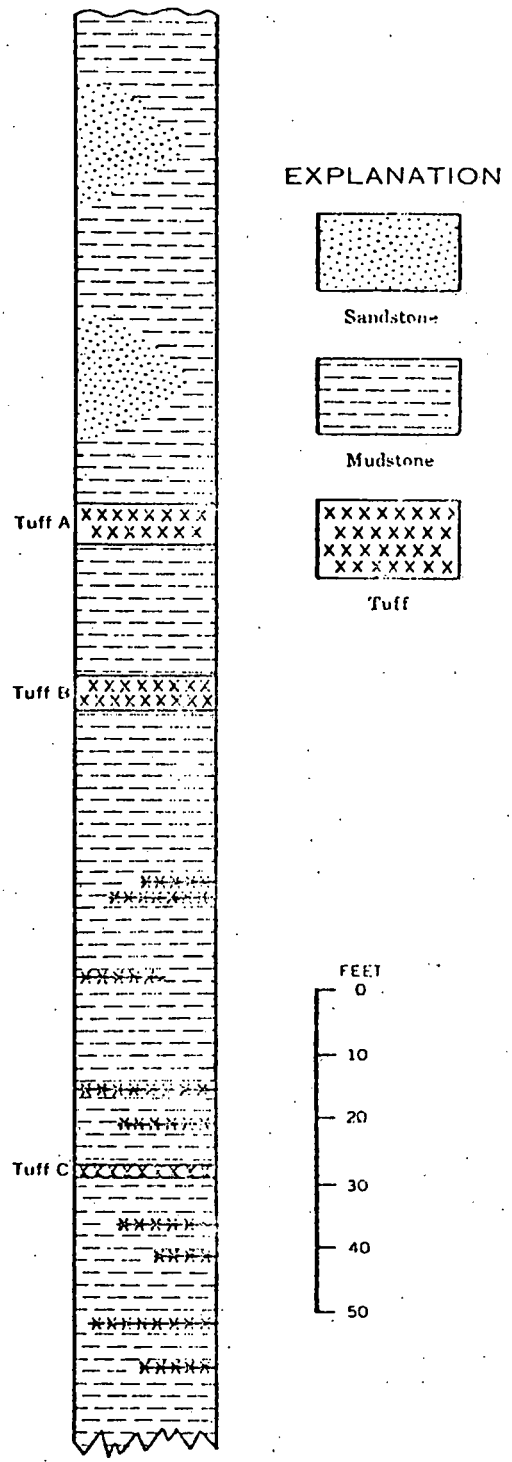

Figure VI-2. Generalized stratigraphic section of the deposits of Lake Tecopa. Base of deposits is not exposed, and top is eroded (from Sheppard and Gude, 1968).

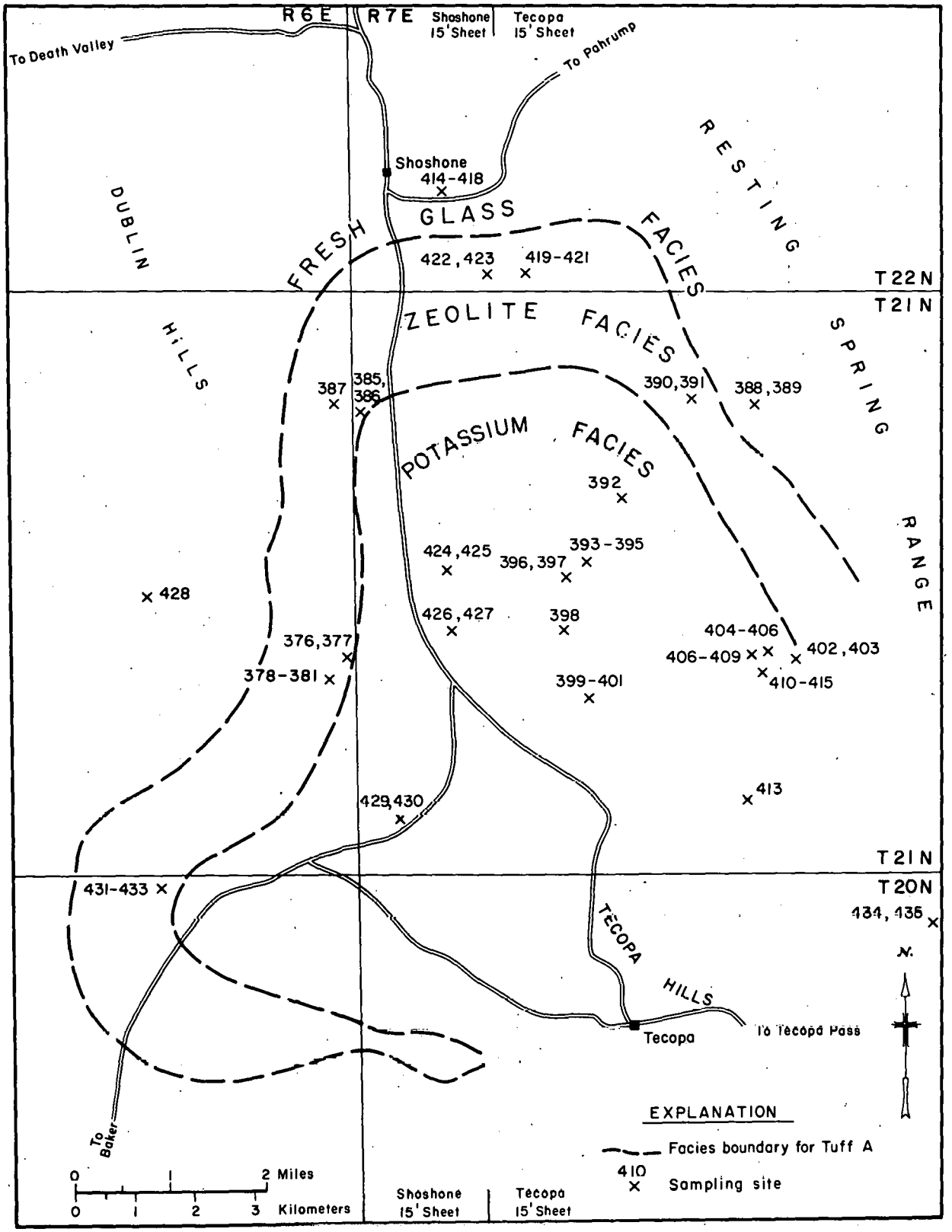

Figure VI-3. Map of Lake Tecopa area showing diagenetic facies for Tuff A (Sheppard and Gude, 1968) and sites where samples were collected for this study.

During the assessment, Bushnell and Morton assigned a favorable designation to the zeolite facies rocks only. The fresh glass and potassium feldspar facies were assumed to be unfavorable for uranium deposits according to NURE guidelines.

The apparent correlation of uranium content with mineralogic zoning raised some interesting questions. It appeared that uranium was released from the tuff units and redistributed throughout the sedimentary sequence during zeolitization. Uranium also appeared to have been mobilized during the transition from the zeolite facies to the potassium feldspar facies.

The major question that was intended to be addressed involves the process responsible for uranium concentration in the zeolite facies. Walton (1978) demonstrated that uranium released during the dissolution of glass in an open hydrologic system does not travel far before it is adsorbed on clays, unless complexing agents are available.

In contrast, in the closed hydrologic system at Lake Tecopa, it is probable that the dissolution of glass and the subsequent formation of zeolites mobilized uranium. The presence of calcite in the lacustrine sequences, especially at sites of fresh-water influx, indicates that the lake and possibly pore waters were carbonate rich. This suggests that carbonate may have served as a complexing agent in solution, thereby permitting uranium migration within the system.

In summary, a major objective of this project was to determine why uranium appeared to be concentrated in the zeolite facies and depleted in the potassium feldspar facies. The available data for Pleistocene Lake Tecopa suggest that uranium concentration may be related to: 1) the mineralogic transformations in the transition from zeolite to potassium feldspar, and (or) 2) differences in pore-water chemistry between the two facies.

METHODS

This study is based on 4 days of field reconnaissance consisting of traverses with a hand-held Mt. Sopris scintillometer, examination of outcrops, and systematic collection of rock samples.

The sampling plan was designed to obtain tuff and mudstone from all three mineralogic facies. Sixty samples were collected from 25 separate locations (Fig. VI-3). Most samples were taken from the zeolite and potassium feldspar facies.

Uranium analysis of all samples was by fluorometric methods to avoid the effects of suspected disequilibrium between uranium and its daughter products (Table VI-1).

M. Dixon (BFEC/Petrology Lab) examined thin sections of samples MAK 383, 384, 385, 386, 387, 407, 408, 409, and 421 with a petrographic microscope. He also performed bulk X-ray analyses of these samples to determine alteration products.

TABLE 1. PLEISTOCENE LAKE TECOPA SAMPLES

Sample Number	Latitude	Longitude	Elevation (ft)	U_3O_8* ppm	Rock Type	Diagenetic Facies**
MAK-376	35°54'11'	116°16'31"	1460	4	Siltstone below B tuff	Zeolite
MAK-377	35°54'11"	116°16'31"	1460	5	B tuff	Zeolite
MAK-378	35°54'01"	116°16'50"	1505	2	Basal A tuff	Zeolite
MAK-379	35°54'01"	116°16'50"	1505	5	A tuff, 2 ft above base	Zeolite
MAK-380	35°54'01"	116°16'50"	1505	9	Silicified lake sediments below A tuff	Zeolite
MAK-381	35°54'01"	116°16'50"	1505	3	Lake sediments below silicified zone	Zeolite
MAK-382	35°56'25"	116°16'29"	1500	3	Mudstone below A tuff	Zeolite
MAK-383	35°56'25"	116°16'29"	1500	5	Basal A tuff -- orange 1" thick bed	Zeolite
MAK-384	35°56'25"	116°16'29"	1500	4	A tuff -- 6" thick orange bed	Zeolite
MAK-385	35°56'25"	116°16'29"	1500	17	Upper, massive A tuff	Zeolite
MAK-386	35°56'25"	116°16'29"	1500	16	A tuff -- interlayered tuff and mudstone	Zeolite
MAK-387	35°56'30"	116°16'47"	1565	1	Calcareous tuffaceous claystone	Zeolite
MAK-388	35°56'29"	116°12'07"	1700	2	Calcified lake sediments	Fresh glass or zeolite?
MAK-389	35°56'29"	116°12'07"	1700	1	Tuff below calcified lake sediments	Fresh glass or zeolite
MAK-390	35°56'33"	116°12'48"	1610	2	Mudstone below tuff	Zeolite
MAK-391	35°56'33"	116°12'48"	1610	2	Tuff with calcite in vugs	Zeolite
MAK-392	35°55'39"	116°13'34"	1440	85	Caliche	Potassium feldspar
MAK-393	35°55'03"	116°13'58"	1400	183	Caliche; composite sample of 1½ ft thick bed	Potassium feldspar

TABLE 1. PLEISTOCENE LAKE TECOPA SAMPLES (continued)

Sample Number	Latitude	Longitude	Elevation (ft)	U_3O_8* ppm	Rock Type	Diagenetic Facies ***
MAK-394	35°55'03"	116°13'58"	1400	13	Mudstone below caliche	Potassium feldspar
MAK-395	35°55'03"	116°13'58"	1400	5	Calcareous mudstone below caliche	Potassium feldspar
MAK-396	35°54'56"	116°14'12"	1400	12	Mudstone below caliche	Potassium feldspar
MAK-397	35°54'56"	116°14'12"	1400	7	Caliche	Potassium feldspar
MAK-398	35°54'27"	116°14'13"	1380	34	Mudstone/claystone with salt crystals	Potassium feldspar
MAK-399	35°53'51"	116°13'56"	1360	6	Tuff	Potassium feldspar
MAK-400	35°53'51"	116°13'56"	1360	4	Mudstone below tuff	Potassium feldspar
MAK-401	35°53'51"	116°13'56"	1360	6	Tuff	Potassium feldspar
MAK-402	35°54'12"	116°11'39"	1500	4	Tuff	Fresh glass(?)
MAK-403	35°54'12"	116°11'39"	1500	3	Mudstone below tuff	Fresh glass(?)
MAK-404	35°54'15"	116°11'59"	1465	5	Mudstone below green A(?) tuff	Potassium feldspar
MAK-405	35°54'15"	116°11'59"	1465	4	A(?) tuff	Potassium feldspar
MAK-406	35°54'15"	116°11'59"	1465	7	Upper A(?) tuff	Potassium feldspar
MAK-407	35°54'13"	116°12'08"	1440	9	Dolomitic claystone	Potassium feldspar
MAK-408	35°54'13"	116°12'08"	1440	8	Calcareous claystone	Potassium feldspar
MAK-409	35°54'13"	116°12'08"	1440	31	Green A(?) tuff	Potassium feldspar
MAK-410	35°54'04"	116°12'00"	1430	5	Mudstone below A(?) tuff	Potassium feldspar
MAK-411	35°54'04"	116°12'00"	1430	12	Orange A(?) tuff	Potassium feldspar
MAK-412	35°54'04"	116°12'00"	1430	6	Upper A(?) tuff	Potassium feldspar
MAK-413	35°52'56"	116°12'11"	1470	5	Green tuff	Fresh glass(?)
MAK-414	35°58'23"	116°15'33"	1600	9	Calcareous siltstone	Fresh glass
MAK-415	35°58'23"	116°15'33"	1600	7	Gray-green tuff	Fresh glass

TABLE 1. PLEISTOCENE LAKE TECOPA SAMPLES (continued)

Sample Number	Latitude	Longitude	Elevation (ft)	U_3O_8* ppm	Rock Type	Diagenetic Facies**
MAK-416	35°58'23"	116°15'33"	1600	9	Sediments above MAK-415	Fresh glass
MAK-417	35°58'23"	116°15'33"	1600	7	Upper tuff?	Fresh glass
MAK-418	35°58'23"	116°15'33"	1600	4	Fossiliferous sediments	Fresh glass
MAK-419	35°57'44"	116°14'39"	1560	7	Basal A(?) tuff	Zeolite
MAK-420	35°57'44"	116°14'39"	1560	8	Glassy tuff above MAK-418	Zeolite
MAK-421	35°57'44"	116°14'39"	1560	8	Upper tuff with concretionary rods	Zeolite
MAK-422	35°57'41"	116°15'03"	1520	10	Mudstone below MAK-419	Zeolite
MAK-423	35°57'41"	116°15'03"	1520	10	Tuff (B?) below MAK-422	Zeolite
MAK-424	35°55'01"	116°15'32"	1400	9	Mudstone	Potassium feldspar
MAK-425	35°55'01"	116°15'32"	1400	12	Tuff	Potassium feldspar
MAK-426	35°54'27"	116°15'27"	1360	4	Mudstone with root casts(?)	Potassium feldspar
MAK-427	35°54'27"	116°15'27"	1360	4	Tuff	Potassium feldspar
MAK-428	35°54'46"	116°18'50"	1700	4	Lake deposits below alluvium	Fresh glass
MAK-429	35°52'44"	116°16'01"	1360	5	Mudstone	Potassium feldspar
MAK-430	35°52'44"	116°16'01"	1360	19	Tuff (?)	Potassium feldspar
MAK-431	35°52'07"	116°18'39"	1490	12	Mudstone below A tuff	Zeolite
MAK-432	35°52'07"	116°18'39"	1490	9	Basal A tuff	Zeolite
MAK-433	35°52'07"	116°18'39"	1490	9	Massive, white A tuff	Zeolite
MAK-434	35°51'48"	116°10'06"	1615	2	Glassy, friable tuff	Fresh glass
MAK-435	35°51'48"	116°10'06"	1615	7	Calcareous siltstone or tuff	Fresh glass

*Fluorometric analyses
**See Sheppard and Gude, 1968

Polished thin sections of samples MAK 392, 393, 394, 429, and 430 were exposed to cellulose nitrate film for approximately 3 weeks. Resultant autoradiographs were examined by Dixon prior to uranium mineral analyses in the scanning electron microscope/energy dispersive spectrometer (SEM/EDS).

RESULTS

Field reconnaissance revealed no anomalous (1.5 times background) radioactivity in the basin. However, initial study by Bushnell and Morton (1980) suggested considerable disequilibrium between uranium and its daughter products. Some of the richest samples (approximately 150 ppm U) from that study produced no anomalous radioactivity in the field.

Distinct stratigraphic units show lateral continuity throughout the basin despite considerable changes in lithology within individual tuff and mudstone units. This is most apparent in the uppermost A tuff of Sheppard and Gude (1968). The A tuff contains a distinctive bright-green or bright-orange marker bed. This thin basal marker bed consists primarily of phillipsite spherules, together with abundant altered glass shards. The marker bed is typically overlain by a light-green or bright-orange altered vitric tuff, which shows evidence of extreme soft-sediment deformation. The upper part of the A tuff is extremely variable in character, depending on location within the basin (Fig. VI-4). The most obvious change is in color, possibly reflecting the variable oxidation state of iron in the tuff. No noticeable difference in uranium content is apparent between the oxidized and reduced tuff. This appears to rule out the possibility of tying uranium concentrations to simple oxidation/reduction processes.

At most sample localities, at least two samples were collected: one of tuff and one of the underlying mudstone. This was done to test for uranium depletion in the tuffs and reconcentration in the mudstones during diagenesis, as suggested by Bushnell and Morton (1980). If any generalization can be made, it is that the uranium content of the tuff generally equals or exceeds that of the mudstone at any particular locality.

Uranium content of tuff samples ranges from 1 to 31 ppm U_3O_8 with a mean (ignoring the lowest and highest values) of 7.4 ppm U_3O_8. This is not unusual for rhyolitic material in the Basin and Range Province. Bushnell and Morton (1980) reported 12 ppm uranium in rhyolite of the Resting Spring Range on the northeast flank of the basin. The tuffs show slight enrichment toward the center of the basin from a mean of 5 ppm U_3O_8 in the fresh glass facies to approximately 8 ppm U_3O_8 in the zeolite facies to approximately 10 ppm U_3O_8 in the potassium feldspar facies.

The mudstones, siltstones, and claystones of the basin have a mean uranium content of approximately 5.5 ppm U_3O_8. This excludes all caliche and mudstones with salt crystals observed in hand specimen. These sediments show no variation in uranium content with diagenetic facies. The mean uranium content does not appear to be unusual for tuffaceous sediments in the Basin and Range Province.

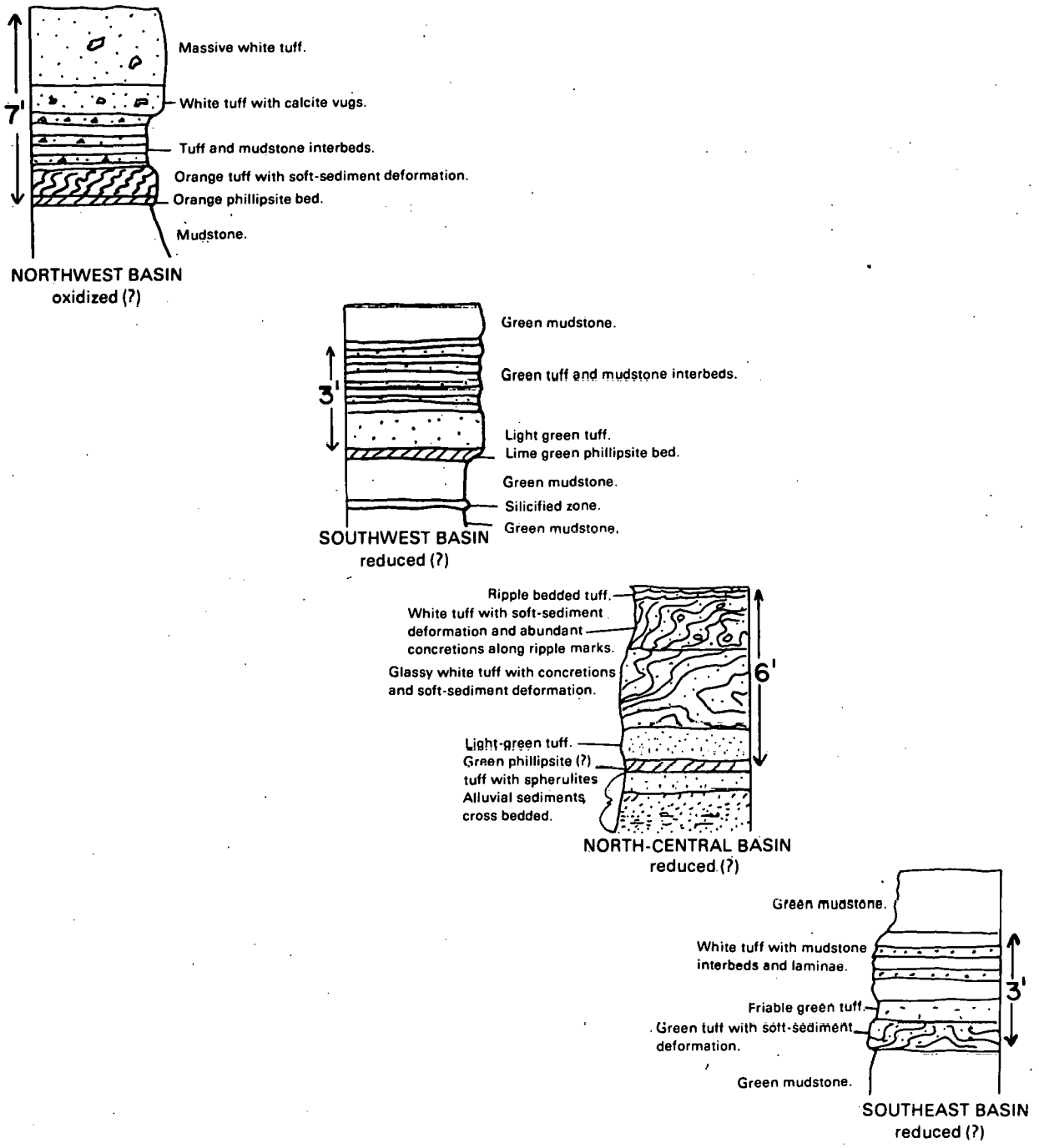

Figure VI-4. Schematic sections of Tuff A zeolite facies.

By contrast, the greatest uranium contents in the basin occur in samples of caliche and mudstone with evaporite minerals. A channel sample of a caliche bed 1.5 ft thick in the center of the basin yielded 183 ppm U_3O_8. The uranium content of caliche samples ranges from 7 to 183 ppm U_3O_8. Uranium in mudstone samples with evaporite minerals ranges from 5 to 34 ppm U_3O_8. No anomalous (1.5 times background) radioactivity was observed in the field in association with these samples.

Alpha track patterns in the caliche and evaporite mineral-bearing mudstone correspond to finely disseminated barite. This can be attributed to radium (a uranium daughter product) substituting for barium in the barite structure and (or) to uranium associated with barite. Thorium-bearing monazite is also responsible for some of the alpha tracks in three samples. No uranium minerals were identified in any of these samples.

DISCUSSION AND CONCLUSIONS

The mechanism for uranium enrichment in tuff from the fresh glass diagenetic facies through the potassium feldspar facies is unclear. The uranium concentrations in the tuffs are too low to permit accurate determination of uranium residence. It is entirely possible that more detailed and systematic sampling may refute this trend of uranium enrichment toward the center of the basin.

The model originally suggested by Bushnell and Morton (1980) is not confirmed, given the results of the present study. Rather than uranium enrichment in the zeolite facies and depletion in the potassium feldspar facies, this study demonstrates a steady increase in uranium content of the tuffs toward the center of the basin. The increase in uranium content does not appear to be directly related to mineralogic transformations from the zeolite to potassium feldspar facies, because there is no sharp increase or decrease in uranium content at the facies boundary. Rather, the increase in uranium content toward the center of the basin may be related to the differences in pore-water chemistry when the basin was a closed system. Further study would be required to establish the actual processes involved.

The apparent diagenetic concentrations of uranium are relatively minor. Most tuff samples contain less than 20 ppm U_3O_8. There appears to be considerable variation in uranium content of the tuffs both vertically and laterally. The results of this study indicate that the tuffs of Pleistocene Lake Tecopa are unfavorable for large, low-grade diagenetic uranium deposits (100 tons U_3O_8 at a cutoff grade of 100 ppm U_3O_8) as defined in the NURE program guidelines.

The lack of variation in the uranium content of the mudstones toward the center of the basin suggests that the proposed model for uranium mobilization from tuffs and redistribution throughout the sediments does not apply. Except where evaporative processes are evident, the sediments are not enriched in uranium. Thus, the lacustrine sediments are also unfavorable for diagenetic uranium deposits as defined in the NURE program.

The uranium concentration in association with evaporative minerals in the center of the basin is probably a relatively recent event. Uranium appears to be concentrated in caliche or mudstone right at the surface. It is probable that uranium was concentrated by an evaporative process that led to the deposition of barite, halite, and minor silver chloride in the saline center of the basin. Uranium may be associated with barite, which is soluble in the presence of chlorides in cold water.

The results of this study do not indicate the presence of a uranium deposit of at least 100 tons of U_3O_8 at a cutoff grade of 100 ppm U_3O_8 at the surface in a caliche-type deposit. It does not rule out the possibility of calcrete/gypcrete-type deposits below the surface in a capillary zone at the upper boundary of the water table. However, because this basin has been open and dissected for a considerable period of time, such deposits appear unlikely.

IMPLICATIONS FOR OTHER BASINS

This study does not eliminate the possibility that Pleistocene closed basins may represent a favorable environment for diagenetic uranium deposits. This investigation merely focused on one Pleistocene closed basin that has been an open system for several million years. Basins that have remained closed since the Pleistocene may contain possible uranium resources. Diagenetic processes operating since the Pleistocene may be efficient enough to produce uranium concentrations in the rock in excess of 100 ppm U_3O_8.

The results of this study also do not rule out calcrete/gypcrete-type models for uranium concentration in closed basins of the Basin and Range Province. Suspected calcrete-type uranium mineralization has been reported for the Amargosa River drainage north of the Tecopa basin (M. McNeil, pers. comm., 1980).

ACKNOWLEDGMENT

Mr. Ken Santini of the Anaconda Minerals Company was extremely helpful to this project.

REFERENCES

Bushnell, M. M., and Morton, P. K., 1980, Uranium resource evaluation, Trona Quadrangle, California: U.S. Department of Energy Open-File Report PGJ-038(80), 226 p.

Mason, J. F., 1948, Geology of the Tecopa area, southeastern California: Geological Society of America Bulletin, v. 59, no. 4, p. 333-352.

Noble, L. F., 1926, Note on a colemanite deposit near Shoshone, California, with a sketch of the geology of a part of Amargosa Valley: U.S. Geological Survey Bulletin 785-D, p. 63-73.

Sheppard, R. A., and Gude, A. J., III, 1968, Distribution and genesis of authigenic silicate minerals in tuffs of Pleistocene Lake Tecopa, Inyo County, California: U.S. Geological Survey Professional Paper 597, 38 p.

Starkey, H. C., and Blackman, D. D., 1979, Clay mineralogy of Pleistocene Lake Tecopa, Inyo County, California: U.S. Geological Survey Professional Paper 1061, 34 p.

Walton, A. W., 1978, Release of uranium during alteration of volcanic glass, in Henry, C. D., and Walton, A. W., eds., Formation of uranium ores by diagenesis of volcanic sediments: U.S. Department of Energy Open-File Report GJBX-22(79), p. VI-1--VI-50.

Plate I.
GEOLOGY OF THE HYLAS AREA, VIRGINIA

Explanation

Cenozoic

Quaternary

Qal—Alluvium

Tertiary

Tgs—Gravel, Sand, and Clay

Mesozoic

Triassic

$\overline{T}$rs—Sandstone and Shale

$\overline{T}$rcm—Coal Measures

$\overline{T}$rcg—Conglomerate

Pg—Pegmatite

Mpb—Petersburg granite

Mississippian

Paleozoic

Precambrian

Sfgn—State Farm gneiss

Sam—Sabot amphibolite

Egnc—Eastern gneiss complex

Geologic contact

Mylonite and (or) ultramylonite boundary

Inferred fault

Quarry

● Water sample locations

◇ Rock sample locations

▲ **HSSR sample site**
(GJBX-18(81))

A= 74.1 ppm
B= 32.7 ppm
(uranium in stream sediment)
C= 3.48 ppb
D= 0.42 ppb
(uranium in ground water)

0 1/2 1 mi.
0 1/2 1 km

77°37'30"
37°45"

37°37'30"
77°45'

37°37'30"
77°37'30"

HYLAS ZONE

MYLONITE
ULTRAMYLONITE

JAMES RIVER

Boscobel

Royal

Luck

Geology modified after Bobyarchick (1976) and Goodwin (1970)

153°00'00"

64°00'00"

7,110,000

7,100,000

7,090,000

7,080,000

490,000

500,000

510,000

520,000

Pluton Boundary

Tape Area

N 25° E

N 70° W

A

B

C

D

E

F

G

D/U

U/D

20

40

60

EXPLANATION

Uranium (Bi-214) anomaly, contour interval =20 cps (approx. 2 ppm eU)

Zoned granitic intrusive with magnetite-poor "core"

Magnetic contours; interval = 2, 10 and 50 gamma

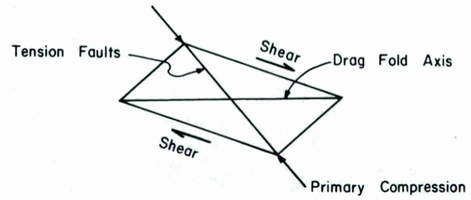

B Inferred faults

FLIGHT ALTITUDE	400 FEET ABOVE TERRAIN
FLIGHT INTERVAL	TRAVERSE 1 MILE, TIE LINE 4 MILES
CONTOUR INTERVAL	2, 10 AND GAMMAS
PROJECTION	10,000 METER GRID, CLARK 1866, ZONE 5
PLANIMETRIC SOURCE	USGS 1:63,360 SERIES
SURVEYED AND COMPILED	1979-1980
A S PROJECT NO	0602

AERO SERVICE

SCALE 1:125,000

0 1 2 3 4 5 MILES

3000 0 3000 6000 9000 12000 15000 18000 21000 FEET

0 1 2 3 4 5 KILOMETERS

TOTAL FIELD
AIRBORNE GAMMA-RAY SPECTROMETER
AND MAGNETOMETER SURVEY
of
FOUR CORNERS AREA
ALASKA
DOE/NURE

Plate 2. GEOPHYSICAL INTERPRETATION MAP